STUDIA
UNIVERSITATIS BABEŞ-BOLYAI

PHYSICA

2

1988

CLUJ-NAPOCA

ANUL XXXIII 1988

STUDIA

UNIVERSITATIS BABEŞ-BOLYAI

PHYSICA

2

Redacţia: 3400 CLUJ-NAPOCA, str. M. Kogălniceanu, 1 Telefon ☎ 1 61 01

SUMAR — CONTENTS — SOMMAIRE

Recenzii — Book Reviews — Comptes rendus

STUDIA UNIV. BABEŞ-BOLYAI, PHYSICA, XXXIII, 2, 1988

ONE DIMENSIONAL MODEL FOR THE HIGH—T_c SUPERCONDUCTORS

L. MACARIE*

Received: June 23, 1988

ABSTRACT. — The one-dimensional electronic system has been considered in order to describe the high-T_c superconductors. The Green function method has been used in order to calculate the critical temperature T_{c1} the lower critical field H_{c_2} and the upper critical field H have been calculated as function of temperature.

1. **Introduction.** In the past two years a large number of modes were proposed in order to explain the high-T_c superconductivity. The importance of the Cu—O has been recently stressed by Rice [1], and Ovshinsky *et al.* [2] proposed a mechanism which explains the occurrence of the "chains" and "sheets" containing Cu atoms. The model proposed in [2] has been applied to explain the superconductivity in the Y—Ba—Cu—O system, but it can be applied to all systems containing the Cu—O.

The aim of this paper is to present a one-dimensional model for the superconductivity of this system which is based on the attractive interaction from the Cu—Cu chains. We will point out the importance of the van Hove singularities in the density of states and the influence of this effect on the critical temperature T_c, the loer critical field H_{c1} and the upper critical field H_{c2}.

2. **The one-dimensional model art $T = 0$.** We start with the mean-field Hamiltonian

$$\mathcal{H} = \sum_{\vec{p},\alpha} (\varepsilon(\vec{p}) - \mu)\, c^{+}_{\vec{p}\alpha}\, c_{\vec{p}\alpha} - \sum_{\vec{p}} (\Delta c_{-\vec{p}\downarrow}\, c_{\vec{p}\uparrow} + h.c.) \tag{1}$$

where the energy of the electrons is

$$\varepsilon(\vec{p}) = -t \cos pa \tag{2}$$

μ is the chemical potential, which can be considered zero only for the half-filled band. The supreconducting gap Δ has been defined as

$$\Delta = g \sum_{\vec{p},\omega} \langle c_{\vec{p}\uparrow}\, c_{-\vec{p}\downarrow} \rangle \tag{3}$$

* *University of Cluj-Napoca, Faculty o Mathematics and Physics, 3400 Cluj-Napoca, Romania*

where g is the electron-electron attractive interaction From (2) we get the energy-dependent density of states as

$$N(\varepsilon) = \frac{1}{\pi} \frac{1}{\sqrt{(2t)^2 - \varepsilon^2}} \tag{4}$$

and for $T = 0$ the equation for the gap is

$$\frac{1}{g} = \int_0^{2t} \frac{d\varepsilon}{2\pi} \frac{1}{\sqrt{(2t)^2 - \varepsilon^2}} \frac{1}{\sqrt{\varepsilon^2 + \Delta_0^2}} \tag{5}$$

where we denoted by $\Delta_0 = \Delta(T = 0)$ From Eg (5) we get the equation

$$\frac{1}{g} = \frac{1}{2\pi} F\left[\frac{\pi}{2}, \frac{2t}{\sqrt{4t^2 + \Delta_0^2}}\right] \tag{6}$$

where the function $F(\varphi, k)$ is defined by

$$\int_0^x \frac{dx}{\sqrt{x^2 + a^2}\sqrt{b^2 - x^2}} = \frac{1}{\sqrt{b^2 + a^2}} F(\varphi, k) \tag{7}$$

and

$$\varphi = \arcsin\left[\frac{x}{b}\sqrt{\frac{a^2 + b^2}{a^2 + x^2}}\right], \quad k = \frac{b}{a^2 + b^2}$$

From (6) we can obtain Δ_0, using the different approximation for the function $F(\pi/2, a)$.

3. **The one-dimensional model at $T \neq 0$.** The equation for the gap at $T \neq 0$ can be obtained using the standard models from (3—4) as

$$\frac{1}{g} = \frac{1}{2\pi} \int_0^{2t} d\varepsilon \frac{1}{\sqrt{(2t)^2 - \varepsilon^2}} \frac{1}{\sqrt{\varepsilon^2 + \Delta^2}} th \frac{\sqrt{\varepsilon^2 + \Delta^2}}{2T} \tag{8}$$

and in order to calculate the critical temperature we approximate (4) by

$$N(\varepsilon) = N(0) + \delta(\varepsilon - 2t) \tag{9}$$

where $N(0) = \frac{1}{2\pi t}$

From (6), (8) and (9) we get the equation

$$\frac{1}{2\pi} F\left(\frac{\pi}{2}, \frac{2t}{\sqrt{(2t)^2 + \Delta_0^2}}\right) = I_{3D}(\Delta) + \frac{1}{4\sqrt{4t^2 + \Delta^2}} th \frac{\sqrt{4t^2 + \Delta^2}}{2T} \tag{10}$$

where

$$I_{3D}(\Delta) = N(0) \int_0^{\omega_D} \frac{d\varepsilon}{2\sqrt{\varepsilon^2 + \Delta^2}} th \frac{\sqrt{\varepsilon^2 + \Delta^2}}{2T} \tag{11}$$

The critical temperature T_c will be obtained from (8) taking $\Delta = 0$ The equation for T_c becomes

$$\frac{1}{g} = \frac{1}{2\pi} \int_0^{2t} \frac{d\varepsilon}{\sqrt{4t - \varepsilon^2}} th \frac{\varepsilon}{2T_c} \tag{12}$$

and using the formula

$$\int x^p th x \, dx = \sum_{k=1}^{\infty} \frac{2^{2k}(2^{2k} - 1)}{(2k + p)(2k)!} B_{2k} x^{k+p}, \quad p \geqslant -1 \tag{13}$$

where B_{2k} are the Bernoulli numbers we get from (12)

$$\frac{1}{g} = \frac{1}{4T_c} \sum_{k=1}^{\infty} \frac{2^k(2^{2k} - 1)(2k - 3)!!}{(2k)!(k - 1)} B_{2k} \left(\frac{t}{T_c}\right)^{2k-2} \tag{14}$$

Using the first two terms from (14) and taking $g = 0\,08$ eV and $2t = 0\,04$ eV, we get $T_c = 84$ K

4 **The lower critical field** H_{c1} The method to calculate H_{c1} for a two-dimensional superconductor has been given recently by Nicula and Crişan [3] using the hypothesis that the high-T_c superconductors are type-II superconductors

The lower critical field $H_{c1}(T)$ can be given by the vortex energy E_v

$$H_{c1}(T) = 2|e|E \tag{15}$$

where E_v can be expressed by

$$E_v = 2\pi \int_0^{\infty} r dr \int_0^{g} d\left(\frac{1}{g}\right) [|\Delta(\vec{r})|^2 - |\Delta(0)|^2] \tag{16}$$

$\Delta(r)$ being the order parameter in the presence of the magnetic field H. The order parameter can be expanded as

$$\Delta(\vec{r}) = \Delta(0) + \Delta_1(\vec{r}) + \quad . \tag{17}$$

and the variation $\Delta_1 = \Delta(r) - \Delta(0)$ will be calculated from (3) written as

$$\frac{1}{g} = T \sum_{\omega, p} \frac{1}{\omega^2 + \varepsilon^2(p) + \Delta^2(p)} \tag{18}$$

where $\omega = 2\pi T(n + 1/2)$
From (18) we get

$$d\left(\frac{1}{g}\right) \cong -\frac{\Delta^2}{4\pi t} T \left[\sum_{\infty} \frac{1}{E^3}\right] \frac{d\Delta}{\Delta} \tag{19}$$

if $\Delta \ll 4t$ and where we introduced the notation $E^2 = \omega^2 + \Delta^2$. Using now the equations (15—19) we get

$$E_v = -\frac{1}{t}\int_0^{\infty} r\,dr \int_0^{\Delta} \Delta \left[\sum_{\omega} \frac{1}{E^3}\right] \Delta_1(\vec{r})ds \tag{20}$$

where

$$\Delta_1(\vec{r}) = -\frac{(ev_0 A(\vec{r}))^2}{3\Delta}\left[\sum_{\omega} \frac{1}{\eta_{tr}E^3}\right] \Big/ \left[\sum_{\omega} \frac{1}{E^3}\right] \tag{21}$$

and

$$\eta_{tr} = 1 + \frac{1}{\tau_{tr} \cdot E}$$

τ_{tr} being the transport scattering time, $A(r)$ the potential vector and v_0 the Fermi velocity.

Taking now $1/\tau_{tr} \cdot E \gg 1$ and for the potential vector the expression [3]:

$$A(\vec{r}) = \frac{1}{s|e|r}\mathbf{K}_1\left(\frac{r}{\lambda}\right) \tag{22}$$

where $\mathbb{K}_1(x)$ is the Bessel function on the imaginary argument, and λ_L is the London penetration. Taking now for (22) the approximation

$$A(\vec{n}) \cong \frac{1}{2|e| \cdot r}$$

the critical field $H_{c1}(T)$ becomes

$$H_{c1}(T) = \frac{\Phi\pi}{4\pi^2\lambda_L^2(T)\,m^2 tv_0} \ln \frac{\lambda_L((T)}{\xi} \tag{23}$$

where $\Phi = \frac{\pi}{2|e|}$ and ξ is the coherence length.

5. **The upper critical field** H_{c2}. The general method for the calculation of the upper critical field H for a superconductor with an energy dependent density of states was given by Crişan [3] and applied for the heavy fermions superconductors. Using the equations (29—30) from the [4] the upper critical field can be obtained from

$$\int d\varepsilon N(\varepsilon)\left[th\frac{\varepsilon}{2T} - th\frac{\varepsilon}{2T}\right] = \frac{Im\Sigma(i0)}{\pi} \times$$

$$\times \int d\varepsilon \frac{N(\varepsilon)}{[\varepsilon + i\Sigma(i0)][\varepsilon - i\Sigma^*(i0)]}\left\{\Psi\left(\frac{1}{2}\right) - \Psi\left(\frac{1}{2}\,\frac{\varepsilon H_{c_2}v_0}{12Im\Sigma(i0)T}\right)\right\} \tag{24}$$

where $\Sigma(i\omega)$ is the self-energy associated with the scattering of the electrons on the non-magnetic impurities and $\Psi(x)$ is the di-gama function.

Using now the same approximation as the one for the calculation of the critical temperature, (24) becomes

$$\frac{1}{2T_c}\sum_{k=1}^{\infty}\frac{2^{2k}(2^{2k}-1)}{(2k)!(k-1)!}B_{2k}\left(\frac{t}{T_c}\right)^{2k-2}-\frac{1}{2T}\sum_{k=1}^{\infty}\frac{2^{2k}(2^{2k}-1)}{(2k)!(k-1)!}\left(\frac{t}{T}\right)^{2k-2}B_{2k}=$$

$$=\frac{Im\,\Sigma(i0)}{\pi}\frac{1}{4t(-Im\,\Sigma(i0))}\frac{ev_0H_{c_2}(T)}{12Im\,\Sigma(i0)T} \tag{25}$$

if we consider

$$4t^2 \gg \Sigma^2(i_\nu)-\varepsilon Im\Sigma(i_\nu)$$

Near the critical temperature T_c from (25) we get

$$H_{c_2}(T)=\frac{24t}{|e|v_0\tau_0 T_c}|T_c-T| \tag{26}$$

where $\tau_0^{-}=-Im\Sigma(i_0)$, an equation which is in agreement with the experimental results [5].

6 **Discussions.** The one-dimensional model for a high-T superconductor has been adopted to explain its unusual properties This model seems to be simple, but a more realistic model has to consider both the "chains" and the "planes" of Cu—O which seem to have a crucial role in the superconducting properties As remarked in many papers, the reduced dimensionality (one dimensional or two-dimensional electronic system) is one of the most important features of these materials.

REFERENCES

1 T M Rice *Nature* **332,** 780 (1988)
2 S. R Ovshinsky, S J Hudgens, R L Lintvedt and D B. Rorabacher *Modern Phys Lett*, **1.** 275 (1987)
3 Al, Nicula and M Crişan, *Helvetica Physica Acta* (to pe published 1988)
4 M Crişan, *J Low Temp Phys*, **64,** 223 (1986).
5 N Kobayashi, T Sasaoka, K. Oh-Ishi, M Kikuchi, M Fukuyama, T Sasaki, K Noto, Y Syomo and Y. Muto, *Jpn Appl. Phys*, 26L, 757 (1987),

STUDIA UNIV. BABEŞ-BOLYAI, PHYSICA, XXXIII, 2, 1988

UPPER CRITICAL FIELD FOR HIGH-T SUPERCONDUCTORS

D. VĂCARU

Received: June 23, 1988

ABSTRACT. — The temperature dependence of the upper critical field H_{c_2} of a high$_c$-T superconductor has been calculated using a two-dimensional model.

1. **Introduction.** The recent discovery of high-T_c superconductivity in $(LaM_2)CuO_4$ systems, where M = Ba, Sr, Ca and $Y_{0\,4}\ Ba_{0\,6}\ CuO_{2\,2}$ has created a strong interest in the basic properties and mechanisms in this class of materials. At the present time the microscopic nature of the high$-T_c$ superconductivity is not clear, but the measurements of the upper critical field H_{c2} [1—3] have shown the following features:

— The high$-T_c$ are type—II high-field superconductors (140 T was predicted [3] for $La_{2-x}Sr_xCuO_{4-y}$);

— There is no Pauli paramagnetic limiting in the high$-T_c$ superconductors;

— A large slope in $H_{c2}(T)$ is observed, and a linear domain near Tc is present in the phase diagram.

The experimental results obtained [1—3] haven been analysed using the standard BCS models, and Schossman *et al.* [4] considered that these results showed an important effect of the electron-phonon interaction which gives rise to the renormalization of the Sommerfeld constant γ which is proportional to the density of states.

In this paper we consider a two-dimensional model for the electronic system with the energy

$$\varepsilon(p) = -2t\ (\cos p_x a + \cos p_y a) \tag{1}$$

where t is the hopping energy and a the lattice constant The density of states calculated by Morita [5] for this system is given by

$$N(\varepsilon) = \frac{1}{2\pi^2 t}\,\theta(4t - \varepsilon)\mathbf{K}[\sqrt{1 - (\varepsilon/4t)^2}] \tag{2}$$

where $\mathbf{K}(x)$ is the complete eliptic integral which can be approximated (for $\varepsilon \ll 4t$) as

$$N(\varepsilon) = \frac{1}{2\pi^2 t}\ln\frac{16t}{\varepsilon} \tag{3}$$

With these results, we calculate the temperature dependence of $H_{c2}(T)$.

* *University of Cluj-Napoca, Faculty of Mathematics and Physics, 3400 Cluj-Napoca Romania*

2. **Upper critical field.** In order to calculate the temperature dependence of the upper critical field H_{c2} for the high$-T_c$ superconductors we will use the general method recently proposed by Crişan [6] to calculate the upper critical field for the heavy fermions superconductors
Using now Eqs (29) and (30) from [6] we have

$$\int \frac{d\varepsilon}{\varepsilon} N(\varepsilon) \left[\text{taugh}\,\frac{\varepsilon}{2T_c} - \text{taugh}\,\frac{\varepsilon}{2T}\right] =$$

$$= \frac{Im\,\Sigma\,(i0)}{\pi} \int \frac{d\varepsilon N(\varepsilon)}{|\,\varepsilon + i\Sigma(i0)\,|^2} \left\{\Psi\left(\frac{1}{2}\right) - \Psi\left(\frac{1}{2} - \frac{eH_{c_2}v_0^2}{12Im\,\Sigma\,(i0)\,T}\right)\right\} \tag{4}$$

where $\Sigma(i\omega)$ is the self-energy describing the scattering of the electrons on the non-magnetic impurities, and $\Psi(x)$ is the di-gama function The integral

$$I_1 = \int_0^{4t} \frac{d\varepsilon}{\varepsilon} N(\varepsilon)\,\text{tangh}\,\frac{\varepsilon}{2T}$$

where $N(\varepsilon)$ is given by (3), gives the simple result

$$I_1 = \ln^2 \frac{4t}{T} \tag{5}$$

and we have to calculate the contribution

$$I_2 = \int_{\varepsilon_0}^{4t} \frac{d\varepsilon}{2\pi^2 t} \ln \frac{16t}{\varepsilon} \frac{1}{[\varepsilon^2 - \varepsilon Im\Sigma(i0) + \Sigma^2(i0)]} \tag{6}$$

This integral has been evaluated as

$$I_2 = -\frac{1}{2\pi^2 t Im\,\Sigma\,(i0)} \left\{\ln X \ln\left[1 - X\frac{Im\Sigma\,(i0)}{16t}\right]\Big|_4^a - \right.$$

$$\left. - L_{i_2}[16t/Im\Sigma(i0)]\right\} \tag{7}$$

where $a = 16t/\varepsilon_0$ and

$$L_{i_2}(z) = \sum_{k=1}^{\infty} \frac{z^k}{k^2},\ |z| < 1$$

Eq (7) will be approximated as

$$I_2 = \frac{a \ln a}{(16\pi t)^2} \tag{8}$$

and from (5) and (8) the equation for $H_{c2}(T)$ becomes

$$\ln^2 \frac{4t}{T_c} - \ln^2 \frac{4t}{T} = c\,\frac{Im\Sigma(i0)}{\pi} \left\{\Psi\left(\frac{1}{2}\right) - \Psi\left(\frac{1}{2} - \frac{ev_0^2 H_{c_2}(T)}{12Im(i0)\,T}\right)\right\} \tag{9}$$

where $C = I_2$.

Near T_c we may use the expansion

$$\Psi\left(\frac{1}{2}+z\right)-\Psi\left(\frac{1}{2}\right)=\frac{\pi^2}{2}z-7\xi(3)z^2+\ldots$$

and from (9) we get

$$H_{c2}(T)=\frac{12\pi}{ce v_0^2}T\ln\frac{16t^2}{T_cT}\ln\frac{T}{T_c} \tag{10}$$

an equation which is in agreement with the experimental data [1—3].

3 **Conclusions.** The two-dimensional model for the high—T_c gives a good agreement between theory and experimental for the $H_{c2}(T)$ near the critical temperature T_c. Eq (9) has to present an agreement with the experimental data also at the lower temperatures, but the measurements in this domain are very difficult because H_{c2} is very high.

REFERENCES

1 B Batlog, A P Ramirez, R J Cava, R B van Dover and E A Rietman, *Phys Rev*, **B 35,** 5340 (1987)
2 W K Kwok, G W Crabtree, D G Hinks, D W Capone, J D Jorgensen and K Zhang, *Phys Rev*, **B. 35,** 5343 (1987)
3 T P. Orlando, K. A Delin, S Foner, E J McNiff Jr, J M. Tarascon, L H Green, W. R McKinnon and G W Hull, *Phys Rev*, **35,** 5347 (1987)
4 M Schossman, F Marsiglio and J P Carbotte, *Phys Rev*, **B 36,** 3627 (1987)
5 T. Morita, *J Math Phys*, **12,** 1744 (1971)
6. M Crişan, *J Low Temp Phys*, **64,** 223 (1986)

STUDIA UNIV BABEŞ-BOLYAI, PHYSICA, XXXIII, 2, 1988

COEXISTENCE OF ANISOTROPIC SUPERCONDUCTIVITY AND ITTINERANT ANTIFERROMAGNETIC ORDER IN HEAVY FERMION SYSTEMS

ZS. GULÁCSI*, M. GULÁCSI* and V. TOŞA*

Received April 22, 1988

ABSTRACT. — The coexistence of anisotropic spin-density-wave and superconductivity is analysed in detail for simple cubic lattice in heavy-fermion systems It is shown that energetically stable coexistence phase occurs only in the presence of an anomalous superconducting pairing Δ_Q connected to the $(k, -\sigma, -k-Q, \sigma)$ pairing in the reciprocal space

There exists experimental evidence for the coexistence of ittinerant antiferromagnetic state and superconducting phase in some heavy-fermion materials like Th doped UBe_{13}. In these materials the superconducting and the spin-density-wave phase are characterized by anisotropic gaps, and the coexistence implies in such a way a coexistence between two anisotropic condensates.

In order to study this problem, we take into account a model hamiltonian H_0 which describes a narrow heavy-fermion band starting from a Kondo lattice type description:

$$H_0 = -\frac{1}{2}\sum_{ij}(ta^+_{i\sigma}a^+_{j\sigma} + h.c.) - \mu\sum_{i\sigma}a^+_{i\sigma}a_{i\sigma} + \frac{1}{2}\sum_{i\sigma}Ua^+_{i\sigma}a_{i\sigma}a^+_{i_1-\sigma}a_{i_1-\sigma} \quad (1)$$

where i and j denote the nearest neighbour sites, the hopping energy t related to the bandwith is given by $t = 2T_K/\pi z$ (where T_K is the Kondo temperature, and z is the number of nearest neighbour sites), μ is the chemical potential, and U represents the renormed T_K dependent on site repulsion between the heavy-electrons.

To describe the condensed phases, we take into account interactions between the nearest-neighbour sites, which are phononic and magnetic in origin [1]:

$$H_i = -\frac{1}{2}\sum_{\{in\},\sigma,\sigma'}K(\{in\}, \sigma, \sigma')\,a^+_{i_1\sigma}a_{i_1\sigma}a^+_{i_4\sigma}a_{i_4\sigma} \quad (2)$$

The phononic terms in Eq (2) do not emphasize the differences which arise in the hamiltonian from different spin configurations of the nearest-neighbour sites. From the phononic contributions we take into account only the greatest contribution, which arises from the $K(ijji; \sigma, \sigma') = \tilde{g}_1$ channel Concerning the spin-dependent interactions between the nearest-neighbour sites, we

* *Institute of Isotopic and Molecular Technology, 3400 Cluj-Napoca 5, P.O Box 700, Romania*

will consider three terms arising from the $K(iijj\,;\,\sigma,-\sigma)=J$, $K(iijj\,,\,\sigma,\,\sigma)=-V$ and $K\,(ijij\,,\,\sigma,\,-\sigma)=I$ like contributions

The model is treated with standard Green functions, allowing the nesting condition $e_{k+Q}=-e_k$ to be satisfied along a fixed Q direction in the reciprocal space

The gaps describing the condensates are defined in the usual manner. The obtained gap equations for the superconducting phase are the following :

$$\Delta(k)=\sum_{i=1}^{3}S_i\,(k)\Delta_i$$

$$\Delta_i=g_i\frac{1}{N}\sum_{k'}S_i(k')\,\Delta(k')\,\mathbf{I}_+(k')\,;\quad g_i=I+\tilde{g}_i \tag{3}$$

The kernel is given by

$$\mathbf{I}_\pm=\frac{1}{4}\left[\frac{1}{\omega_+}\tanh\frac{\beta\omega_+}{2}\pm\frac{1}{\omega_-}\tanh\frac{\beta\omega_-}{2}\right]$$

$$\omega_\pm^2=\Delta^2(k)+[\sqrt{\zeta_k^2+\Delta_S^2(k)}\pm\Delta_Q]^2\,,\ \zeta_k=-S_1(k) \tag{4}$$

and the orthogonal symmetry set (S_i) for the simple cubic lattice (the lattice which is analysed in detail) can be expressed as

$$\begin{aligned}S_1(k)&=2\,(\cos ak_x+\cos ak_y+\cos ak_z)\\ S_2(k)&=\sqrt{6}(\cos ak_x-\cos ak_y)\\ S_3(k)&=\sqrt{2}(\cos ak_x+\cos ak_y-2\cos ak_z)\end{aligned} \tag{5}$$

a being the lattice constant.

For the spin-density-wave, we have

$$\Delta_S(k)=\sum_{i=0}^{6}S_i(k)\Delta_{Si}\,,\qquad \Delta_{Sj}=g_j^S\frac{1}{N}\sum_{k'}\Delta_S(k')S_j(Tk')\,\mathbf{J}_+(k') \tag{6}$$

where the coupling constants (g_j), and the suplimentary symmetry functions (S_j) are

$$\begin{aligned}g_0^S&=U+6(V+J+\tilde{g}_1)\,;\quad g^S_{i/i=1,2,3}=V-I\,;\quad g^S_{i/i=1,2,3}=V+I\\ S_0&=1,\ S_4=\sin ak_x,\ S_5=\sin ak_y,\ S_6=\sin ak_z\end{aligned} \tag{7}$$

The kernel function for this case has the form

$$\mathbf{J}_+=\mathbf{I}_+-\frac{\Delta_Q}{\sqrt{\xi_k^2+\Delta_S^2}}\mathbf{I}_- \tag{8}$$

Besides Δ_i and Δ_{Si} we consider an anomalous superconducting pairing Δ_Q connected to the $\langle a_{k,-\sigma}a_{-k-Q,\sigma}\rangle$ average

$$\Delta_Q=g_Q\frac{1}{N}\sum_k\langle a_{k,-\sigma}a_{-k-Q,\sigma}\rangle \tag{9}$$

The equation for the Δ_Q order-parameter can be expressed as·

$$\Delta_Q = g_Q \frac{1}{N} \sum_{k'} [\Delta_Q \, \mathbb{I}_+(k') + \sqrt{\zeta_{k'}^2 + \Delta_S^2(k')} \, \mathbb{I}_-(k')]; \quad g_Q = 6I - U \tag{10}$$

For any solution of the gap equations (3), (6) and (9) we analyse the free energy (F) in comparison with the free energy of the desordered (paramagnetic) state (F_0) $\delta F = F - F_0$. The obtained solution is stable energetically only if $\delta F < 0$ The free energy can be expressed as

$$\delta F = \delta F_S + \delta F_{SDW} + \delta F_Q + \delta F_{ln} \tag{11}$$

where the first three individual contributions are:

$$\delta F_S = \sum_{i=1}^{3} \frac{\Delta_i^2}{g_i}; \quad \delta F_{SDW} = \sum_{i=0}^{6} \frac{\Delta_{S_i}^2}{g_i^S}; \quad \delta F_Q = \frac{\Delta_Q^2}{6I - U} \tag{12}$$

The last contribution can be written in the following way.

$$\delta F_{ln} = -\frac{\beta^{-1}}{N} \sum_{k'} \ln \left[\frac{ch^3 \frac{\beta\omega_+}{2} + ch^3 \frac{\beta\omega_-}{2} \, ch^{-1} \frac{\beta\omega_+(\Delta_Q = 0)}{2} \, ch^{-1} \frac{\beta\omega_-(\Delta_Q = 0)}{2}}{ch \frac{\beta\omega_+(\Delta = 0)}{2} \, ch \frac{\beta\omega_-(\Delta = 0)}{2} \, ch \frac{\beta\omega_+(\Delta_S = 0)}{2} \, ch \frac{\beta\omega_-(\Delta_S = 0)}{2}} \right]$$

$$ch_x = \frac{1}{2}(e^x + e^{-x}); \quad ch_x^{-1} = \frac{1}{ch_x}; \quad \beta = \frac{1}{k_B T} \tag{13}$$

The δF_{ln} term in the $T = 0$ limit becomes.

$$\delta F_{ln} = -\frac{1}{N} \sum_{k'} \left[\frac{3}{2} (\omega_+ + \omega_-) - \frac{1}{2} \{\omega_+ (\Delta = 0) + \omega_-(\Delta = 0) + \right.$$

$$\left. + \omega_+(\Delta_S = 0) + \omega_-(\Delta_S = 0) + \omega_+ + (\Delta_Q = 0) + \omega_-(\Delta_Q = 0)\} \right]; \tag{17}$$

$$\omega_+ (\Delta_Q = 0) + \omega_-(\Delta_Q = 0) = 2\sqrt{\zeta_{k'}^2 + \Delta_S^2(k') + \Delta^2(k')}$$

First of all we analysed the $\Delta_Q \neq 0$ phase ($\Delta = \Delta_S = 0$). For the critical temperature of these phase (T_{cQ}) we obtain.

$$\frac{1}{2 g_Q N(0)} = th \frac{\Omega}{2 T_{cQ}} \tag{15}$$

Eq. (15) shows that $g_Q < 1/2N(0)$ give $T_{cQ} = 0$. Because $g_Q = 6I - U$ and usually I is smaller in comparison with the one-site repulsion U, it results that the $\Delta_Q \neq 0$ phase cannot appear alone (in fact the $T = 0$ phase diagram of the system for finite g_Q does not contain an energetically stable $\Delta_Q \neq 0$ phase).

The importance of Δ_Q is underlined by the fact that stable coexistence $\Delta_S \neq 0$, $\Delta \neq 0$ solution does not exist for $\Delta_Q = 0$. On the other hand, $\Delta_Q \neq 0$ allows stable coexistence solution, which theoretically explains the experimentally measured coexistence.

REFERENCES

1. M. Gulácsi and Zs. Gulácsi, *Phys. Rev.*, **B36**, 748 (1987).
M. Gulácsi and Zs. Gulácsi, *Solid State Commun.*, **64**, 1075 (1987).
Zs. Gulácsi and M. Gulácsi, *Phys. Rev.*, **B36**, 699 (1987).

STUDIA UNIV. BABEŞ-BOLYAI, PHYSICA, XXXIII, 2, 1988

DIGITAL DATA ACQUISITION IN MAGNETIC RESONANCE IMAGING

AL. NICULA*, M. TODICĂ*, S. AŞTILEAN*, G. BUZAŞ** and I. BERINDEAN**

Received June 28, 1988

ABSTRACT. — The paper present some general considerations concerning the filtering and the sampling of the magnetic resonance imaging recorded spectrum A concret sketch of an A/D converter, used in conection with the NMR spectrometer, is presented

Introduction. The image projection reconstruction method, used both in "RMN and RES imaging", is allready well known [1, 2, 3]. It has at its basis the Fourier transform, which implies a great calculus volume and consequently a digitization of the recorded signal.

The wide use of personal computers, having a limited operating capacity and a processing of the information in real time, implies the adaptation of computing programs [4] as well as building adequate interfaces between the computer and the spectometer [5].

Usually, the practical achievement of the aquisition and computing data is done according to the method, aim and the employed apparatus.

We are interested in the data acquisition of the JEOL JNM 3H—60 spectrometer and their processing by HC—85 computer for measurement within both homogeneous magnetic field and gradient magnetic field.

The NMR absortion spectrum. In the case of JNM 3H—60 spectrometer the magnetic field is linearly time variable

$$H(t) = h_0 + \alpha t \tag{1}$$

where h_0 is the remaining magnetization, α is the speed rise of magnetic field.

In the case of a magnetic field gradient G_x parallel to the homogeneous field.

$$H_{tot} = h_0 + \alpha t + G_x \cdot X \tag{2}$$

The resonance condition is

$$\omega_0 = \gamma H_{tot} = \text{const.} \tag{3}$$

The absorption spectrum, $s_g(x, t)$, in the presence of the field gradient is a convolution between the absorption spectrum when lacking the gradient $s_0(t)$ and the spatial distribution function $g(x)$, [7]

$$s(t) = \int_{-\infty}^{+\infty} g(x) s_0(t - x) dx \tag{4}$$

* *University of Cluj-Napoca, Faculty of Mathematics and Physics, 3400 Cluj-Napoca, Romania*
** *Institute for Computer Technique and Informatics, 3400 Cluj-Napoca, Romania*

Digital treatment of the signal. The absorbtion signal is observed for a time delay $t_0 - T$, $t_0 + T$, which is equivalent to a gate function filtering, $f(t)$

$f(t)$ is equal to 1 within this time delay and has a zero value outside this interval

This Fourier transform is

$$F(\nu) = 2T \quad \frac{\sin 2\pi T\nu}{2\pi T\nu} \cos\left[2\pi t_0\nu - j \sin 2\pi t_0\nu\right] \tag{5}$$

The recorded signal is a convolution between $s(t)$ and $f(t)$. Its Fourier transform, according to the Plancherel theorem is

$$s(t) \cdot f(t) \rightleftharpoons S(\nu) \times F(\nu) \tag{6}$$

where $S(\nu)$ and $F(\nu)$ are the Fourier transform of the $s(t)$ and $f(t)$.

It results that the temporal filtering affects the frequency spectrum Such a time interval, T, has to be closed so that the frequency spectrum should not semnificatively modified.

The sampling of the signal is the next operation regarding the digital processing The ideal sampling implies the use of a succession of Dirac impulses

$$\Pi_{Fe}(t) = T_e \cdot \sum_{k=-\infty}^{+\infty} \delta\left(t - \frac{k}{Te}\right) \tag{7}$$

where Fe is the sampling frecvence and $\delta\left(t - \frac{k}{Te}\right)$ is the Dirac function.

If $s(t)$ is the original signal, then, the sampled signal $s(t)$ is a convolution between $s(t)$ and the Π_{Fe} function.

$$\hat{s}(t) = s(t) \quad T_e \quad \sum_{k=-\infty}^{+\infty} \delta\left(t - \frac{k}{Te}\right) \tag{8}$$

Its Fourier transform is

$$\hat{s}(t) \rightleftharpoons S(\nu) * \sum_{k=-\infty}^{+\infty} \delta(\nu - k \cdot F_e) \tag{9}$$

The sampling frequency Fe should be greater or equal to $2F_M$, in order that the signal spectrum should not be altered

F_M is the maximum frequency contained by the $S(\nu)$ spectrum [8].

The signal can be reconstructed out of the pieces

$$s(t) = \sum_{k=-\infty}^{+\infty} s\left(\frac{k}{Fe}\right) \cdot \frac{\sin \pi \cdot F_e\left(t - \frac{k}{F_e}\right)}{\pi \cdot F_e \cdot \left(t - \frac{k}{F_e}\right)} \tag{10}$$

A low frequency component, the "aliasing effect" appears if the above condition is not fulfilled and the T_e period is a little smaller than the signal period

The limited duration θ impulses are practically used. Thus, $s(t)$ is a signal average for the θ time interval

$$s(k, T_e) = \frac{1}{\theta} \int_{-\infty}^{+\infty} \Pi_{\frac{\theta}{2}} \left(t - k \cdot T_e - \frac{\theta}{2} \right) \cdot s(t) dt = \\ = \frac{1}{\theta} s(t) \ast \Pi_{\frac{\theta}{2}} (t) \Big|_{t = K T_e} \tag{11}$$

$\Pi_{\frac{\theta}{2}}$ is the gate function which has the value 1 in the interval $-\frac{\theta}{2}, \frac{\theta}{2}$ and zero value outside.

The signal Fourier transform is

$$\hat{s} \rightleftharpoons \left[S(\nu) \cdot \frac{\sin \pi \theta \nu}{\pi \nu \theta} \cdot e^{-2\pi \nu j \cdot \frac{\theta}{2}} \right] \ast \sum_{k=-\infty}^{+\infty} \delta \left(\nu - \frac{k}{T_e} \right) \tag{12}$$

The process flows as is $S(\nu)$ in relation (8) were substituted by $S_1(\nu) = S(\nu) \frac{\sin \pi \nu \theta}{\pi \theta \nu} e^{-2\pi \nu j \cdot \frac{\theta}{2}}$

In this case only the amplitude is modified by $\frac{\sin \pi \nu \theta}{\pi \nu \theta}$ factor and the frequency spectrum is not affected. Besides, a defasage term $e^{-2\pi \nu j \cdot \frac{\theta}{2}}$ appears.

Thus, it results that the measurements precision is altered by the width of the sampling impulsions.

These effects can be eliminated employing an adequate module filtering.

The pointed edges of the sampling impulsins introduce high frequencies in the digitized spectrum. This effect is often taken for the "aliasing effect". It can be eliminated either by increasing the sampling frequency or by the employment of a low-passing filter [9].

The use of the equidistant impulsions method is most frequently used. In this case, sometimes the pointed edges of the signal can pass unnoticed. Lately, the nonequidistant impulsions, which observe a certain previously established rule or succession, has been used.

This method gives good results if the form of the signal is beforehand approximated or if a corelation between the signal evolution and the sampling rule can be established. This method presents the advantage that the waste of the significant details can be avoided. At the same time the memory of the data aquisition system is better exploited.

To know the minimum distance between the two impulses is practically important in order to recunstruct the signal by the simplest interpolation rule, e.g. the lineary interpolation rule.

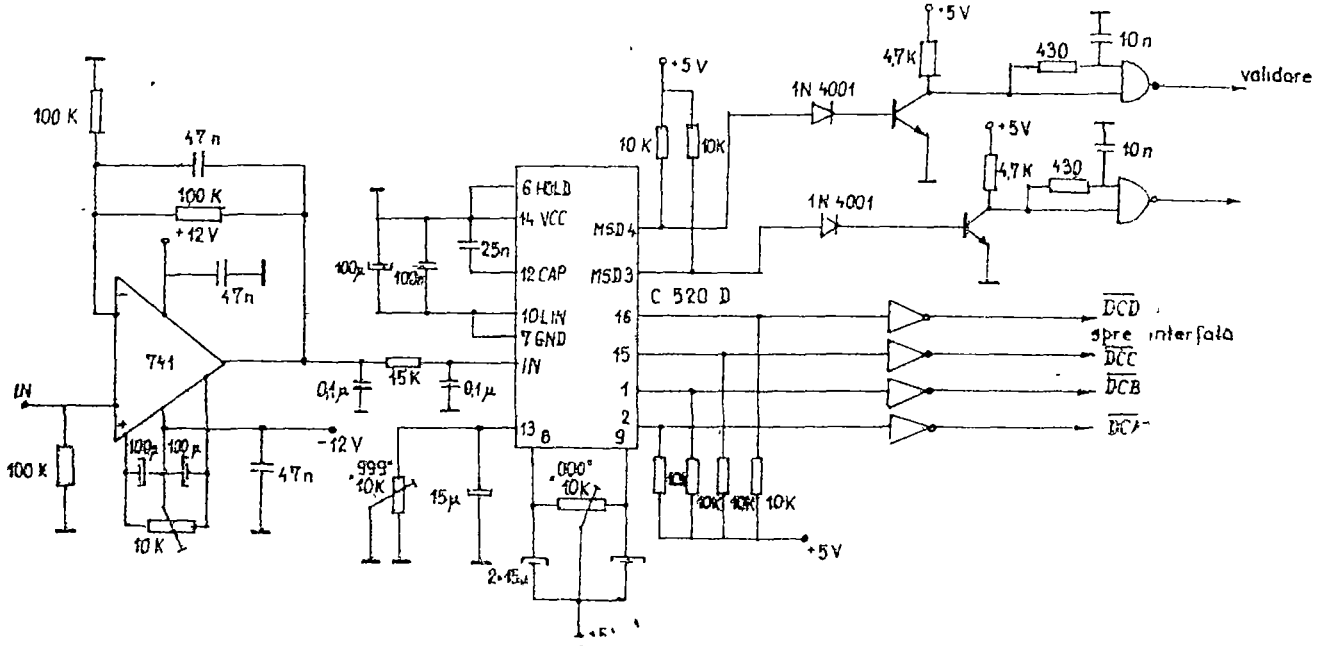

Fig 1. The functioning principles sketch of the A/D converter

The A/D converter. This paper presents a digitisor based on the equidistant sampling impulsions which can be connected to the JNM 3H—60 spectrometer. Fig. 1 shows the functioning principles sketch.

The C 520 D integrated circuit is the basic component. This chip makes an analogue digital conversion BCD with a parallel output multiplexed on three digits.

A numerical display can be directly connected, or a TTL computer interface can be used.

The automatical sampling of the signals can be achieved using the internal clock generator. The conversion is done at every 5 ms.

The circuit can also receive external impulsions either from a separate clock generator or from the computer clock generator.

The sweep time of the magnetic field of the spectrometer takes some minutes. In this case the conversion speed of the convertor is convenient.

The RMN absorbtion signals are broad and do not register sudden variations. Thus the risk of not recording the pointed edges of the signals is minimal. The above are true both for the homogeneous field and for he NMR field gradients.

There still is the risk to digitalize the noise of the signals because the convertor has no noise filters. The noise can be reduced using the spectrum accumulation method

High frequency components of the Fourier transform appear due to the noises. These can be eliminated, using an adequate filtering during the computation process.

Conclusions. In this paper general theoretical and practical aspects of the sampling of the signals, applied to the RMN spectroscopy were analized. The advantages and disadvantages of the above method, according to most recent studies were discussed. A concrete principle sketch of the digital processing or the signal, adaptable to the JNM 3H—60 spectrometer was presented.

It is estimated that the use of this digital method will lead to a rise in the spectrometre resolution both in homogeneous magnetic field and gradient magnetic field.

REFERENCES

1. P. C. Lauterbur, C. M. Lai, *IEEE Trans. Nucl Sci.*, vol NS—27, 3 (1980).
2. P. Mansfield, P. C. Morrsi, *NMR imaging in biomedicine*, Academic Press, 1982.
3. P. Bottomeley, *Rev. Sci. Instrum.*, 53 (9), 1982
4. Al. Nicula, S Aştilean, M. Todică, *Studia-Physica*, 1 (1988).
5. Richard W. Quine, G. R. Eaton, S. Eaton, *Journal of Magn. Reson*, 66, 164—167 (1986).
6. P. H. Oksman, M. E. S. Komv, E. K. Koivula, M Punkkinen, *Annales Academiae Scientiarum Fennicae, VI Physica*, 428, Helsinki 1981.
7. P. Hornak, J. K. Mosacki, D. J. Schneider, J. H Freck, *J. Chem. Phys.*, 84 (6) 1986.
8. Max J., *Traitement du signal*, Masson (1972) Paris.
9. Tomasz Daniel, *These*, Universite de Paris-Sud, 1985.

STUDIA UNIV BABEŞ-BOLYAI, PHYSICA, XXXIII, 2, 1988

DETERMINATION OF SOME STRUCTURAL MAGNITUDES FROM ULTRASONIC MEASUREMENTS IN BINARY LIQUID SYSTEMS

I. LENART*, A. CIUPE*, D. AUSLANDER*, and E. LENDER*

Received. July 1, 1988

ABSTRACT. — Some properties of the systems benzene-i-propanol, and benzene-butanol are studied in the whole concentration range at the temperature of 20°C Measurements of ultrasonic velocity and absorption by attenuation of the ultrasound, of density and dynamic viscosity were made From experimental data, the relaxation absorption, the volume viscosity, the activation energies corresponding to the dynamic viscosity, the relaxation frequencies, the available volumes, the vaporisation energies, as well as the excess quantities which evidence the presence of interactions between molecules of the components of the studied systems were calculated

Introduction. The propagation of the ultrasound in a liquid is accompanied by the dissipation in the environment of a part of the acoustic energy as a result of the effects of dynamic viscosity, thermal conductibility, as well as the relaxation processes, characterizes by aditivity properties [1], [2]

Summing up the first two effects, where the prevailing part is due to the viscosity absorption, represents the classical absorption described by Stokes-Kirchhoff's laws Reduced thermal conductibility of the studied liquids allows neglecting the corresponding absorption term as compared to that of viscosity, thus resulting.

$$\frac{\alpha_V}{f^2} = \frac{8\pi^2}{3\rho v^3}\eta \tag{1}$$

A considerable part of the acoustic energy is dissipated through the molecular processes of thermal, respectively structural relaxation. As a result, the experimental value of the attenuation constant, for most liquids, is much higher than that calculated by relation (1) The inclusion of the relaxation terms allowed to establish the relation.

$$\frac{\alpha_{exp}}{f^2} = \frac{\alpha_V}{f^2} + \frac{\alpha_{rel}}{f^2} = \frac{2\pi^2}{\rho v^3}\left(\frac{4}{3}\eta + \eta_V\right) \tag{2}$$

where: α_{exp} represents the experimental attenuation, α_V the viscosity attenuation, α_{rel} the relaxation attenuation constant respectively, f is the ultrasonic frequency, ρ the density, η_V the dynamic viscosity coefficient, η the volumic viscosity coefficient of the liquid, and v the ultrasonic propagation velocity.

Material and Method. In the mixtures benzene-i-propanol and benzene-butanol the ultrasonic propagation velocity was measured, using an optical installation of diffraction The attenuation constant was determined by an impulse method on the basis of repeated echoes at fixed distance,

* *University of Cluj-Napoca, Faculty of Mathematics and Physics, 3100 Cluj-Napoca, Romania*

at the 8 MHz frequency The density of the mixtures by the picnometric method, and the dynamic viscosity by means of the Höppler viscosimeter were also measured

All determinations were made under constant temperature conditions of 20 °C

By means of the obtained data the classical attenuation constant (1), that of relaxation (2), and the volumic viscosity were calculated

On the basis of Eyring's celular model [3]

$$\eta = \frac{N h}{V} e^{W/RT} \tag{3}$$

where η is the dynamic viscosity, h — Planck's constant, N — Avogadro's number, W — activation energy of viscous flow per mole of liquid, R — the universal constant of gases, the activation energies of the studied systems were calculated as well

There have also been evaluated the relaxation frequencies of viscosity by means of the relation

$$f = \frac{1}{2\pi\beta_{ad}(2\eta + \eta_V)}$$

where $\beta_{ad} = 1/\rho v^2$

Results. The variation of the ultrasonic velocities and of the adiabatic compressibility with the alcohol concentration in the mixture is presented in Fig 1 The behaviour of the two mixtures is analogous, noticing the superior value of the compresibility, respectively, the inferior one of the velocity into the benzene-1-propanol system.

From the velocity data the available volume was calculated $V_a = V\left(1 - \frac{v}{v_\infty}\right)$ where $v_\infty = 1600$ m/s, its dependence on concentration, presented in Fig 2, illustration for both mixtures positive deviation from ideality, more pronounced in the case of the system benzene-1-propanol These excesses of the available volume are determined by the interactions among the molecules of the components, concomitantly with affecting the equilibrium of the alcohol structure

The attenuation constants calculated by the relation (1) and the experimental ones are given in Fig. 3.

It has been ascertained that the values of α_{exp}/f^2 are much higher than those of α_V/f^2 with a different dependence on concentration Thus, while α_V/f^2 slowly increases with the alcohol concentration, α_{exp}/f^2 strongly decreases in the smaller alcohol concentration ranges, tending to a certain level at high concentrations

The arranging according to the type of the alcohol in the mixture is of opposite direction for α_{exp}/f^2 and α_V/f^2 The decreasing of the relaxation absorption in the direction benzene to alcohol according to the graph of Fig. 4 is due to the variation in the opposite direction of the intensity of the intermolecular interactions of the two components, the first one nonpolar, the second one polar.

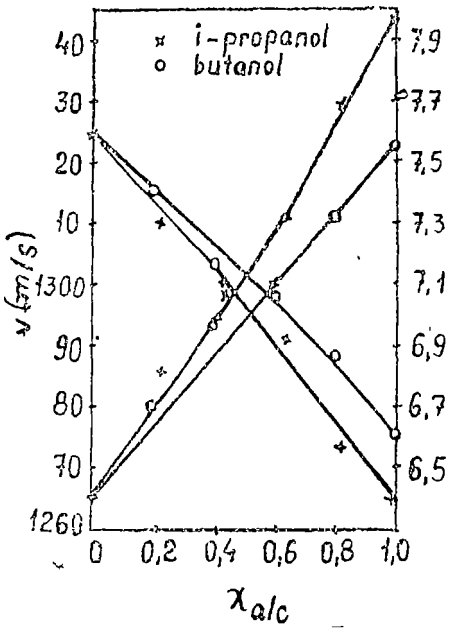

Fig. 1

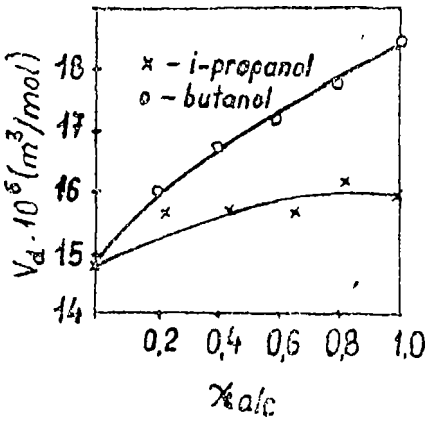

Fig. 2

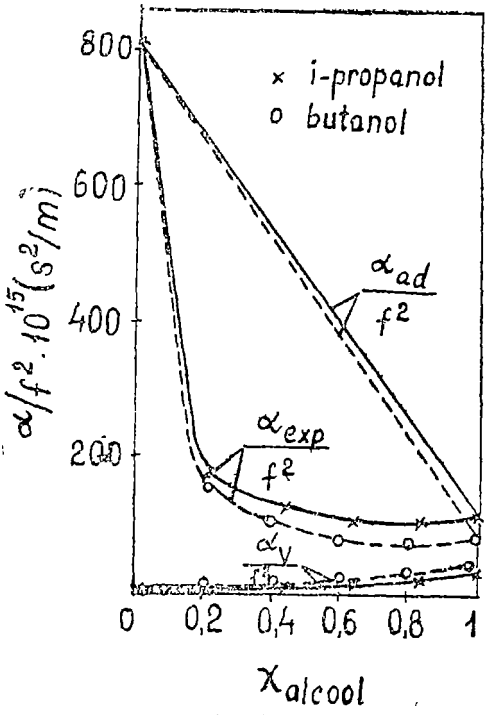

Fig. 3

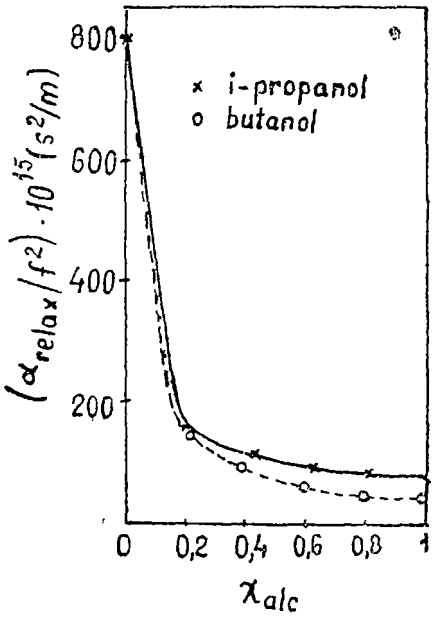

Fig. 4

The negative deviations from aditivity illustrated in Fig. 5 have at the origin the presence of certain interactions among the molecules of the mixture components This type of interaction appears at low alcohol concentrations as a result of the breaking of the hydrogen bonds between the alcohol molecules, followed by the progressive decreasing of the bonds number of the type polar — nonpolar on the advantage over those of the type polar — polar

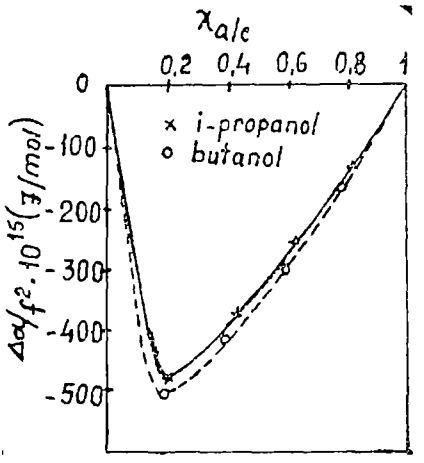

Fig 5

Fig 6 comprises the volume viscosity variation of the mixtures with alcohol concentration, and Fig. 7 — the concentration dependence of the activation energy of the viscous flow

The relaxation frequencies are presented in Table 1 Of the order of GHz, the frequencies increase in the mixtures from benzene towards alcohols along certain curves having maxima situated in the high alcohol concentration ranges.

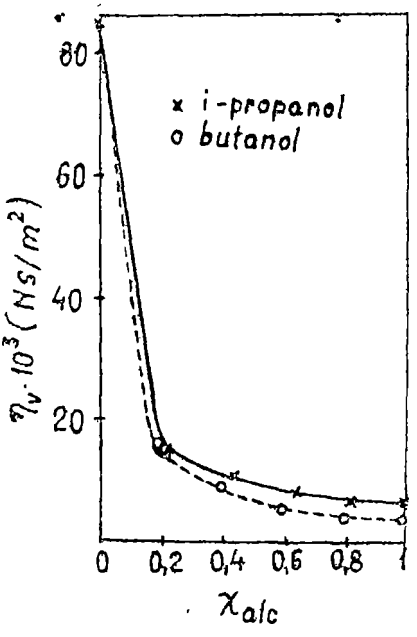

Fig. 6

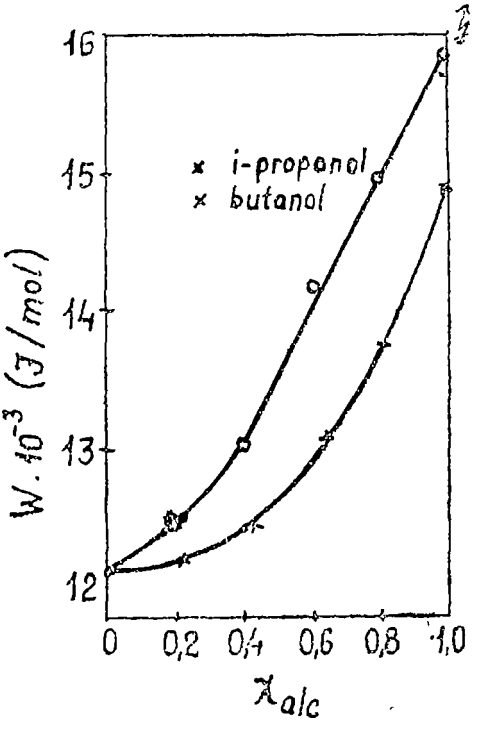

Fig. 7

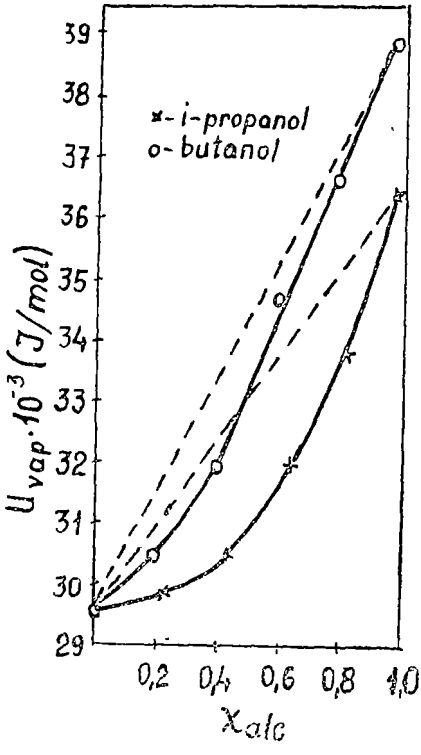

Fig 8

Table 1

$\chi_{i\text{-propanol}}$	f[GHz]	$\alpha_{butanol}$	f[GHz]
0	2 88	0	2 88
0 224	14 74	0 196	13 99
0 435	18 78	0 394	21 47
0 636	21 71	0 594	27 49
0 822	21 78	0 796	27 28
1	18 15	1	23 02

The intermolecular interaction changes due to concentration emphosised by means of the excesses of the presented, molecular-acoustic magnitudes, can be checked by means of the vaporization energy values calculated from the activation energy of the viscous flow [4], [5], [6].

For the pure components from the two types of mixtures the obtained values are presented in Table 2, comparatively with the experimental data from the literature, and with those obtained by means of Trouton's rule, respectively

The low values in the last column, corresponding to the alcohols are caused by their structure, characterized by hydrogen bonds. As concerning the differences between the vaporization energies calculated from the activation energy, and the experimental ones we consider that they can be assigned to the used value of the constant, discussed in the literature [7].

Table 2

Substance	T_f [K]	Vaporization Energy [J/mol]		
		From activation energy	Experimental data	From Trouton's rule
benzene	353.35	29597 1	30723	27612 2
i-propanol	355 15	36523 4	40420 6	27756 7
n-butanol	390 15	38933 2	43764 6	30492 2

The vaporization energy — concentration curves calculated from the activation energy of flow, are presented in Fig 8.

The agreement with the former results concerning the intermolecular interactions in the system can be noticed In mixtures, especially at not too high concentrations of alcohol, the appearace of the polar — nonpolar interactions affect the interactions among the alcohol molecules. This effect, prevailing in i-propanol, leads to the weakening of the mixture's intermolecular forces as a whole.

REFERENCES

1 J Ambrus, H Dardy, C Moynihan, *J Phys Chem*, **76, 23,** 3495 (1972)
2 V S Kononenko, *Akusticeskii jurnal*, Tom XXII, 1, 688 (1987)
3 M Solomon, Viscozimetrie şi elemente de teorie a viscozităţii", Editura Tehnică, Bucureşti (1958)
4 D V S Jain, A Pethrick, *Trans Farad Soc*, **70,** 1293 (1974)
5 R K Nigam, B S Mahl, *Ind J Chem*, **9,** 1255 (1971)
6 K Ram Moorthy, *Ind J Pure & Appl Phys*, **11,** 554 (1973)
7 Ram Lakhan Mishra, „Some Acoustical & Thermodynamic Parameters", *Ph D Thesis*, Allahabad, India (1977)

STUDIA UNIV BABEŞ-BOLYAI, PHYSICA, XXXIII, 2, 1988

THE RELATIVISTIC ACCELERATION PRODUCED BY A ROTATIONLESS, ELECTRICALLY CHARGED, SPHERICAL, CENTRAL BODY ON AN OUTER MATERIAL POINT WITHOUT ELECTRICAL CHARGE

HUBA SASS*

Received July 4, 1988

ABSTRACT. — The paper points out the existence of a force produced by an electrical charge on a chargeless body The expression of this force is determined This force is shown to be capable of playing an important part in determining the inner structure of some elementary particles, as for instance the electron

In the frame of the General Relativity Theory, the knowledge of the spacetime metric also means the knowledge of the motion laws The metric of the spacetime outside a spherically symmetrical central body can be written in generalized spherical coordinates as follows [2]·

$$ds^2 = g_{00}(dx^0)^2 + g_{11}(dx^1)^2 + g_{22}(dx^2)^2 + g_{33}(dx^3)^2, \tag{1}$$

where x^0 is the temporal coordinate, while $x^1 = r$, $x^2 = \theta$, $x^3 = \varphi$ are the space spherical coordinates.

The fundamental metric tensor g_{ij} depends only on the radial coordinate r We shall use, as habitually, the geometrized quantities

$$\begin{aligned} l &= l_{ph} \ \text{(cm)}, \\ t &= ct_{ph} \ \text{(cm)}, \\ v &= v_{ph}/c \ \text{(dimensionless)}, \\ m &= (G/c^2)M_{ph} \ \text{(cm)}, \\ Q &= (G^{1/2}/c^2)Q_{ph} \ \text{(cm)}, \\ a &= a_{ph}/c^2 \ \text{(cm}^{-1}\text{)}, \end{aligned} \tag{2}$$

where c = speed of light, G = constant of gravitation, while the index ph signifies that the length, l, the time t, the velocity v, the mass M, the electrical charge Q and the acceleration a are measured in physical units

The three-dimensional components of the acceleration, in geometrized units, are [3]:

$$a^i = -\Gamma^i_{00}/g_{00}, \qquad i = \overline{1, 3}, \tag{3}$$

* *Industrial Secondary School No 4, 4800 Baia Mare, Romania*

and the module of the acceleration is·

$$a = (a^i a^j \gamma_{ij})^{1/2}, \tag{4}$$

where:

$$\gamma_{ij} = -g_{ij} + g_{0i}g_{0j}/g_{00}, \qquad i,j = \overline{1,3}, \tag{5}$$

are the components of the three-dimensional metric tensor, and

$$\Gamma^l_{nk} = g^{lm}(g_{mk,n} + g_{nm,k} - g_{kn,ri})/2 \tag{6}$$

are Christoffel's symbols of the second kind [3].

In our case, only the components·

$$\gamma_{11} = -g_{11}, \quad \gamma_{22} = -g_{22}, \qquad \gamma_{33} = -g_{33} \tag{7}$$

are nonzero; hence:

$$\Gamma^1_{00} = -g_{00,1}/(2g_{11}) \tag{8}$$

From (3) and (8) we obtain the geometrized components of the acceleration:

$$\begin{aligned} a^1 &= a^r = (g_{00,1}/g_{00})/(2g_{11}), \\ a^2 &= a^\theta = 0, \\ a^3 &= a^\varphi = 0, \end{aligned} \tag{9}$$

and the module of this one:

$$a = (a^r a^r \gamma_{11})^{1/2} = (-g_{11})^{-1/2}|g_{00,1}/g_{00}|/2 \tag{10}$$

Consider now a rotationless, spherical, central body of mass m, radius R and electrical charge Q Outside such a body ($r \geqslant R$) the spacetime is featured by the Reissner-Nordström metric [1]

$$\begin{aligned} ds^2 = (1 - 2m/r + Q^2/r^2)dt^2 - (1 - 2m/r + Q^2/r^2)^{-1}dr^2 - \\ -r^2(d\theta^2 + \sin^2\theta\, d\varphi^2), \end{aligned} \tag{11}$$

where:

$$\begin{aligned} g_{00} &= 1 - 2m/r + Q^2/r^2, \\ g_{11} &= -1/g_{00}. \end{aligned} \tag{12}$$

From (9) and (10) it results:

$$a^1 = -g_{00,1}/2 = -(\partial g_{00}/\partial r)/2 \tag{13}$$

and:

$$a = |a^1|(g_{00})^{-1/2}. \tag{14}$$

Replacing g_{c0} from (12), we obtain

$$a^r = -m/r^2 + Q^2/r^3 \tag{15}$$

and

$$a = |-m/r^2 + Q^2/r^3|(1 - 2m/r + Q^2/r^2)^{-1/2} \tag{16}$$

Since a^r from (15) and a from (16) are expressed in geometrized units, we shall express them in physical units, but omitting this time the index *ph* Therefore, *in physical units*, the components of the acceleration outside the body will be

$$\begin{aligned} a^r &= -GM/r^2 + GQ^2/(c^2r^3), \\ a^\theta &= 0, \\ a^\varphi &= 0, \end{aligned} \tag{17}$$

and the module of the acceleration

$$\begin{aligned} a = |-GM/r^2 + GQ^2/(c^2r^3)|(1 - 2GM/(c^2r) + \\ + GQ^2/(c^4r^2))^{-1/2}. \end{aligned} \tag{18}$$

If the body is not electrically charged, the above formulae become respectively

$$a^r = -GM/r^2, \tag{17'}$$

$$a = (GM/r^2)(1 - 2GM/(c^2r))^{-1/2}. \tag{18'}$$

Introducing a characteristic radius

$$r_0 = Q^2/(c^2M) \tag{19}$$

and denoting

$$r = r_0x, \tag{20}$$

then

$$a^r = (GM/r_0^2)(1 - x)/x^3, \tag{21}$$

and x represents the distance from the centre of the body, in units of characteristic radius

The function $a^r = a^r(x)$ is plotted in Fig 1. One sees that inside the sphere of radius r_0 ($R < r < r_0$) the acceleration is positive, hence there exists a repulsive force which acts on a chargeless material point. Outside this sphere ($r > r_0$) the acceleration is negative, then there will exist an attractive force On the surface of the sphere of radius r_0 the acceleration is zero (from both outside and inside), hence the substance will tend to accumulate on this surface

It is interesting to observe that if we consider a body having the mass m_e of the electron and the charge e of this one, then one obtains for r_0

$$r_0 = e^2/(c^2m_e), \tag{22}$$

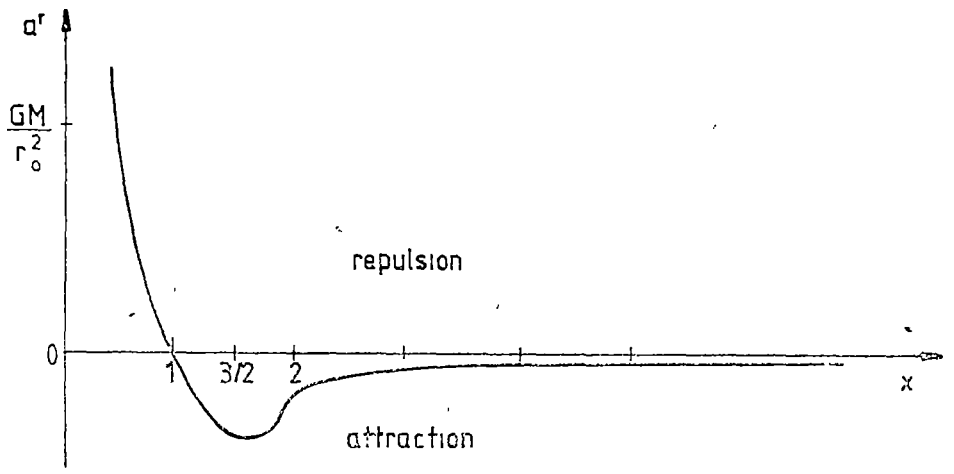

Fig 1

that is just the classical radius of the electron Also for a (the module of the acceleration measured in the point x)

$$a = (Gm_e/r_0^2)|(1 - x)/x^3|(x^2 - 2\alpha x + \alpha)^{-1/2}, \tag{23}$$

where $\alpha = Gm_e^2/e^2 = 2\,4 \quad 10^{-43}$ and $Gm_e/r_0^2 = 7\,65 \cdot 10^{-10}$ cm/s^2.

Since α is very small, the relativistic effect of spacetime curvature is negligible Obviously, at a macroscopic scale ($x \gg 1$), the quantity

$$a_Q = GQ^2/(c^2r^3) \tag{24}$$

is negligible as against

$$g = -GM/r^2, \tag{25}$$

but it is different for elementary particles

REFERENCES

1 Lang, K R , *Astronomical Formulae,* Vol 2, „Mir" Publ House, Moscow, 1978 (Russ)
2 Sass, I H A , *The Space-Time Metric and the Quadrivelocity inside a Rotating Relativistic Body,* Babeş—Bolyai Univ , Fac Math Res, Sem Preprint 2 (1985), 89—104
3 Zeldovich, Ya B , Novikov, I D , *Stars and Relativity,* University of Chicago Press, Chicago, London, 1971

STUDIA UNIV BABEŞ-BOLYAI, PHYSICA, XXXIII, 2, 1988

SOLAR FLARE INFLUENCE ON THE LOW IONOSPHERE

GEZA SZÖCS*, ALEXNDRU NICULA** and HUBA SZÖCS***

Received July 4, 1988

ABSTRACT. — An analysis of the correlation between the solar activity (during 1969) and the ionospheric disturbances is performed The variations (especially the sudden ones) of the solar activity are superposed on a roughly constant level of the ionization factors (UV, X and gamma radiation, respectively the corpuscular radiation) due to the galactic and solar radiation („quiet Sun") The study of such variations constitutes a contribution to the attempts at clearing up the very complex phenomena featuring the magnetosphere and the ionosphere, generally the atmosphere

1 **Introduction.** The state of the ionosphere can be featured directly by the ionic and electronic concentration, and indirectly by various physical parameters depending on them. attenuation of the electromagnetic waves, critical frequency, limit frequency, real or virtual height of the ionospheric layers (in the case of the ordinary component) for vertical or skew incidence, etc.

The state of the "quiet" ionosphere is determined by the permanent ionizing agents, as the galactic radiation and the solar one: EUV, X, gamma and corpuscular (fluxes of protons, electrons or other particles). During the cosmic (less frequent) and solar (more frequent) events, the ionosphere is strongly disturbed, with negative effects on radiocommunications and biological phenomena

2. **Solar Flare Effects.** Taking into account the sudden growth of the level of the electromagnetic and corpuscular radiation, the effects of the solar flares on the ionosphere are various. So, the group of the sudden ionospheric disturbances (SID) contains

a) the sudden growth of the atmospheric radio noise on 27 kHz (SEA), as a consequence of the superposition of the LF and VLF waves generated by the permanent atmospheric discharges, therefore, the radio noise attenuation features the state of the low ionosphere;

b) the sudden variation of the phase altitude (SFA),

c) the sudden flares in the radiowave range (SRB — sudden radio burst, the disturbances in the microwave range SSWF, SCNA, SRB- "micro"), namely the sudden microwave emissions which disturb the radiocommunications in the range of decimetric, centimetric, millimetric and micrometric waves.

3. **Statistical Analysis of Solar Flare Effects between February — October 1969.** In order to perform such a study, we processed the data published in [1]. The number of the SEA, SFA and SRB solar flare effects during the considered period is given in Table 1.

* *Industrial Secondary School No 3, 4050 Tîrgu Secuiesc, Romania*
** *University of Cluj-Napoca, Faculty of Mathematics—Physics, 3100 Cluj-Napoca, Romania*
*** *Polytechnical Institute, Institute for Subengineers, 4800 Baia Mare, Romania*

Table 1

Month	Number of SEA	Number of SFA	Number of SRB
February (F)	15	25	24
March (M)	35	77	60
April (A)	17	22	18
May (M)	26	32	28
June (J)	27	32	27
July (J)	6	10	9
August (A)	15	22	22
September (S)	10	13	10
October (O)	16	23	19

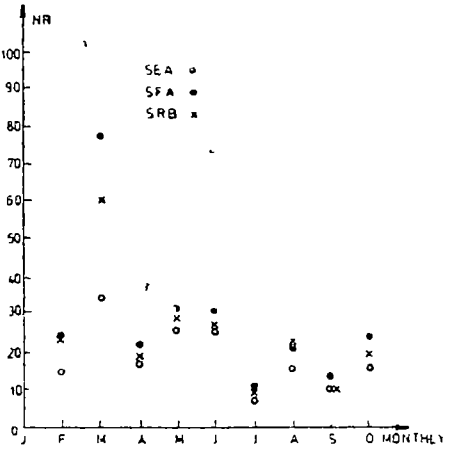

Fig 1

Figure 1, which plots the monthly variation of these numbers, points out a maximum in March and a minimum in July.

The close evolution of these effects can also be noticed (the SRB number interfering with SEA and SFA numbers, respectively). This situation is illustrated by the high values of the correlation coefficients ($r = 0.894$ for SEA—SFA, $r = 0{,}993$ for SFA—SRB) The total number of effects is $N = 167$ for SEA and $N = 256$ for SFA.

Table 2 lists for each considered month the total observation duration T_0 (in units of 100 minutes), the totalized duration of the effects T_e (in minutes) and the relative duration of these ones p (in units of 10 percents)

Table 2

Month	SEA T_0	SEA T_e	SEA p	SFA T_0	SFA T_e	SFA p
F	60	650	1.083	78	880	1 128
M	78	970	1 244	126	1995	1 583
A	66	650	0.982	84	541	0 644
M	96	860	0 896	96	1265	1 318
J	72	910	1 264	84	1225	1 458
J	24	170	0 708	42	435	1 036
A	48	405	0 844	72	715	0.993
S	60	340	0.567	66	585	0 886
O	78	555	0 712	78	765	0 981
	mean 9 5%			mean 11 5%		

Table 3

Month	SEA T_{min}	SEA T_{max}	SFA T_{min}	SFA T_{max}	SRB T_{min}	SRB T_{max}
F	15	115	10	120	1	165
M	15	80	10	110	1	216
A	20	60	10	70	3	47
M	20	60	15	85	2	124
J	20	50	20	125	1	315
J	20	45	20	105	2	170
A	10	45	15	70	3	134
S	20	50	25	75	7	82
O	20	60	10	130	3	146
mean	17 78	62 78	15 00	98 89	2.56	144 11

One notices that the relative monthly averages are small; however the importance of these effects can be significant, as Table 3 shows. This table contains for each month the minimum (T_{min}) and maximum (T_{max}) durations (in minutes).

The maximum duration of these effects can exceed 1 hour 115, 130 and 315 minutes for SEA, SFA and SRB, respectively (see Table 3) So, even if their relative durations are short as against the total observation duration, they are able to cause disturbances and even breakings of the radiocommunications (including radiotelephone and TV) for some hours.

In the international code, the intensity of the effect is featured by I (the index of importance), which takes the values 1, 2, 3 and 3+ (this last one being replaced by 4 in calculations). The boundary values (1 and 3+) represent respectively attenuation of less than 1 dB and more than 7 dB for SEA; variation of the phase altitude of less than 1 km and more than 7 km for SFA, very weak and very strong for SRB The value $I = 0$ which appears in some tables signifies the fact that the solar flare does not have effects in the ionosphere.

Table 4

Month	SEA T	SEA T_m	SEA I_m	SFA T	SFA T_m	SFA I_m
F	650	43 33	2 7 8	880	35 20	1 18
M	970	27 71	1 14	1995	25 90	1 10
A	650	38 24	0 94	541	24 60	0 86
M	860	33 07	0 92	1265	39 53	0 94
J	910	33 70	1 11	1225	38 28	0 94
J	170	28 33	1 00	435	43 50	0 50
A	405	27 00	0 53	715	32 50	0 23
S	340	34 00	1 40	585	45 00	0 85
O	555	34 69	0 94	765	33 26	1 39
mean	459 2	37 48	1 086	700 5	32 84	0 888

Table 5

Month	SEA $T_m - T_{m,m}$	SEA $I_m - I_{m,m}$	SFA $T_m - T_{m,m}$	SFA $I_m - I_{m,m}$
F	+5.85	+1 699	+2 36	+0 293
M	−9 77	+0 056	−6 94	+0 216
A	+0 65	−0 146	−8 24	−0.028
M	−4 41	−0.166	+6 74	+0 052
J	−3 78	+0 024	+5.44	+0 052
J	−9 15	−0 086	+10 66	−0 388
A	−10 84	−0 556	−0 34	−0 658
S	−3 48	+0 314	+12 16	−0 038
O	−2 79	−0 146	+0 42	+0.502

Table 4 contains the durations T of the effects (T_e of Table 2, in minutes), the mean monthly durations T_m (in minutes) and the mean monthly values I_m of the index of importance. Table 5 lists the deviations of T_m (in minutes) and I_m from the corresponding mean values (denoted by $T_{m,m}$ and $I_{m,m}$, respectively) calculated from the total number of cases Table 6 contains the deviations of T_e (in minutes) from the monthly mean value (denoted by $T_{m,mon}$).

Table 6

Month	SEA $T_e - T_{m,mon}$	SFA $T_e - T_{m,mon}$
F	+191	+180
M	+511	+1296
A	+191	−159
M	+401	+565
J	+451	+525
J	−289	−265
A	−54	+15
S	−119	−115
O	+96	+65

Figures 2 and 3 plot for SEA and SFA, respectively, for each month, the values T_m and I_m, together with their deviations from the corresponding mean values. Figures 4 and 5 plot for SEA and SFA, respectively, also for each month, the variations of the total duration of these effects and the respective deviations from the monthly average.

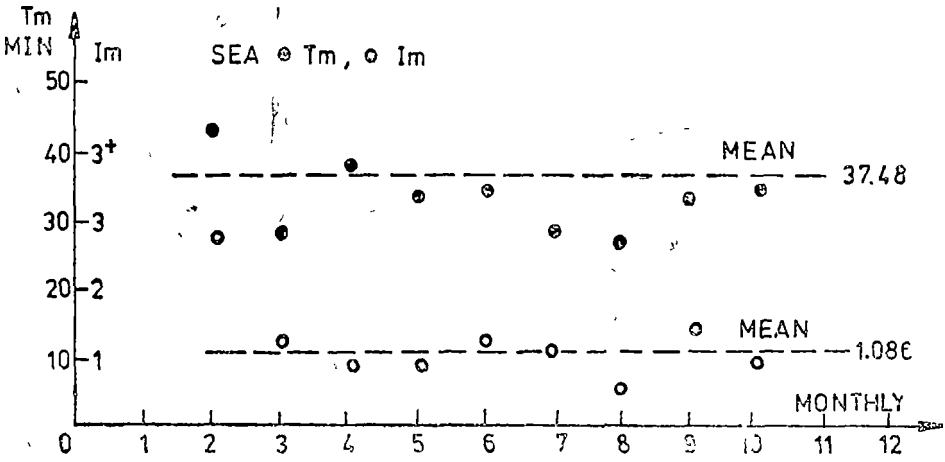

Fig 2

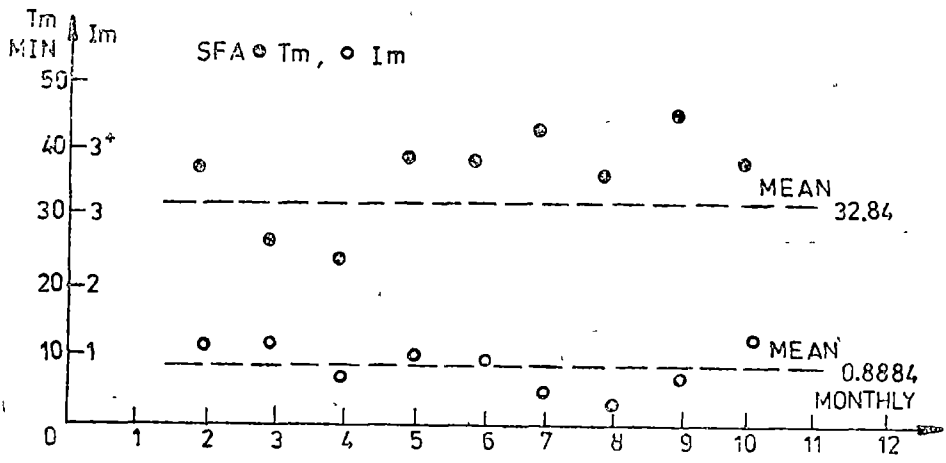

Fig 3

In order to estimate the correlation between the duration T (in minutes) and the index of importance I, Table 7 gives these values for February 1969. The duration of growth Δt (the time interval elapsed between the start of the effect and the maximum) is also listed (in minutes) in Table 7

For SEA (14 events, total duration 610 minutes), the average values are 10 143 minutes for Δt, 43 57 minutes for T, 2.785 for I. In the case of SFA (22 events, total duration 850 minutes), the average values are: 9 0 minutes for Δt, 38.64 minutes for T, 2 09 for I.

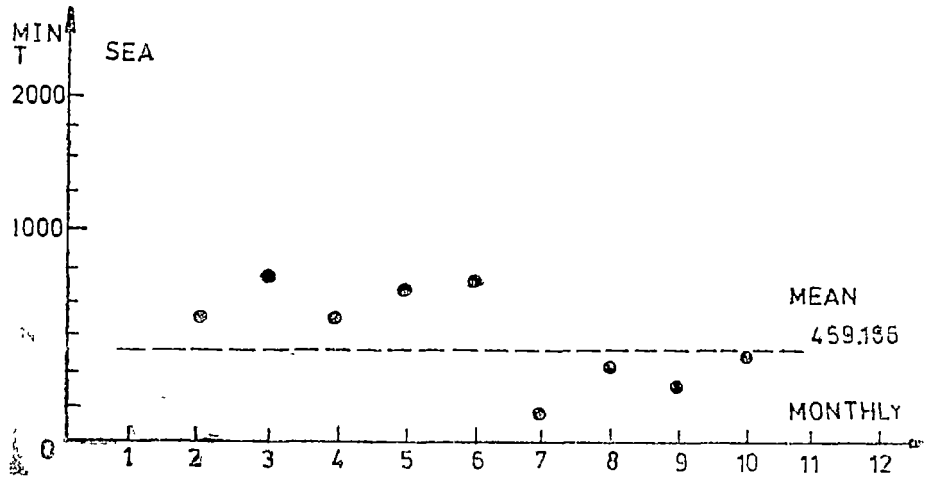

Fig 4

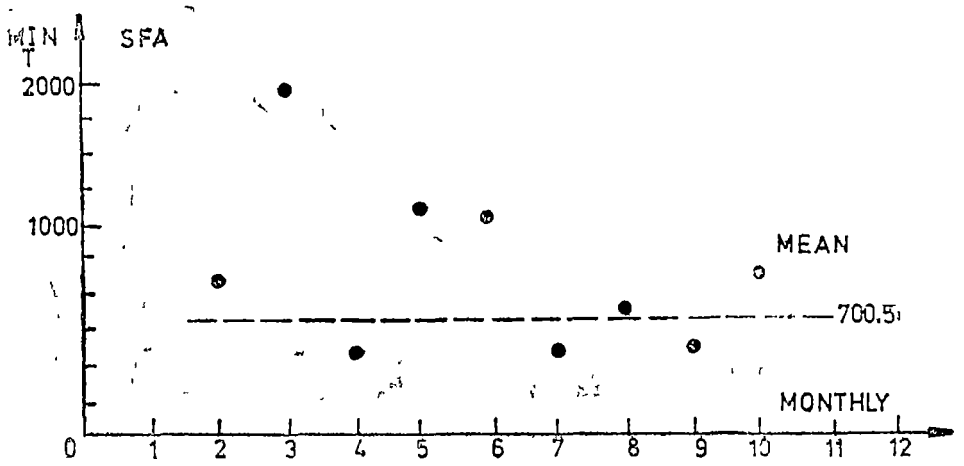

Fig. 5

Estimating the correlation coefficients between T and I, we obtained $r_{SEA} = 0.6924$, $r_{SFA} = 0\,8139$.

4. **Concluding Remarks.** We can formulate some conclusions.

(a) The high correlation coefficients ($r = 0\,894$ for SEA—SFA and $r = 0.993$ for SFA—SRB) point out the fact that these effects appear and act generally together, being associated. The VLF and VF waves are less affected (due to SEA and SFA), the VHF and UHW ones are more affected (due to SRB)

(b) Although the relative duration of these ones is small (9 5% for SEA, 11.54% for SFA), their influence on the radiocommunications can be signifi-

Table 7

SEA			SFA		
Δt	T	I	Δt	T	I
7	35	3	7	50	3
7	30	1	5	30	1
6	15	0	4	25	0
7	30	0	8	40	1
8	40	3	8	45	3
20	45	2	13	35	1
—	—	—	8	40	1
4	15	0	6	20	0
—	—	—	5	30	0
—	—	—	9	30	1
—	—	—	5	10	0
—	—	—	5	20	0
—	—	—	5	25	0
12	100	3	21	120	3+
—	—	—	10	20	0
7	20	0	5	20	0
—	—	—	4	15	0
9	30	3	10	30	3
18	40	3	19	60	2
17	115	3+	16	85	3+
10	35	1	12	55	1
17	60	2	15	45	1

cant if we take into account the long duration of these effects · the average values of T_{max} exceed 60 minutes for SEA and 90 minutes for SFA; the maxima are 115, 130 and 315 minutes (for SEA, SFA and SRB, respectively).

(c) The high correlation coefficients between T and I ($r = 0.6924$ for SEA, $r = 0\,8139$ for SFA) point out a very probably linear dependence between these quantities.

(d) Taking into account the fact that the sudden variation undergone by the level of the low frequency radio noise (27 kHz) and by the phase altitude (SEA and SFA, respectively) are strongly connected with the electronic and ionic concentration [2], the study of these ones shows the quantitative relations between the solar activity and the state of the ionosphere (especially the low ionosphere).

REFERENCES

1 * * * *Geophysikalische Beobachtungsergebnisse Geophysical Data Ionosphere, Atmospheric Noise Cosmic Rays, February—October 1969*, Heinrich Hertz Institut, DDR, Berlin.

2 S A Bowhill, *Review of Recent Progress in Ionospheric Research*, Space Research, XIII, Akademie—Verlag, Berlin, 1973, 423—433.

STUDIA UNIV BABEŞ-BOLYAI, PHYSICA, XXXIII, 2, 1988

REPULSIVE SPHERES AROUND STARS

VASILE MIOC*, ALEXANDRU V. POP* and IOACHIM GIURGIU**

Received July 4, 1988

ABSTRACT. — The paper deals with the motion of a solid grain in the neighbourhood of a star The case when the radiative force exceeds the gravitation is studied by using dimensionless variables The existence of a forbidden sphere around the star, which cannot be penetrated by the grain, is pointed out The radius of such a repulsive sphere is estimated in some concrete cases

1 **Introduction.** Using a simplified model (but constituting a good enough approximation), in the neighbourhood of a star a solid body is subject to two main forces the gravitational attractive force F_g and the repulsive force F_r due to the radiation pressure Of course, for large enough such bodies, F_r is generally negligible with respect to F_g, but if these bodies are sufficiently small their motion is significantly altered by F_r, which can, under certain conditions, exceed F_g In this paper we shall consider the motion of such a small body (*i e* a solid grain of water ice or dust), for which the ratio F_r/F_g is supraunitary in module

2. **Basic Equations.** Let us firstly remind a theorem from mechanics Consider two material points of masses m and M, $m \ll M$, and let $\vec{r}$ be the position vector of m with respect to M Let also $\vec{F}_g$ and $\vec{F}_r$ be two central forces of fixed point M, in whose field the point m is moving The force $\vec{F}_r$ is repulsive, while $\vec{F}_g$ is attractive If the following conditions are fulfilled

(i) $|\vec{F}_g| < |\vec{F}_r|$;
(ii) m approaches M with a finite initial speed,

then m and M cannot collide

Let now impose a new condition the two considered forces obey to an inverse square law The motion of m will be plane and featured by an equation of the form [2]

$$r - C^2/r^3 = -\mu/r^2, \tag{1}$$

written using modules, in which C is the constant angular momentum, while μ is called the effective gravitational parameter This is an abuse of terms, since the nature of the two forces was not specified, however, we shall keep the term "gravitational", because (1) has the same form as the motion equation in the well-known two body problem [3].

For $\mu > 0$, the problem is analogous to the standard Kepler problem, which is well studied Subsequently we shall deal only with the case $\mu \leqslant 0$ ($|F_r/F_g| \geqslant \geqslant 1$)

* *Centre for Astronomy and Space Sciences, 3400 Cluj-Napoca, Romania*
** *Industrial Secondary School, 3379 Baia de Arieş, Romania*

The case $\mu = 0$ is simple The two forces counteract each other and the resulting force is zero Therefore m will conserve its initial motion (or rest) with respect to M as in the absence of this mass

Let us now consider $\mu < 0$ For simplicity, we shall introduce two dimensionless variables

$$x = r/R, \tag{2}$$

where R is an arbitrary length, and

$$\tau = \imath R^{-3/2}\mu^{1/2}t, \tag{3}$$

which is a dimensionless time (here the factor $\imath = \sqrt{-1}$ was introduced in order to obtain real values for τ)

Consider that the motion of m is rectilinear In this case, its velocity $V = dr/dt$ will become with (2) and (3)

$$V = \imath R^{-1/2}\mu^{1/2}v, \tag{4}$$

where $v = dx/d\tau$ is the dimensionless velocity

With these considerations, the energy integral $V^2 = 2\mu/r + h$ (where $h =$ = energy constant) will acquire the dimensionless from

$$v^2 = -2/x + h', \tag{5}$$

where the dimensionless constant of energy h' has the expression

$$h' = v_i^2 + 2/x_i, \tag{6}$$

x_i and $v_i = (dx/d\tau)_i$ being the initial conditions

Consider x_f and v_f as being final values for x and v, respectively With (5) and (6) we can write

$$v_f^2 = v_i^2 + 2(1/x_i - 1/x_f) \tag{7}$$

3 **Repulsive Spheres.** It is clear from (7) that, if m moves away from M, we shall have $x_i < x_f$ and the final velocity will be higher than the initial one This fact is natural, since the repulsive force is dominant Obviously, the velocity cannot increase indefinitely, when x_f tends to infinity, $v_f^2 \to h'$ (which is finite)

Suppose now that m moves towards M Then $x_f < x_i$ and the final velocity will be lower than the initial one At limit, when m is coming from a very far region, $1/r_i \to 0$ and (7) becomes

$$x_f = 2/(v_i^2 - v_f^2) \tag{8}$$

One easily observes that if the final dimensionless radius vector reaches the value .

$$x_f = x_s \equiv 2/v_i^2, \tag{9}$$

then we have $v_f = 0$ This means that, whatever be its initial (finite) speed, m cannot approach M at a distance smaller than x_s

Let us see what happens later Let m be in the situation $x = x_s$, $v = 0$. We shall consider these values as initial conditions, replacing them in (7), we observe that m moves away indefinitely from M. When its distance tends to infinity, its speed tends to return to its primary value (but this time it is directed outward); we are in the first case considered in this section.

In conclusion, there exists around M a sphere of dimensionless radius x_s, given by (9), and m cannot get into this sphere In our conditions, the frontier of the field of the resulting force acts like an elastic barrier m is gradually slowed down; it stops at the distance x_s, then is thrown backwards with a monotonically increasing speed and cannot return

4. **Circumstellar Forbidden Spheres.** Let the central body be a star of mass M, radius R and luminosity L Let the other body be a homogeneous, spherical grain of radius r', density ς and mass m, with constant albedo, moving in the neighbourhood of the star. Then the attractive gravitational force will be:

$$F_g = -GMm/r^2, \tag{10}$$

and the repulsive radiative force will have the expression [4]:

$$F_r = (AL/(4\pi c))/r^2, \tag{11}$$

where G = gravitation constant, A = effective cross-sectional area of the grain, c = speed of light.

Thus the effective gravitational parameter will be

$$\mu = GM(1 - AL/(4\pi mcGM)). \tag{12}$$

The case $\mu > 0$ is mathematically modelled by the two body problem The case $\mu = 0$ is also clear: if the grain fulfils one of the following equivalent conditions (which lead to $\mu = 0$):

$$A/m = 4\pi cGM/L, \tag{13}$$

$$r'^2/m = 4cGM/L, \tag{13'}$$

$$r'\varsigma = 3L/(16\pi cGM), \tag{13''}$$

then it will keep its initial motion (or rest) with respect to the star

With (2), (4), (9) and (13''), the radius of the repulsive sphere becomes

$$r_s = 2GM(3L/(16\pi cGMr'\varsigma) - 1)/V_i^2, \tag{14}$$

where we identified the arbitrary distance R appearing in (2) with the radius of the star.

This result can be briefly stated as follows if a given spherical grain (defined by r' and ς) moves towards a given star (defined by M, L and R), and if the following conditions are fulfilled

(i) the grain is coming from infinity with an initial speed V_i;

(ii) $r'\varsigma < 3L/(16\pi cGM)$,

then there exists around the star a forbidden sphere whose radius r_s is given by (14), and the grain cannot penetrate inside. If the supplementary condition

$r_s > R$ $(x_1 > 1)$ is also fulfilled, the grain cannot reach the star Obviously, r_s (for a given star) will differ for different grains (according to their dimensions and densities)

If we denote by $F_{g,0}$ and $F_{r,0}$ the values of F_g and F_r, respectively, at the surface of the star, (14) can also be written in the from (see [1])

$$r_s = 2(F_{g,0} + F_{r,0})(R/V_t)^2/m \tag{15}$$

5 **Numerical Estimate.** We performed a numerical application in the case of a spherical grain with $r' = 10^{-5}$ cm, $\varsigma = 3\,4$ g/cm^3 (silicate), $V_t = 20$ km/s. Considering four representative concrete stars, we obtained the following values of r_s

Star	$M/M_\odot$	$L/L_\odot$	R (km)	r_s (km)
α Sco	19	34 000	$3\,69 \quad 10^8$	$3\,8 \quad 10^{13}$
α Boo	4 2	130	$1\,81 \quad 10^7$	$1\,4 \quad 10^{11}$
α CMa	3 3	61	$1\,67 \quad 10^6$	$6\,6 \quad 10^{10}$
Sun	1	1	$6\,96 \cdot 10^5$	$4\,6 \quad 10^8$

For the Sun we considered $M_\odot = 1\,989 \quad 10^{33}$g, $L_\odot = 3\,826 \quad 10^{33}$ cm^2 g/s^3. One sees that a grain with the above features can get into the inner planetary region of our solar system

REFERENCES

1 Dufay, J, *Nébuleuses galactiques et matière interstellaire*, Albin Michel, Paris, 1954
2 Mioc, V, Pál, A, Giurgiu, I, *Orbital Motion with Periodically Changing Gravitational Parameter*, Studia Univ Babeş–Bolyai, **33** (1988) (to appear)
3 Moulton, F R, *An Introduction to Celestial Mechanics*, 13-th ed, Macmillan, New York, 1959
4 Saslaw, W C, *Motion around a Source whose Luminosity Changes*, Astrophys, J, **226** (1978), 240–252

STUDIA UNIV BABEŞ-BOLYAI, PHYSICA, XXXIII, 2, 1988

ON THE DIRECT CONNEXION FUNCTIONS OF A DYNAMIC SYSTEM ACCELERATIONS

CONSTANTIN TUDOSIE*

Received March 30, 1987

ABSTRACT. — An approximate method is given for calculating the higher order accelerations of a dynamic system The method consists in using some unknown functions, of the time variable, called „direct connexion functions"

Introduction. The higher order accelerations appear directly in the study of all phenomena whose variation in time is very fast The differential equations describing the dynamism of these phenomena become more and more complicated as the more one attempts to catch the phenomenon in all its complexity. Their resolution implies special mathematical methods of investigation, the result of which leads to new and superior orientations in the field of technical creation.

As an example the third order acceleration is given (considering velocity as first order acceleration), which appears in the vertical vibrations of autotrucks and tractors [3], supported without danger by the drivers of these vehicles, on condition it does not exceed a certain admissible value.

Such accelerations also appear when fast passenger trains pass through curves. That is why projecting and constructing railway curves cannot lack knowledge of these accelerations

In this paper an approximate method is given for calculating higher order accelerations of a dynamic system. The method consists in introducing some unknown functions, of t time variable, called "direct connexion functions"

Description of the Method. Let us consider, in general, the differential equation of a dynamic system

$$\sum_{i=0}^{n} a_i(t)\overset{(i)}{x} = f(t), \tag{1}$$

with the initial conditions $\overset{(\sigma)}{x}(0) = \overset{(\sigma)}{x}_0$, $(\sigma = 0, 1, 2, \ldots, n-1)$, assuming the functions $a_i, f \in C[0, a]$, $a > 0$.

By introducing the "direct connexion functions" $\varepsilon_{i,0}(t)$, we have the relation

$$\overset{(i)}{x} = \varepsilon_{i,0}\, x, \quad (i = 0, 1, 2, \ldots, n), \quad (\varepsilon_{0,0} = 1), \tag{2}$$

and equation (1) becomes

$$x \sum_{i=0}^{n} a_i(t)\varepsilon_{i,0}(t) = f(t). \tag{3}$$

*Polytechnical Institute of Cluj-Napoca, 3400 Cluj-Napoca, Romania

By integrating equation (2), for $i = 1$, it follows

$$x = x_0 \exp\left[\int_0^t \varepsilon_{1,0}(s)ds\right], \tag{4}$$

and substituting in (3), one obtains

$$x_0 \exp\left[\int_0^t \varepsilon_{1,0}(s)ds\right]\left[a_0(t) + \sum_{i=1}^{n} a_i(t) \quad \varepsilon_{i,0}(t)\right] = f(t) \tag{5}$$

By introducing the "direct connexion functions" $\varepsilon_{i,i-1}(t)$, $(i=1, 2, 3, \quad ., n)$, we have the relations

$\dot{x} = \varepsilon_{1,0}\ x$, $\ddot{x} = \varepsilon_{2,1}\ \dot{x}$, . ., $\overset{(n)}{x} = \varepsilon_{n,n-1}\ \overset{(n-1)}{x}$, obtaining, for $n = i$, the expression

$$\overset{(i)}{x} = \varepsilon_{i,i-1}\ \varepsilon_{i-1,i-2} \quad . \quad \varepsilon_{3,2}\ \varepsilon_{2,1}\ \varepsilon_{1,0}\ x \tag{6}$$

By noting

$$\prod_{\sigma=1}^{i} \varepsilon_{\sigma,\sigma-1} = \varepsilon_{1,0}\ \varepsilon_{2,1}\ \varepsilon_{3,2} \quad . \quad \varepsilon_{i-1,i-2}\ \varepsilon_{i,i-1}, \tag{7}$$

relation (6) is written

$$\overset{(i)}{x} = \prod_{\sigma=1}^{i} \varepsilon_{\sigma,\sigma-1}\ x. \tag{8}$$

From (2) and (8) it follows

$$\varepsilon_{i,0} = \prod_{\sigma=1}^{i} \varepsilon_{\sigma,\sigma-1} \tag{9}$$

By making use of (9), equation (5) becomes

$$x_0 \exp\left[\int_0^t \varepsilon_{1,0}(s)ds\right]\left[a_0(t) + \sum_{i=1}^{n} a_i(t) \prod_{\sigma=1}^{i} \varepsilon_{\sigma,\sigma-1}(t)\right] = f(t) \tag{10}$$

By generalizing relation (4), we have

$$\overset{(i-1)}{x} = \overset{(i-1)}{x_0} \exp\left[\int_0^t \varepsilon_{i,i-1}(s)ds\right],$$

and substituting it in expression

$$\overset{(i)}{x} = \varepsilon_{i,i-1} \cdot \overset{(i-1)}{x},$$

one obtains

$$\overset{(i)}{x} = \overset{(i-1)}{x_0}\ \varepsilon_{i,i-1}(t)\exp\left[\int_0^t \varepsilon_{i,i-1}(s)ds\right], \tag{11}$$

$$(i = 1, 2, 3, \quad , n)$$

From (4), (8) and (11) it results

$$x_0 \prod_{\sigma=1}^{i} \varepsilon_{\sigma,\sigma-1}(t)\exp\left[\int_0^t \varepsilon_{1,0}(s)ds\right] -$$

$$-\overset{(i-1)}{x_0}\ \varepsilon_{i,i-1}(t)\exp\left[\int_0^t \varepsilon_{i,i-1}(s)ds\right] = 0, \tag{12}$$

$$(i = 1, 2, 3, \quad , n)$$

By observing that $\varepsilon_{i,i-1} \neq 0$, for $\sigma = i$, expression (12) becomes

$$x_0 \prod_{\sigma=1}^{i-1} \varepsilon_{\sigma,\sigma-1}(t)\exp\left[\int_0^t \varepsilon_{1,0}(s)ds\right] -$$

$$-\overset{(i-1)}{x_0}\exp\left[\int_0^t \varepsilon_{i,i-1}(s)ds\right] = 0, \tag{13}$$

$$(i = 2, 3, \ldots, n)$$

Expressions (10), (4), (11) and (13) make up a system(A) of $2n + 1$ equations with $2n + 1$ unknown values

$$\overset{(i)}{x}(t),\ (i = 0, 1, 2, \quad , n),\ \varepsilon_{\sigma,\sigma-1}(t),\ (\sigma = 1, 2, \quad , n)$$

Determination of system (A) solution. The approximate solution of system (A) is determined by a method of numerical integration We apply on the interval $[0, a]$, $a > 0$, a method analogous to that of polygonal lines We divide the interval $[0, a]$ by the points $t_k = k\frac{a}{m}$, $k = \overline{1, m}$, and we consider the quadrature formula

$$\int_0^{k\frac{a}{m}} f(x)dx \approx \frac{a}{m}\sum_{\nu=1}^{k} f\left(\nu\frac{a}{m}\right), \tag{14}$$

$$(k = 1, 2, \quad , m)$$

Writing that system (A) is verified for $t_k = k\frac{a}{m}$, and making use of formula (14) for the approximate calculation of integrals, we obtain a system of $m(2n+1)$ algebraic equations with $m(2n+1)$ unknown values

$$\begin{cases} x_0 \exp\left[\frac{a}{m}\sum_{\nu=1}^{k}\varepsilon_{1,0}\left(\nu\frac{a}{m}\right)\right]\left[a_0\left(k\frac{a}{m}\right)+\right. \\ \left.+\sum_{i=1}^{n}a_i\left(k\frac{a}{m}\right)\prod_{\sigma=1}^{i}\varepsilon_{\sigma,\sigma-1}\left(k\frac{a}{m}\right)\right]-f\left(k\frac{a}{m}\right)=0, \\ x\left(k\frac{a}{m}\right)-x_0\exp\left[\frac{a}{m}\sum_{\nu=1}^{k}\varepsilon_{1,0}\left(\nu\frac{a}{m}\right)\right]=0, \\ \overset{(i)}{x}\left(k\frac{a}{m}\right)-\overset{(i-1)}{x_0}\cdot\varepsilon_{i,i-1}\left(k\frac{a}{m}\right)\exp\left[\frac{a}{m}\sum_{\nu=1}^{k}\varepsilon_{i,i-1}\left(\nu\frac{a}{m}\right)\right]=0, \\ (i=1,\ 2,\ 3,\ \ldots,\ n), \\ x_0\prod_{\sigma=1}^{i-1}\varepsilon_{\sigma,\sigma-1}\left(k\frac{a}{m}\right)\exp\left[\frac{a}{m}\sum_{\nu=1}^{k}\varepsilon_{1,0}\left(\nu\frac{a}{m}\right)\right]- \\ -\overset{(i-1)}{x_0}\exp\left[\frac{a}{m}\sum_{\nu=1}^{k}\varepsilon_{i,i-1}\left(\nu\frac{a}{m}\right)\right]=0, \\ (i=2,\ 3,\ 4,\ \ldots,\ n) \end{cases} \tag{15}$$

The unknown values of system (15) are

$$\overset{(i)}{x}\left(k\frac{a}{m}\right),\ \varepsilon_{\sigma,\sigma-1}\left(k\frac{a}{m}\right),$$

$$(i=0,\ 1,\ 2,\ \ldots,\ n;\ \sigma=1,\ 2,\ 3,\ \ldots,\ n,\ k=1,\ 2,\ \ldots,\ m).$$

The values of functions $\varepsilon_{\sigma,\sigma-1}(t)$, for $t=0$, are determined with the relations

$$\varepsilon_{\sigma,\sigma-1}(0)=\overset{(\sigma)}{x_0}\left[\overset{\sigma-1}{x_0}\right]^{-1},\quad(\sigma=1,\ 2,\ 3,\ \ldots,\ n)$$

The value $\overset{(\sigma)}{x_0}$, for $\sigma=n$, results from (1)

$$\overset{(n)}{x_0}=[a_n(0)]^{-1}\left[f(0)-\sum_{i=0}^{n-1}a_i(0)\cdot\overset{(i)}{x_0}\right]$$

The variation diagrams of functions $\overset{(i)}{x}(t)$ and $\varepsilon_{\sigma,\sigma-1}(t)$, constructed by points, represent the approximate solution of system (A), on the interval $[0,\ a]$, $a>0$.

In numerical values, solution of system (15) is obtained by making use of the known methods [2].

REFERENCES

1 Buzdugan, Gh, Fetcu, L, Radeş, M, „Vibraţiile sistemelor mecanice", Editura Academiei Republicii Socialiste România, Bucureşti, 1975
2 Démidovitch, B, Maron, I, „Éléments de calcul numérique", Éditions Mir Moscou, 1973
3 Harris, C, M, Crede, C, E „Şocuri şi vibraţii", Vol III, Editura tehnică, Bucureşti, 1969
4 Tudosie, C, „Mecanică teoretică", Centrul de multiplicare al Institutului politehnic din Cluj, 1972

STUDIA UNIV BABEŞ-BOLYAI, PHYSICA, XXXIII. 2 1988

A METHOD FOR DETERMINING HIGHER ORDER ACCELERATIONS IN COMPLEX

CONSTANTIN TUDOSIE*

Received March 30, 1987

ABSTRACT. — A method is given for determining the higher order accelerations when the fast dynamic phenomena are described by differential equations in complex The method consists in introducing some unknown functions, of the time t variable, called „functions of direct connection"

Introduction. In the technical sphere of nature there are a lot of phenomena suited to be placed in mathematical structure by functions of complex variable This procedure of totally including the phenomenon may develop towards the domain of real variable functions, by corresponding mathematical methods

In what follows a method is given for determining the higher order accelerations occurring in phenomena whose variation in time is very fast, when these ones are described by differential equations in complex This method consists in introducing some unknown functions, of time variable t, which we called "functions of direct connection" [2], [3]

To the end that the order of acceleration should be given by the order of the derivative, we have called the space x as zero order acceleration, the speed $\dot{x}$ as first order acceleration, and the derivative $\ddot{x}$ as second order acceleration Accelerations $\overset{(\iota)}{x}$, $(\iota > 2)$ are of higher order

Description of the method. One considers the differential equation, in complex, of a dynamic phenomenon

$$f(z)\ddot{z} + g(z)\dot{z} + h(z)\dot{z} + e(z) = F(z), \tag{1}$$

with the given initial conditions $\overset{(\iota)}{z}(0) = \overset{(\iota)}{z}_0$, $(\iota = 0, 1, 2)$, where functions f, g, h, e, F $\mathbf{C} \to \mathbf{C}$ are continuous and have continuous derivatives and

$$\begin{cases} f(z) = P(x, y) + \iota Q(x, y), \\ g(z) = R(x, y) + \iota S(x, y), \\ h(z) = U(x, y) + \iota V(x, y), \\ e(z) = C(x, y) + \iota D(x, y), \\ F(z) = A(x, y) + \iota B(x, y) \end{cases} \tag{2}$$

By substituting (2) and the derivatives in relation with the time

$$\overset{(\sigma)}{z} = \overset{(\sigma)}{x} + \iota \overset{(\sigma)}{y}, \quad (\sigma = 0, 1, 2, 3),$$

* *Polytechnical Institute of Cluj-Napoca, 3400 Cluj-Napoca, Romania*

in (1), the following system of differential equations results

$$\begin{cases} P\ddot{x} + R\dot{x} + U\dot{x} - (Q\ddot{y} + S\dot{y} + Vy) + C = A, \\ Q\ddot{x} + S\ddot{x} + V\dot{x} + P\ddot{y} + R\dot{y} + Uy + D = B \end{cases} \tag{3}$$

By introducing the "functions of direct connection" $\omega_{i,0}(t)$, $\varepsilon_{i,0}(t)$, $(i = 1, 2, 3)$, one can write the equations

$$\overset{(i)}{x} = \omega_{i,0}x, \quad \overset{(i)}{y} = \varepsilon_{i,0}y, \qquad (i = 1, 2, 3) \tag{4}$$

By integrating the first equation, for $i = 1$, one obtains

$$x(t) = x_0 \exp\left[\int_0^t \omega_{1,0}(s)ds\right]. \tag{5}$$

Generally, we have

$$\overset{(i)}{x}(t) = \overset{(i)}{x}_0 \exp\left[\int_0^t \omega_{i+1,0}(s)ds\right], \quad (i = 0, 1, 2) \tag{6}$$

By observing (5), $\ddot{x}$ from (4) becomes

$$\ddot{x}(t) = x_0\omega_{3,0}(t) \exp\left[\int_0^t \omega_{1,0}(s)ds\right] \tag{7}$$

For y we have, analogically,

$$\overset{(i)}{y}(t) = \overset{(i)}{y}_0 \exp\left[\int_0^t \varepsilon_{i+1,0}(s)ds\right], \quad (i = 0, 1, 2), \tag{8}$$

$$\ddot{y}(t) = y_0\varepsilon_{3,0}(t) \exp\left[\int_0^t \varepsilon_{1,0}(s)ds\right] \tag{9}$$

Constants $\ddot{x}_0$ and $\ddot{y}_0$ result from system (3), for t = 0, being given

$$\overset{(i)}{x}(0) = \overset{(i)}{x}_0, \quad \overset{(i)}{y}(0) = \overset{(i)}{y}_0, \qquad (i = 0, 1, 2).$$

By substituting (4) in (3), one obtains

$$x(\omega_{3,0}P + \omega_{2,0}R + \omega_{1,0}U) - y(\varepsilon_{3,0}Q + \varepsilon_{2,0}S + \varepsilon_{1,0}V) + C = A, \tag{10}$$

$$x(\omega_{3,0}Q + \omega_{2,0}S + \omega_{1,0}V) + y(\varepsilon_{3,0}P + \varepsilon_{2,0}R + \varepsilon_{1,0}U) + D = B \tag{11}$$

Expressions (4) for $i = 1, 2$, (6) for $i = 0, 1, 2$, (7), (8) for $i = 0, 1, 2$, (9), (10) and (11) make up a system (E) of 14 equations with 14 unknown quantities

$$\overset{(i)}{x}(t), \ \overset{(i)}{y}(t), \ (i = 0, 1, 2, 3), \ \omega_{i,0}(t), \ \varepsilon_{i,0}(t), \ (i = 1, 2, 3)$$

Determination of system (E) solution. The approximate solution of system (E) is determined by a method of numerical integration. On the interval $[0, a]$,

$a > 0$, we apply a method analogous to that of polygonal lines We divide the interval $[0,\ a]$ through the points $t_k = k\frac{a}{m}$, $k = \overline{1,\ m}$ and we consider the quadrature formula

$$\int_0^{k\frac{a}{m}} G(s)ds \approx \frac{a}{m}\sum_{\nu=1}^{k} G\left(\nu\frac{a}{m}\right), \qquad (12)$$

$$(k = 1,\ 2,\ 3,\ \ldots,\ m).$$

By writing that system (E) is verified for $t_k = k\frac{a}{m}$, and by using formula (12) for the approximate calculus of the integrals, we obtain a system of $14m$ algebraic equations with $14m$ unknown quantities

With the notations

$$\overset{(i)}{x}_k = \overset{(i)}{x}\left(k\frac{a}{m}\right),\ \overset{(i)}{y}_k = \overset{(i)}{y}\left(k\frac{a}{m}\right),\ (i = 0,\ 1,\ 2,\ 3),$$

$$\omega_{i,0k} = \omega_{i,0}\left(k\frac{a}{m}\right),\ \varepsilon_{i,0k} = \varepsilon_{i,0}\left(k\frac{a}{m}\right),\ (i = 1,\ 2,\ 3),$$

the algebraic system is

$$\begin{cases}
\overset{(i)}{x}_k - \omega_{i,0k}x_k = 0,\ \overset{(i)}{y}_k - \varepsilon_{i,0k}y_k = 0,\ (i = 1,\ 2),\\
\overset{(i)}{x}_k - \overset{(i)}{x}_0 \exp\left(\frac{a}{m}\sum_{\nu=1}^{k}\omega_{i+1,0\nu}\right) = 0,\ (i = 0,\ 1,\ 2),\\
\ddot{x}_k - x_0\omega_{3,0k}\exp\left(\frac{a}{m}\sum_{\nu=1}^{k}\omega_{1,0\nu}\right) = 0,\\
\overset{(i)}{y}_k - \overset{(i)}{y}_0 \exp\left(\frac{a}{m}\sum_{\nu=1}^{k}\varepsilon_{i+1,0\nu}\right) = 0,\ (i = 0,\ 1,\ 2),\\
\ddot{y}_k - y_0\,\varepsilon_{3,0k}\exp\left(\frac{a}{m}\sum_{\nu=1}^{k}\varepsilon_{1,0\nu}\right) = 0,\\
x_k[\omega_{3,0k}P(x_k,\ y_k) + \omega_{2,0k}R(x_k,\ y_k) + \omega_{1,0k}U(x_k,\ y_k)] -\\
- y_k[\varepsilon_{3,0k}Q(x_k,\ y_k) + \varepsilon_{2,0k}S(x_k,\ y_k) + \varepsilon_{1,0k}V(x_k,\ y_k)] +\\
+ C(x_k,\ y_k) - A(x_k,\ y_k) = 0,\\
x_k[\omega_{3,0k}Q(x_k,\ y_k) + \omega_{2,0k}S(x_k,\ y_k) + \omega_{1,0k}V(x_k,\ y_k)] +\\
+ y_k[\varepsilon_{3,0k}P(x_k,\ y_k) + \varepsilon_{2,0k}R(x_k,\ y_k) + \varepsilon_{1,0k}U(x_k,\ y_k)] +\\
+ D(x_k,\ y_k) - B(x_k,\ y_k) = 0,\ (k = 1,\ 2,\ 3,\ \ldots,\ m).
\end{cases} \qquad (13)$$

The unknown quantities of system (13) are

$$\overset{(i)}{x}_k,\ \overset{(i)}{y}_k,\ (i = 0,\ 1,\ 2,\ 3),\ \omega_{i,0k},\ \varepsilon_{i,0k},\ (i = 1,\ 2,\ 3),$$
$$(k = 1,\ 2,\ 3,\ \ldots,\ m),$$

and its solution is obtained by the known methods [1]

Constants $\omega_{i,0}$ (0) and $\varepsilon_{i,0}$ (0), $(i = 1,\ 2,\ 3)$ are obtained from (4), for $t = 0$

$$\omega_{i,0}(0) = x_0^{-1}\overset{(i)}{x}_0,\ \varepsilon_{i,0}(0) = y_0^{-1}\overset{(i)}{y}_0$$

The variation diagrams of functions $\overset{(i)}{x}(t)$, $\overset{(i)}{y}(t)$, $(i = 0,\ 1,\ 2,\ 3)$ and $\omega_{i,0}(t)$, $\varepsilon_{i,0}(t)$, $(i = 1,\ 2,\ 3)$, on the interval $[0,\ a]$, $a > 0$, are built up through points.

Relations

$$\overset{(\sigma)}{z}_k = \overset{(\sigma)}{x}_k + i\overset{(\sigma)}{y}_k,\ (\sigma = 0,\ 1,\ 2,\ 3),\ (k = 1,\ 2,\ 3,\ \ldots,\ m),$$

permit to trace the variation diagrams of functions $\overset{(\sigma)}{z}$, on the interval considered

REFERENCES

1 Démidovitch, B., Maron, I., „Éléments de calcul numérique", Éditions Mir, Moscou, 1973

2 Tudosie, C., „Deduction of higher order accelerations by the method of associated angular velocity", *Strojnicky Časopis*, **34**, č 3, pp 337–341, 1983

3. Tudosie, C., „Determination of higher order accelerations by a functional method", *Acta Technica*, ČSAV, No 2, pp 218–224, 1983

4 Tudosie, C., „A method for calculating the higher order accelerations", *Mathematica*, Tome 25 (48), No. 1, pp 69–74, 1983.

STUDIA UNIV BABEŞ-BOLYAI, PHYSICA, XXXIII, 2, 1988

MÖSSBAUER STUDIES OF SOME IRON MINERALS

O. COZAR*, M. MORARIU, V. ZNAMIROVSCHI* and I. MASTAN***

Received August 25, 1988

ABSTRACT. — Mössbauer measurements of some iron minerals were performed at room temperature The sublattices corresponding to different minerals and their characteristic Mössbauer parameters were determined. In the case of magnetite were evidenced four magnetic sublattices from which two are similar with those obtained below the Verwey transition temperature (110—120 K) where the Fe^{2+} and Fe^{3+} states are discret.

Mossbauer spectroscopy is one of the most utilized methods for the structural investigations of iron minerals proceeding from terrestrial and extraterrestrial samples (meteorites and lunar rocks) [1—4]. Distinct minerals give different hyperfine structure patterns usually. Also, ferrous and ferric sites may be distinquished by their isomer shifts and their quadrupolar splittings [2].

The aim of this paper is to report our results concerning the structure of some iron minerals as Dobrogea one, magnetite (Băiţa — Bihor) and limonite (Konigsberg). The structural sublattices and their weights were determined.

Mossbauer effect measurements were performed at room temperature using an ELRON type spectrometer working in a constant acceleration mode. A ^{57}Co source of 10 mCi activity in copper matrix was used All data were accumulated using a Nuclear Data multichannel analyser on 512 channels. The isomer shift is given relative to α-iron. The experimental spectra were fitted using a Fortran IV program, assuming lorentzian shape of the lines.

For the Dobrogea one, the experimental spectrum (fig 1) was decomposed into two subspectra belonging to α-Fe_2O_3 [1] and $FeCO_3$ [5, 6] The characteristic parametres of these sublattices are given in Table 1 The first sublattice is due to the Fe^{3+} ions showing a magnetic hyperfine structure, while the second sublattice which is due to the Fe^{2+} ions shows only a quadrupolar splitting [5, 6].

Table 1

Mössbauer parameters of Dobrogea ore sublattices

Identified sublattice	Isomer shift (mm/s) ±0.007	Quadrupole splitting (mm/s) ±0.007	Magnetic field (kG) ±3	Line width (mm/s) ±0.004	Relative area (%) ±2
(1) —αFe_2O_3	0 378	0.162	523	0.279	52
(2) —$FeCO_3$	1.210	1.857	—	0 333	48

* *University of Cluj-Napoca, Faculty of Mathematics and Physics, 3400 Cluj-Napoca, Romania*
** *Institute for Physics and Technology of Materials, Bucharest, Romania*

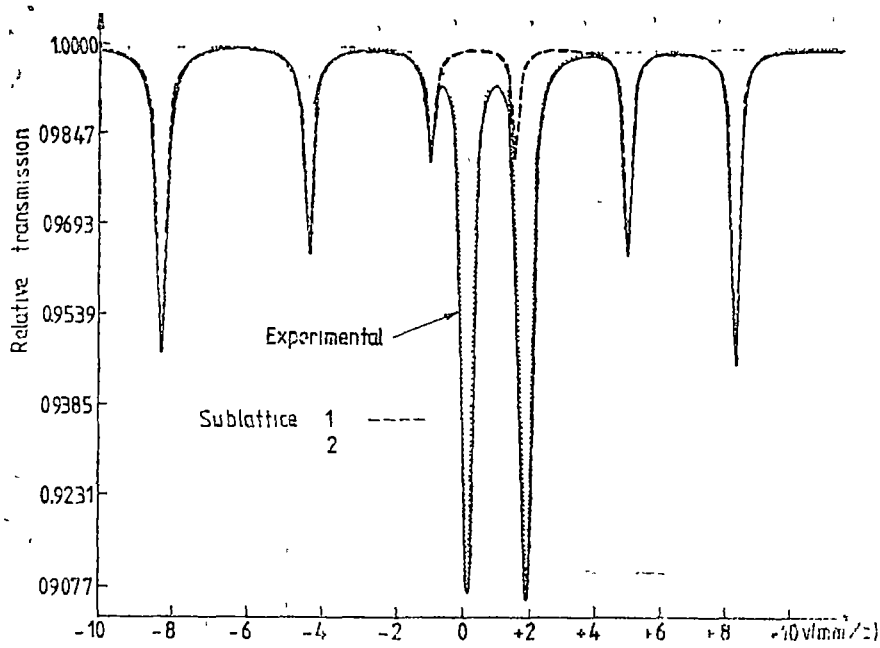

Fig 1. Experimental spectrum and sublattices of the Dobrogea ore

The experimental spectrum of magnetite (Fe_3O_4) was decomposed into four sublattices having all the magnetic hyperfine structure (Fig 2). The characteristic parameters of these sublattices are given in Table 2

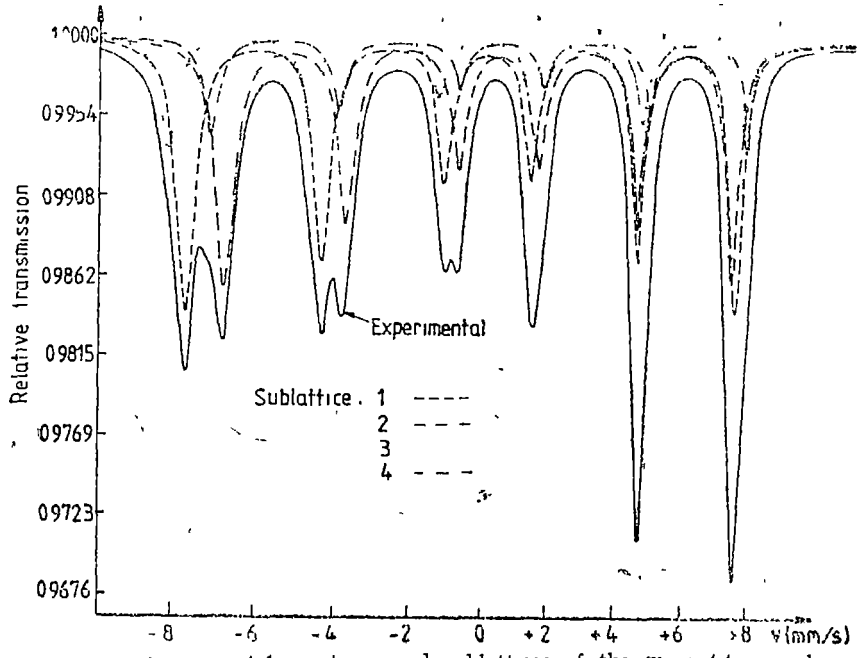

Fig. 2. Experimental spectrum and sublattices of the magnetite sample.

Table 2

Mössbauer parameters of magnetite sublattices

Sublattice	Isomer shift (mm/s) ±0.007	Quadrupole splitting (mm/s) ±0.007	Magnetic field (kG) ±3	Line width (mm/s) ±0.004	Relative area (%) ±2
1	0.341	0.070	482.3	0.524	39 4
2	0.697	0.020	449.7	0.553	36 1
3	0.263	0.011	507.0	0.466	13.8
4	0.765	0.023	476 8	0.465	11 7

Magnetite is a spinel ferrite which can be written as $Fe^{3+}[Fe^{2+}Fe^{3+}]O_4$ or (AB_2O_4) [1] The type "A" cations are situated into a tetrahedric oxygen coordination and those of the "B" type into an octahedral symmetry site with a trigonal distortion. The sublattices 1 and 2 characterized by the following values of the magnetic field, 482.3 kG and 449.7 kG, may be attributed to the Fe^{3+} ions from the A site and to the B site ($Fe^{2+} + Fe^{3+}$) cations respectively A fast electron-transfer process (electron hopping) exist between the Fe^{2+} and Fe^{3+} ions on the octahedral B sites above the Verwey transition temperature (110—120 K) [1, 7]. The sublattices 3 and 4, characterized by the magnetic field of 507 kG and 476.8 kG respectively, are similar with those obtained by Banerjee *et al.* [7] at 77 K where the Fe^{2+} and Fe^{3+} states are

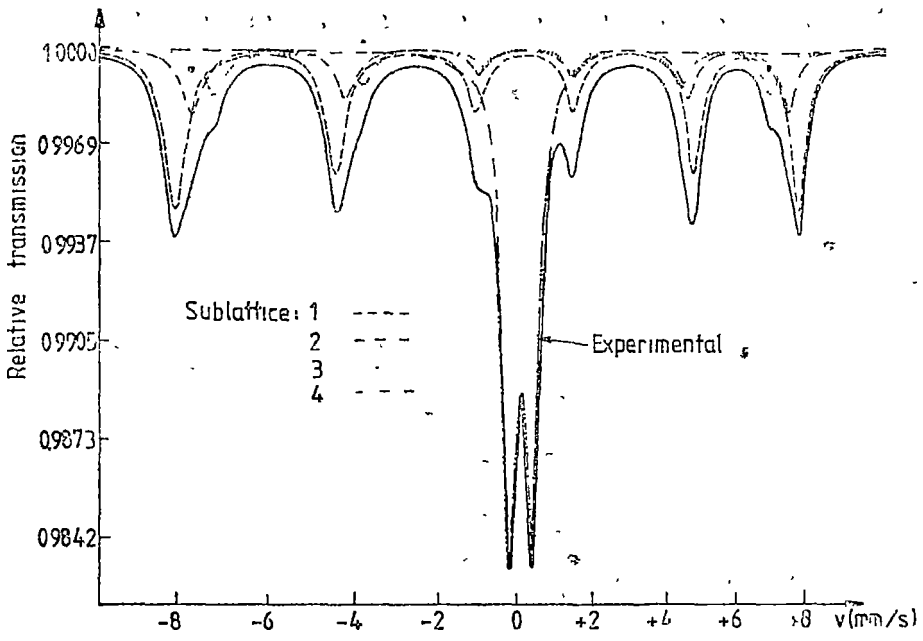

Fig. 3. Experimental spectrum and sublattices of the limonite sample.

discret, one apparently sees two partially resolved hyperfine patterns with fields of 503 kG and 480 kG The 507 kG field corresponds to the Fe^{3+} ions on both A and B sites and the 476.8 kG field is due to the B site Fe^{2+} ions In this case do not exist the electron-transfer processes between the Fe^{2+} and Fe^{3+} ions from the B sites.

The simultaneous evidence of the four characteristic sublattices of magnetite, as under as above the Verwey transition temperature, may be explained by the presence of some cation vacances in the studied sample which prevent the development of the electron-transfer process between Fe^{2+} and Fe^{3+} ions situated in B site Table 2 shows that the weights of these sublattices (3, 4) are three times smaller than others

Table 3

Mössbauer parameters of limonite sublattices

Sublattice	Isomer shift (mm/s) ±0 007	Quadrupole splitting (mm/s) ±0.007	Magnetic field (kG) ±3	Line width (mm/s) ±0 004	Relative area (%) ±2
1 $-(\alpha Fe_2O_3)$	0 303	0 22	502	0 582	37 4
2 $-\gamma Fe_2O_3$	0 316	0 25	478 5	0 578	13 2
3 $-\gamma Fe_2O_3$	0 352	0 35	447	0 589	11.3
4 $-\alpha$FeOOH	0 282	0 57	—	0 465	39 2

For the limonite were also evidenced four structural sublattices (Fig. 3). The Mossbauer parameters for these are given in Table 3. The first sublattice characterized by the magnetic field of 502 kG may be attributed to the hematite ($\alpha-Fe_2O_3$) and the other two (2, 3) sublattices characterized by the magnetic field of 478.5 kG and respectively 447 kG to A and B sublattices of $\gamma-Fe_2O_3$ [8] The fourth non-magnetic sublattice with an weight of 39.2% is due to the presence of goethite (α—FeOOH) having a particle size granulation smaller than 70 Å [9]

REFERENCES

1. T. C. Gibb, N N Greenwood, *Mössbauer Spectroscopy*, Chapmann and Hall, London 1972
2. D. Barb, *Efectul Mossbauer şi aplicatiile sale*, Ed Acad, Bucureşti, 1972
3. A. G Maddock, „Mössbauer spectroscopy in mineralogy", in *Mossbauer spectroscopy and its applications*, IAEA Vienna, 329—347, 1972
4. D. Barb, M. Morariu, L. Diamandescu, V Znamirovschi, D Ciuchea, A. Moţiu, *Ann Geophys.*, **38**, 8 (1982).
5. V. I. Goldanskii, E F Makarov, I. P Suzdalev, I A Vinogradov, *Phys. Rev Lett*, **20**, 137 (1968)
6. K. Ono, A Ito, *J Phys Soc Japan*, **19**, 899 (1964)
7. S K Banerjee, W O'Reilly, C E Johnson, *J Appl Phys*, **38**, 1289 (1967)
8. R J Armstron, A H Morrish, G A Sawatzky, *Phys Lett*, **23**, 414 (1966).
9. A. Govaert, C Danwe, E de Grame, *Solid State Commun*, **18**, 389 (1976).

STUDIA UNIV BABEŞ-BOLYAI, PHYSICA, XXXIII, 2, 1988

L'ÉQUATION DE DISPERSION D'UN FLUIDE VISQUEUX—ÉLASTIQUE, IONISÉ, EN PRÉSENCE DU L'EFFET RAYLEIGH-BÉNARD

M. VASIU* et T. BEU*

Manuscrit reçu le Octobre 17, 1988

ABSTRACT. — Dispersion Equation of a Visco-Elastic Conducting Fluid. The Rayleigh-Bénard model for a visco-elastic fluid has been studied to include the Hall effects and the uniform rotation on the thermal convection

Introduction. Dans le présent article nous nous proposons de déduire l'équation de dispersion pour le cas d'un fluide visqueuxélastique de type Oldroyd [1], ionisé, ayant une conductivite électrique finie, en présence d'un effet de conductivité thermique de type Rayleigh—Bénard, du l'effet Hall et du mouvement de rotation uniforme, avec une vitesse angulaire $\vec{\Omega}(0,\ 0,\ \Omega)$ Le fluide se trouve sous l'action d'un champ magnétique uniforme $\vec{B}(0,\ 0,\ B_0)$ et de l'accélération gravitationnelle $\vec{g}(0,\ 0,\ -g)$

Nous utilisons les resultats obtenus par S Chandrasekhar [2], R Sharma, K Sharma [3], R Sharma [4], P Bhatia, J Steiner [5], M Vasiu [6], À la différence des travaux cités nous prenons en considération l'influence simultanée du l'effet Hall et du mouvement de rotation

Équations fondamentales pour l'état perturbé du fluide ionisé. Admettons que des petites perturbations se propagent dans le fluide Le système des équations magnéto-hydrodynamique pour l'état perturbé du fluide, en projection sur l'axe Oz, s'écrit de la manière suivante [3], [4]

$$\left(1+\lambda\frac{\partial}{\partial t}\right)\left\{\frac{\partial}{\partial t}(\Delta w)-g\alpha\left(\frac{\partial^2\theta}{\partial x^2}+\frac{\partial^2\theta}{\partial y^2}\right)+2\Omega\frac{\partial\zeta}{\partial z}-\right.$$
$$\left.-\frac{B_0}{\mu_0\rho_0}\frac{\partial}{\partial z}[\Delta(\delta B_z)]\right\}=\nu\left(1+\lambda_0\frac{\partial}{\partial t}\right)\Delta^2 w \tag{1}$$

$$\left(\frac{\partial}{\partial t}-\nu_m\Delta\right)\delta B_z=B_0\frac{\partial w}{\partial z}-HB_0\frac{\partial\xi}{\partial z}, \tag{2}$$

$$\left(\frac{\partial}{\partial t}-\varkappa\Delta\right)\theta=\beta w \tag{3}$$

$$\left(\frac{\partial}{\partial t}-\nu\Delta\right)\zeta=2\Omega\frac{\partial w}{\partial z}+\frac{B_0}{\mu_0\rho_0}\frac{\partial\xi}{\partial z} \tag{4}$$

$$\left(\frac{\partial}{\partial t}-\nu_m\Delta\right)\xi=B_0\frac{\partial\zeta}{\partial z}+HB_0\frac{\partial}{\partial z}[\Delta(\delta B_z)], \tag{5}$$

* *Universite de Cluj-Napoca, Faculté de Mathematique et Physique, 3100 Cluj-Napoca, Roumanie*

où w est la composante sur l'axe Oz de la perturbation de la vitesse $\vec{v}(u, v, w)$, θ — la perturbation de la température du fluide, δB_z — la perturbation sur l'axe Oz du vezteur champ magnètique $\vec{B}$, λ — le temps de relaxation des tensions, λ_0 — le temps de retardement des déformations, ν — — le coefficient de viscosité cinématique, ρ_0 — la densité du fluide pour $z = 0$, ou la température T du fluide est T_0 (admettons une rélation entre la densité ρ et la densité ρ_0 sous la forme $\rho = \rho_0[1 - \alpha(T - T_0)]$, où T est la temperature pour $z \neq 0$, α este le coefficient dé expansion thermique du volume), $\varkappa$ — le coefficient de conductivité thermique, $\beta = \left|\frac{dT}{dz}\right|$ (le fluide est chauffée de bas en haut de sorte que $T = T_0 - \beta z$), ν_m — le coefficient de diffusion magnétique, $H = 1/\mu_0 Ne$, où μ_0 est la perméabilité magnétique du vide, N est le nombre des ions (électrons) dans l'unité de volume du fluide, e — la charge électrique, Δ — l'opérateur de Laplace et

$$\zeta = rot_z\vec{v}, \qquad \xi = rot_z\delta\vec{B}. \tag{6}$$

Dans le fluide se propagent des petites perturbations sous la forme

$$\varphi'(x, y, z, t) = \Phi(z) \exp(ik_x x + ik_y y + nt) \tag{7}$$

ou $\varphi' = w$, δB_z, θ, ζ, ξ, $\Phi(z)$ est l'amplitude de la perturbation, k_z, k_x sont les composantes du vecteur d'onde $\vec{k}$, n est la pulsation d'onde La substi tution des perturbations (7) dans les équations (1)—(5) et tenant compte de la forme du l'opérateur $\Delta = \frac{\partial^2}{\partial x^2} + \frac{\partial^2}{\partial y^2} + \frac{\partial^2}{\partial z^2} = D^2 - k^2$ où $D^2 = \frac{d^2}{dz^2}$ et $k^2 = k_x^2 + k_y^2$, nous conduit au système d'équations

$$(1 + \lambda n)[n(D^2 - k^2)W(z) + \alpha g k^2 \Theta(z) + 2\Omega DZ(z) - \frac{B_0}{\mu_0\rho_0}(D^2 - k^2)DK(z)] = \nu(1 + \lambda_0 n)(D^2 - k^2)W(z) \tag{8}$$

$$[n - \nu_m(D^2 - k^2)K(z) = B_0 DW(z) - HB_0 DX(z) \tag{9}$$

$$[n - \varkappa(D^2 - k^2)]\Theta(z) = \beta W(z) \tag{10}$$

$$[n - \nu(D^2 - k^2)]Z(z) = 2\Omega DW(z) + \frac{B_0}{\mu_0\rho_0} DX(z) \tag{11}$$

$$[n - \nu_m(D^2 - k^2)]X(z) = B_0 DZ(z) + HB_0(D^2 - k^2)DK(z), \tag{12}$$

où $D = \frac{d}{dz}$, $W(z)$,$\Theta(z)$, $K(z)$ $X(z)$ et $Z(z)$ sont les amplitudes $\Phi(z)$ des perturbations: w, θ, δB_z, ξ et ζ.

Introduisons maintenant les grandeurs

$$a = kd, \quad \sigma = \frac{nd^2}{\nu}, \quad p_1 = \frac{\nu}{\varkappa}, \quad p_2 = \frac{\nu}{\nu_m}, \quad F = \frac{\lambda\nu}{d^2}, \quad \Gamma = \frac{\lambda_0\nu}{d^2}, \quad A = \frac{1 + \sigma\Gamma}{1 + \sigma F}, \tag{13}$$

où d est une longueur caractéristique pour le fluide (le fluide est confiné entre les plans $z = 0$ et $z = d$)
Remplaçons les grandeurs (13) en équations (8) — (12) Faisant les calculs nous obtiendrons

$$(D^2 - a^2)[A(D^2 - a^2) - \sigma]W + \frac{B_0 d}{\mu_0 \rho_0 \nu}(D^2 - a^2)DK - \frac{2d^3\Omega}{\nu} - \left(\frac{\alpha g d^2}{\nu}\right)a^2\Theta = 0 \tag{14}$$

$$(D^2 - a^2 - p_2\sigma)K = -\left(\frac{B_0 d}{\nu_m}\right)DW + \left(\frac{HB_0 d}{\nu_m}\right)DK \tag{15}$$

$$(D^2 - a^2 - p_1\sigma)\Theta = -\left(\frac{\beta d^2}{\varkappa}\right)W \tag{16}$$

$$[A(D^2 - a^2) - \sigma]Z = -\left(\frac{2\Omega d}{\nu}\right)DW - \left(\frac{B_0 d}{\mu_0 \rho_0 \nu}\right)DX \tag{17}$$

$$(D^2 - a^2 - p_2\sigma)X = -\left(\frac{B_0 d}{\nu_m}\right)DZ - \left(\frac{HB_0}{d\nu_m}\right)(D^2 - a^2)DK \tag{18}$$

Introduisons les nouvelles constantes

$$c_1 = \frac{\beta d^2}{\varkappa},\ c_2 = \frac{B_0 d}{\mu_0 \rho_0 \nu},\ c_3 = \left(\frac{\alpha f g d^2}{\nu}\right)a^2,\ c_4 = \frac{B_0 d}{\nu_m},$$
$$c_5 = \frac{2\Omega d^3}{\nu},\ c_6 = \frac{2\Omega d}{\nu},\ c_7 = \frac{B_0}{\nu_m d} \tag{19}$$

et les opérateurs

$$O = D^2 - a^2,\ O_1 = D^2 - a^2 - p_1\sigma,\ O_2 = D^2 - a^2 - p_2\sigma$$
$$O_A = A(D^2 - a^2) - \sigma \tag{20}$$

Les équations (14) — (18) s'écrivent sous la forme

$$OO_A W + c_2(ODK) - c_5 DZ - c_3\Theta = 0 \tag{21}$$

$$O_2 K = -c_4 DW + Hc_4 DX \tag{22}$$

$$O_1\Theta = -c_1 W \tag{23}$$

$$O_A Z = -c_6 DW - c_2 DX \tag{24}$$

$$O_2 X = -c_4 DZ - c_7 H(ODK). \tag{25}$$

L'équation de dispersion Si l'on applique l'opérateur D dans (24) et l'opérateur O_A dans (25), introduisant le nouvel opérateur

$$L_A = O\ O_2 - c_2 c_4 D^2, \tag{26}$$

on obtient l'égalité

$$L_A X = c_4 c_6 D^2 W - Hc_7 O_A ODK, \tag{27}$$

Si l'on applique l'opérateur L_A dans (22), en tenant conpte de (27), l'égalité (22) prend la forme

$$L_A O_2 K = -c_4(L_A DW) + Hc_4 D(L_A X) = -c_4(L_A DW) + \\ + Hc_4 D(c_4 c_6 D^2 W - c_7 HO_A ODK). \tag{28}$$

Introduisons maintenant les opérateurs

$$L_{AH} = L_A O_2 + c_4 c_7 H^2 O_A O D^2 \tag{29}$$

et

$$O_D = c_4^2 c_6 H D^3 - c_4 L_A D. \tag{30}$$

En tenant compte de (29) et de (30), l'égalité (28) s'écrit

$$L_{AH} K = O_D W. \tag{31}$$

Nous pouvons éliminer la fonction X entre les équations (24) et (25) Si l'on applique l'opérateur O_2 dans (24) et l'opérateur D dans (25) nous obtiendrons

$$L_A Z = -c_6 O_2 DW + c_2 c_7 HOD^2 K \tag{32}$$

Si l'on applique l'opérateur L_{AH} dans (32), en tenant compte de (31), l'égalité (32) prend la forme

$$L_{AH} L_A Z = (-c_6 L_{AH} O_2 D + c_2 c_7 HOD^2 O_D) W. \tag{33}$$

Si l'on applique l'operateur $L_{AH} L_A O_1$ dans l'équation (21) et tenant compte de (19), de (23), de (26), de (29), de (30), de (31) et de (33), on obtient l'égalité

$$O_1 \Big\{ O \Big\{ L_{AH} L_A O_A + \left(\frac{B_0 d}{\mu_0 \rho_0 \nu}\right) L_A \left[\left(\frac{B_0 d}{\nu}\right)^2 \left(\frac{2\Omega d}{\nu}\right) HD^4 - \\ - \left(\frac{B_0 d}{\nu_m}\right) L_A D^2 \right] \Big\} - \left(\frac{2\Omega d^3}{\nu}\right) \Big\{ - \left(\frac{2\Omega d}{\nu}\right) L_{AH} O_2 D^2 + \\ + \left(\frac{B_0^2 H}{\mu_0 \rho_0 \nu \nu_m}\right) O D^2 \left[\left(\frac{B_0 d}{\nu_m}\right)^2 \left(\frac{2\Omega d}{\nu}\right) HD^4 - \\ - \left(\frac{B_0 d}{\nu_m}\right) L_A D^2 \right] \Big\} \Big\} W = - \left(\frac{\alpha g \beta d^4}{\nu \varkappa}\right) a^2 L_{AH} L_A W. \tag{34}$$

Introduisant les constantes

$$Q = \frac{B_0^2 d^2}{\mu_0 \rho_0 \nu \nu_m}, \quad T = \frac{4\Omega^2 d^4}{\nu^2}, \quad M = \frac{H^2 B_0^2}{\nu_m^2}, \quad R = \frac{\beta \alpha g d^4}{\nu \varkappa}, \tag{35}$$

où Q est le nombre de Chandrasekhar, T est le nombre de Taylor, M est le nombre qui caractérise l'effet Hall, R est le nombre de Rayleigh, après un arrangement des terms, l'égalité (34) prend la forme

$$O_1 \} O [L_{AH} L_A O_A + 2Q\sqrt{TM} L_A D^4 - TMQD^6 - \\ - QL_A^2 D^2] + TL_{AH} O_2 D^2 \} W = -Ra^2 L_{AH} L_A W. \tag{36}$$

Cette égalité est exactement l'équation de dispersion cherchée.

Cas particuliers 1 Pour le cas d'un modèle de fluide visqueuxélastique ionisé, en l'absence du l'effect Hall ($H = 0$, $M = 0$), l'opérateur L_{AH} prend la forme

$$L_{AH} = L_A O_2$$

et l'équation de dispersion (36) se réduit à la forme

$$O_1[OL_A^2 + TD^2O_2^2]W = -Ra^2L_AO_2W \tag{37}$$

2 Pour le cas d'un modèle de fluide visqueux-élastique ionisé, en l'absence du l'effet Hall ($H = 0$, $M=0$) et du mouvement de rotation ($\Omega = 0$, $T = 0$), l'équation de dispersion (36) se réduit à l'équation obtenue par R Sharma [4]

$$O_1OL_AW = -Ra^2O_2W. \tag{38}$$

3 Un autre cas est celui d'un modèle de fluide ionisé, en l'absence du l'effet visqueux-élastique ($\lambda = 0$, $\lambda_0 = 0$, $A = 1$) et du l'effet Hall ($H = 0$, $M = 0$) mais en présence du mouvement de rotation ($T \neq 0$) Les opérateurs L_{AH}, O_A et L_A prennent la forme

$$L_{AH} = L_AO_2 = L^xO_2,$$

$$L^x = O\,O_2 - QD^2,$$

$$O_A = O^x = D^2 - a^2 - \sigma,\ L_A = L^x$$

et l'équation de dispersion (36) se réduit à l'équation obtenue par S Chandrasekhar [2]

$$O_1[OL^{x2} + TO_2^2D^2]W = -Ra^2L^xO_2W \tag{39}$$

Dans un autre travail nous nous proposons de résoudre l'équation de dispersion (36) et d'établir les critères de l'instabilité magnétohydrodynamique

BIBLIOGRAPHIE

1 J Oldroyd, *Proc Roy Soc*, A **245**, 278 (1958)
2 S Chandrasekhar, *Hydrodynamic and Hydromagnetic Stability*, Oxford, Clarendon Press, 1961, § 51.
3 R. Sharma, K. Sharma, *Aust J Phys*, **31**, 181 (1978)
4 R Sharma, *Acta Phys. Hung* **38** (4), 293 (1975)
5. P Bhatia, J Steiner, *Phys Lett*, **37** A, 419 (1971)
6 M Vasiu, *Studia Univ Babeş—Bolyai, Physica*, **30**, 40 (1985)

STUDIA UNIV BABEŞ-BOLYAI, PHYSICA, XXXIII, 2, 1988

POLYCRYSTALLINE YIG RESONATORS

D. IANCU* and D. STĂNILĂ*

Received September 20, 1988

ABSTRACT. — We present a calculus method of resonance frequency for a polycrystalline YIG cylindrical body, with internal metallical bar This resonator may be employed for microwave measurements and applications Such a resonator has been used as resonance cavity for an IMPATT microwave oscillator A good concordance may be observed between the theoretical and experimental values, for the resonance frequency of such a resonator

Theoretical introduction. We consider a polycrystalline YIG cylinder shown in Fig 1 We assume that this cylinder has mettalical walls at $\rho = R_1$, $z = 0$ and $z = 1$, and a magnetical wall at $\rho = R_a$ We also assume the resonator situated in uniform d c magnetic field oriented along z axis

The equation of the magnetic potential is given by the following expression .

$$\mu\left(\frac{\partial^2\psi}{\partial\rho^2} + \frac{1}{\rho}\frac{\partial\psi}{\partial\rho} + \frac{1}{\rho^2}\frac{\partial^2\psi}{\partial\varphi^2}\right) + \frac{\partial^2\psi}{\partial z^2} = 0 \qquad (1)$$

Where μ is the magnetic permeability

$$\Psi = \begin{matrix} I_m \\ Y_m \end{matrix}\left(\frac{K_z}{\sqrt{-\mu}}\rho\right)\begin{matrix}\cos \\ \sin\end{matrix}(K_z z e^{-jml}) \qquad (2)$$

is the wave function

$k_z = \frac{\pi p}{l}$ is the wave number,

$$\begin{matrix} I_m \\ Y_m \end{matrix}\left(\frac{K_z}{\sqrt{-\mu}}\rho\right) = AI_m\left(\frac{K_z}{\sqrt{-\mu}}\rho\right) + BY_m\left(\frac{K_z}{\sqrt{-\mu}}\rho\right) \qquad (3)$$

and

$$\begin{matrix}\cos \\ \sin\end{matrix}(K_z Z) = e^{\pm jK_z z}$$

The other notations are given in reference [1] Taking into account the periodicity condition $\varphi = \varphi + 2\pi$, as well as the bor-

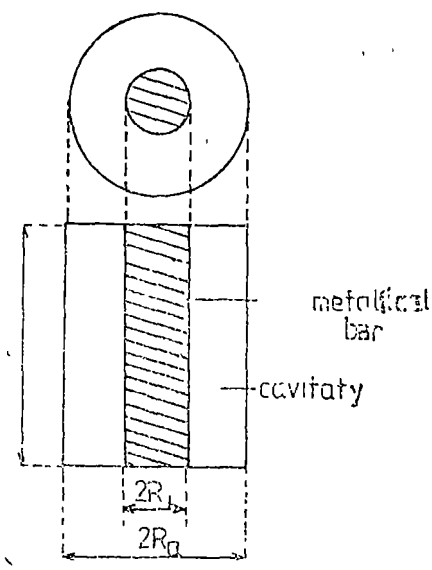

Fig 1 The representation of the resonance cavity

* University of Cluj-Napoca, Faculty of Mathematics and Physics, 3400 Cluj-Napoca, Romania

der conditions at $z = 0$ and $z = 1$, we will obtain for the wave function the following expression.

$$\Psi = \underset{Y_m}{I_m}\left(\frac{K_z}{\sqrt{-\mu}}\rho\right)\cos(K_z z)e^{-jm\varphi} \tag{4}$$

At the margin between the metallical bar and the giromagnetic medium, the border condition is given by

$$\mu\frac{\partial\psi}{\partial\rho} + j\mu_a\frac{1}{\rho}\frac{\partial\psi}{\partial\varphi} = 0 \tag{5}$$

Raplacing eq (4) in eq (5) we will obtain at $\rho = R_1$

$$\sqrt{-\mu}\,\underset{Y'_m}{I'_m}\left(\frac{K_z}{\sqrt{-\mu}}R_1\right) + \frac{\mu_a m}{K_z R_1}\,\underset{Y_m}{I_m}\left(\frac{K_z}{\sqrt{-\mu}}R_1\right) = 0 \tag{6}$$

Outside the resonator the equation of the magnetic potential may be written

$$\frac{\partial^2\psi_0}{\partial\rho^2} + \frac{1}{\rho}\frac{\partial^2\psi}{\partial\varphi^2} + \frac{\partial^2\psi_0}{\partial z^2} + \frac{\partial^2\psi_0}{\partial z^2} = 0 \tag{7}$$

The eq (7) has the solution.

$$\Psi_0 = \underset{K_m}{I_m}(K_z\rho)\cos(K_z z)e^{-jm\varphi} \tag{8}$$

The border condition for the magnetic wall, at $\rho = R_a$ is given by

$$\mu\frac{\partial\psi}{\partial\rho} + j\mu_a\frac{1}{\rho}\frac{\partial\psi}{\partial\varphi} = \frac{\partial\psi_0}{\partial\rho} \tag{9}$$

Uisng eq (6) and (7) results:

$$\sqrt{-\mu}\,\underset{Y'_m}{I'_m}\left(\frac{K_z}{\sqrt{-\mu}}R_a\right) + \frac{\mu_0 m}{K_z \cdot R_a}\,\underset{Y_m}{I_m}\left(\frac{K_z}{\sqrt{-\mu}}R_a\right) - \underset{K_m}{I'_m}(K_z R_a) = 0 \tag{10}$$

The equations (6) and (10) form a system in function of the constants A and B This system cannot have vanishing solutions for A and B Putting the condition for the determinant to be zero we will obtain for $m = 0$ [2] the following equation

$$I'_0(qR_1)[\sqrt{-\mu}Y'_0(qR_a) - K'_0(K_z R_a)] - Y'_0(qR_1)[\sqrt{-\mu}I'_0(qR_a) - I'_0(K_z R_a)] = 0 \tag{11}$$

For a giromagnetic material with electromagnetic loss, the magnetic permeability may be written [3] as

$$\mu = 1 + \chi'_{zz}$$

where χ'_{zz} is given by

$$\chi'_{zz} = \frac{\omega_M\omega_0[\omega_0^2 - \omega^2 + 1/T^2]}{[\omega_0^2 - \omega^2 - 1/T^2]^2 - 4\omega_0^2/T^2} \tag{12}$$

In this way we will obtain for the magnetic permeability

$$\mu = 1 + \chi'_{xx} = \omega_M \omega_0 \left(\omega_0^2 - \omega^2 + \frac{1}{T^2}\right) + \left(\omega_0^2 - \omega^2 - \frac{1}{T^2}\right)^2 + \frac{4\omega_0^2}{T^2} = -\left(\frac{\pi p}{q_t l}\right)^2 \tag{13}$$

where q_t represents the solutions of the eq (11) The eigenvalues of the electromagnetic mods, result from eq (13), for $m = 0$

$$\omega_{0pt} = \frac{1}{2}\left(2\omega_0^2 - \frac{2}{T^2} + \frac{\omega_M \omega_0}{1 + \left(\frac{\pi p}{q_t l}\right)^2} \pm \sqrt{\Delta}\right) \tag{14}$$

Where

$$\Delta = \left[\frac{\omega_M \omega_0}{\left(\frac{\pi p}{q_t l}\right)^2 + 1}\right]^2 - \frac{2}{T^2}\frac{4\omega_M \omega_0}{\left(\frac{\pi p}{q_t l}\right)^2 + 1} - \frac{16\omega_0^2}{T^2}$$

In eq (14) only the positiv value is retained, because, at $T = \infty$ (lossless material) the value of ω_{opt} cannot be equal to the value coresponding to an infinit extended medium

The values of q_t obtained by a computer method for different cylindrical resonators, may be seen in Table 1

Experiment. Several YIG resonators have been prepared by conventional ceramic method [4] For a peculiar resonator with the following parameters $4\pi M_s = 2200$ Gs, $T = 876 \times 10^{-10}$ sec,

Table 1

The values of q for different dimensions of the resonators

p,	L (m),	$R_a(m)$	$R_i(m)$,	q_t	oscillating mode
1	10×10^{-3}	8×10^{-3}	3×10^{-3}	722 15	011
1	10×10^{-3}	8×10^{-3}	4×10^{-3}	541 82	011
1	10×10^{-3}	8×10^{-3}	5×10^{-3}	433 5	011
				1080 16	
1	10×10^{-3}	8×10^{-3}	6×10^{-3}	361 25	011
				900 08	012
2	10×10^{-3}	8×10^{-3}	3×10^{-3}	732 31	021
2	10×10^{-3}	8×10^{-3}	4×10^{-3}	519 28	021
2	10×10^{-3}	8×10^{-3}	5×10^{-3}	439 43	021
				1085 90	022
2	10×10^{-3}	8×10^{-3}	6×10^{-3}	366 18	021
				904 92	022
3	10×10^{-3}	8×10^{-3}	3×10^{-3}	732 37	031
3	10×10^{-3}	8×10^{-3}	4×10^{-3}	549 28	021
3	10×10^{-3}	8×10^{-3}	5×10^{-3}	439 43	031
				1085 93	032
3	10×10^{-3}	8×10^{-3}	6×10^{-3}	366 18	031
				904 95	032

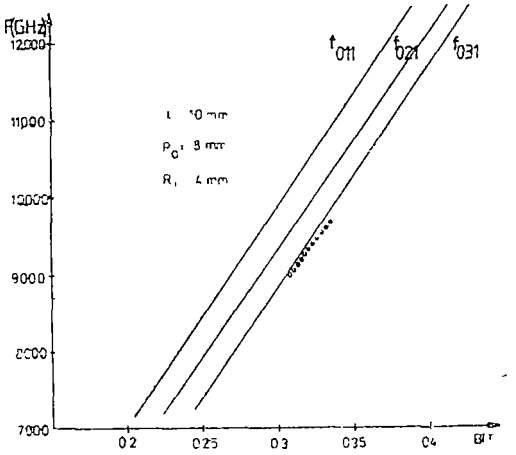

Fig 2 Plot of resonance frequency as a function of external d c magnetic field

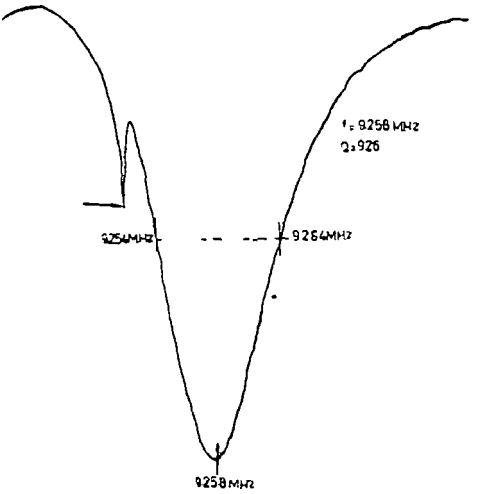

Fig 3 Rnancesoe curve of the resonator

f = 10 mm, R_a = 8 mm, R_i = 4 mm, the theoretic and experimental resonance frequency as a function of the external d c magnetic field is plotted in Fig. 2 Fig 3, shows the resonance curve of such a resonator plotted with a experimental set-up presented in Fig 4 Fig 5 and Fig 6 present the theoretical resonance frequency as functions of R_i and R_a.

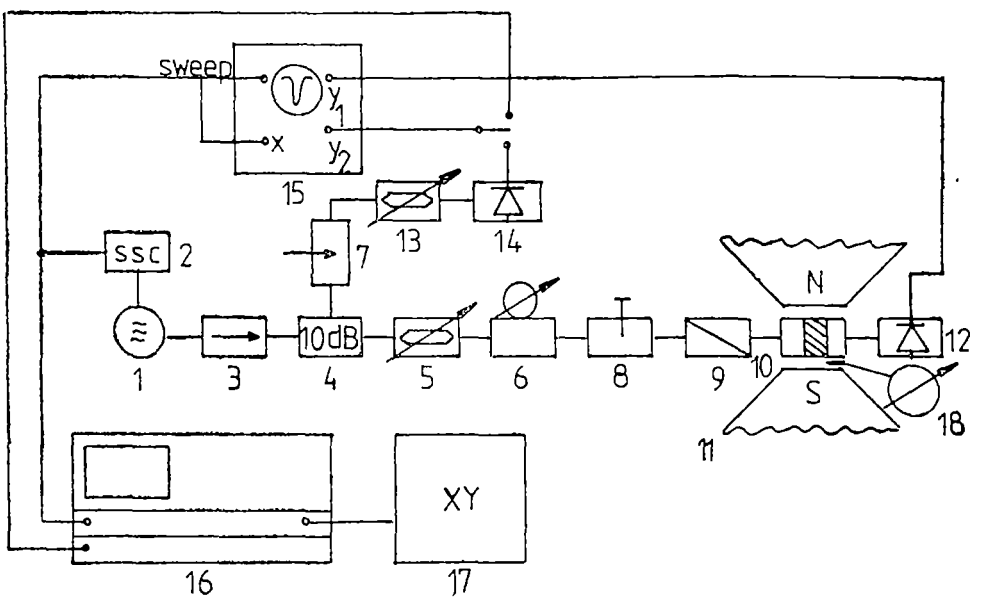

Fig 4 Experimental set-up 1 IMPATT oscillator, 2 current supply, 3 izlator, 4 cupler; 5. attenuator, 6 frequenvcymeter, 7 skrew; 8 skrew, 9 twist, 10. YIG resonator monture, 11 electromganet, 12 detector, 1e3. alternator, 14 detector, 15 oscilloscope, 16 processore type TR—4910/9, 17 plotter, 18 Tesla-meter.

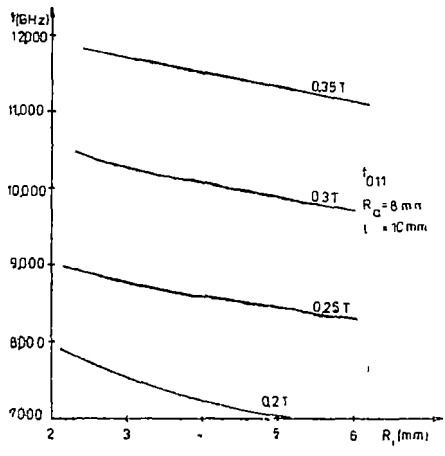

Fig 5 Theoretical curves as a function of R_i for different values of the external magnetic field

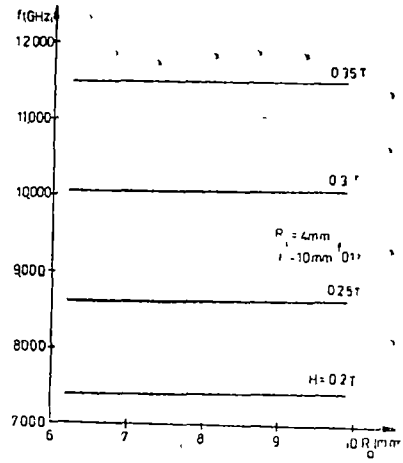

Fig 6 Theoretical curves as a function of R_a for different values of the external magnetic field

Application. Such a resonator as described previously has been employed as resonant cavity for a rectangular waveguide oscillator with IMPATT diode.

The R, L, C parameters of the Yig oscillator have been determined as follows

1 From the resonance curve plotted in Fig. 2 may be accounted the quality factor of the resonator, $Q_0 = 926$,

2 The parameters of the bar have been determined by a measurement method described in reference [5] We found for the bar quality factor, $Q_{\text{bar}} = 166$;

3 We assume that the loss (in principal) is given by the loss of the bar. In this way knowing that $Q_0 \simeq \frac{\omega_0 L}{R_{\text{bar}}}$ and $f_0^2 = \frac{1}{4\pi^2 LC}$ we found $L = 0.27$ nH, $C = 1\,08$ pF and $R = R_{\text{bar}} = 0\,017\ \Omega$.

The schematic of the oscillator is shown in Fig 7 The equivalent circuit for the oscillator is represented in Fig 8, where R, L, C are the parameters of the giromagnetic resonator and Z_s is the impedance of the short circuit.

Writting that the imaginary part of the resonator impedance must be equal with the imaginary part of the active device impedance, it follows:

$$\frac{R_D^2 X_p - (X_s - X_D)^2 X_p + X_D(X_s - X_D)}{R_D^2 + (X_s - X_D - X_p)} = X_L - X_C$$

where

$$Z_0 = -\frac{X_p[R_D + j(X_s - X_D)]}{R_D + j[(X_s - X_D) X_p]} \quad \text{and} \quad Z_{rez} = R + j(X_Z - X_C)$$

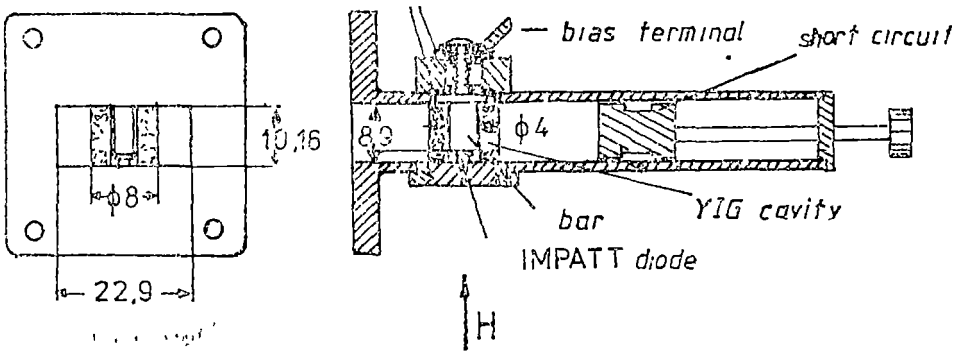

Fig 7 The representation of the oscillator

According to those previously described, we obtained for the resonance frequency the theoretical value $f = 9100$ MHz, at an external field $B = 3800$ Gs The experimental value was $f_{exp} = 9460$ MHz at 40 mA bias current of IMPATT device

The comparison between the experimental and theoretical values of the frequency put in evidence a good concordance of the theory with the experiment

The 4% difference between the theoretical and experimental value appears because of several facts

1 The IMPATT's parameters depend strongly on the bias current and the configuration of the experimental set-up.

2 The equivalent circuit used for the IMPATT diode is a simplified one.

3 The calculus of the parameters of the resonator has been made without taking into account the magnetic loss of the material

4 The parameters of the bar have been determined with 5% precision.

The frequency characteristic for such an oscillator, swept by current variation, is plotted in Fig 9 The plots of the frequency and the power as a func-

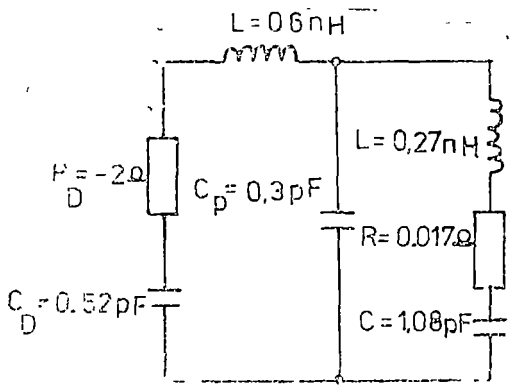

Fig 8 The equivalent scheme of the oscillator

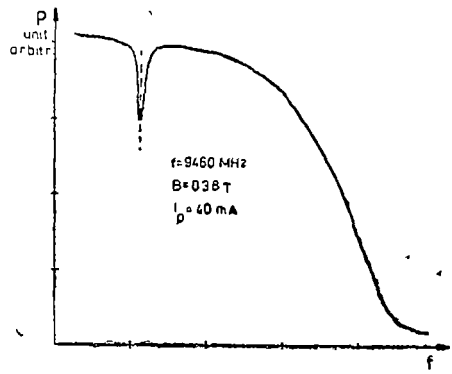

Fig 9 Power characteristic for a current sweeped oscilator.

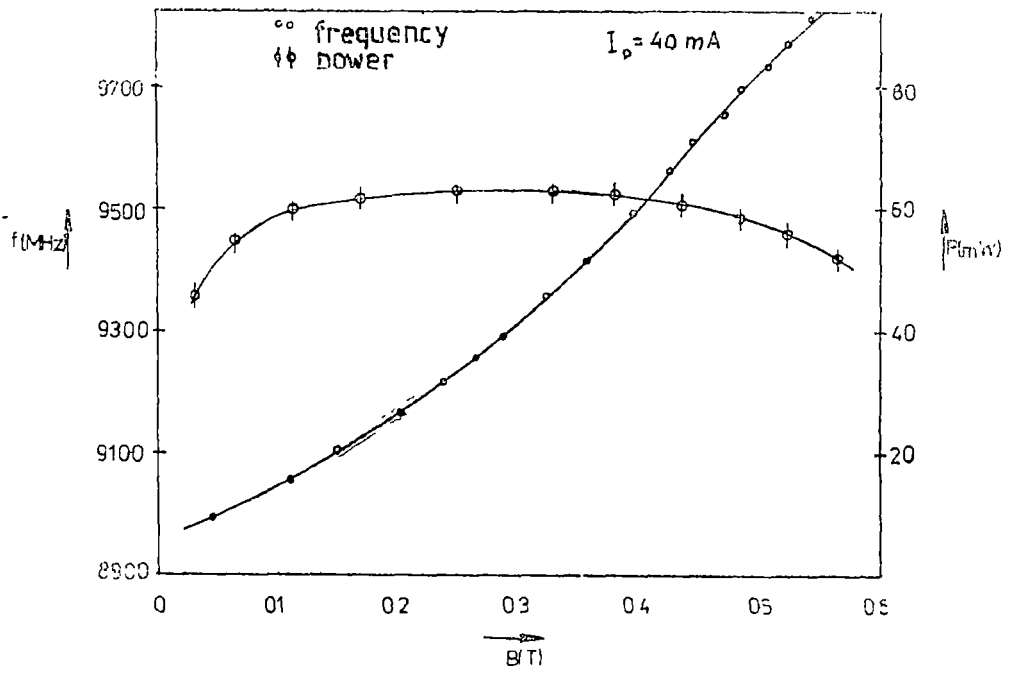

Fig 10 Power and frequency characteristics as a function of external d c magnetic field

tion of the external magnetic field is given in Fig. 10. From Fig 10 it also may be seen that the oscillator may be swept for more than 900 MHz, using a variable magnetic field from zero to 6000 Gs

REFERENCES

1 St Derwischev, I Hedkov, *Nachrichtentechnik*, **9**, p. 381 (1983)
2 A G Gurevici, „Magnitnii rezonans v ferritah i antiferromagneticah", Ed Nauka, Moskva, 1973
3 B Lax, K Button, „Microwave ferrites and ferrimagnetics", Mc Grow-Hill Book, Com. Inc New-York, 1973
4 E Sterk, M Balla, *Proc Conf on Soft Magn Mat*, **6**, Eger 6—9 Sept 1983.
5 G Grosh, B R Nag, *IEEE*, vol 47, nr 10, p 460, oct 1977

STUDIA UNIV BABEŞ-BOLYAI, PHYSICA, XXXIII, 2, 1988

LONG-LIFE RADIOISOTOPES IN RADIOACTIVE DEPOSITS OF CLUJ-NAPOCA CITY AREA

C. COSMA*, MARIA SĂLĂGEAN**, ANA PANTELICĂ**, T. FIAT*, L. MÂNZAT* and R. BULDUŞ***

Received October 28, 1988

ABSTRACT. — Data on the May 1986 radioactive fall-out in Cluj-Napoca area are presented. The measurements were performed by high resolution gamma ray spectrommetry The concentrations of long-lived isotopes ^{134}Cs, ^{137}Cs, ^{141}Ce, ^{106}Ru, ^{125}Sb, ^{110m}Ag were quantitatively determined and subsequently the concentrations of the short lived isotopes ^{132}Te, ^{132}I, ^{131}I, ^{140}Ba, ^{140}La, ^{103}Ru The total activity of the fall-out was more than 1000 kBq/m^2

Introduction. Following the accident of the Tchernobyl atomo-electrical center, a great quantity of radionuclides ($\simeq$100 MCi) escaped from the reactor. It is estimated that 13% of the inventory activity of Cs representing 1 5 MCi and 4% of the inventory activity of Sr representing 2.2 MCi of $^{89}Sr + ^{90}Sr$ left the reactor [1—2] Table 1 presents the radionuclides identified by gamma spectrommetry in the radioactive deposits of Cluj-Napoca City area.

Table 1

Radionuclides identified in samples from Cluj-Napoca

Nuclide	$T_{1/2}$	Fission efficiency (%)	Main gamma rays emitted (keV) and abundance (%)	Nuclide obtained
^{132}Te	3 2 days	4.7	228 (85%)	^{132}I (2 3 h)
^{132}I	2.3 h	—	673 (98%) 775 (66%) 520 (22%) 650 (20%)	^{132}Xe (stable)
^{131}I	8 1 days	3	364 (79%) 638 (9 3%)	^{131}Xe (stable)
^{140}Ba	12 8 days	6 3	537 (24%)	^{140}La (40 h)
^{140}La	40 h	1	1596 (95%) 487 (43%)	^{140}Ce (stable)
^{137}Cs	30 years	6 2	662 (85%)	^{138}Ba (stable)
^{134}Cs	2.06 years	—	605 (97%) 795 (85%)	^{134}Ba (stable)
^{136}Cs	13 days	0,007	1047 (80%) 818 (100%)	^{137}Ba (stable)
^{103}Ru	40 days	2 9	495 (88%) 611 (5%)	^{103}Rh (stable)
$^{106}Ru+$ ^{106}Rh	1 year	0 4	513 (21%) 624 (11%)	^{106}Pd (stable)
^{95}Zr	65 days	0.3	726 (55%) 760 (43%)	^{95}Nb (35 days)
^{95}Nb	35 days	0.4	768 (99%)	^{95}Mo (stable)
$^{99}Mo+$ ^{99}Tc	67 h + 6 h	6+1.2	142 (95%) 740 (10%)	^{99}Ru (stable)
^{129m}Te	41 days	0.35	475 (15%) 1120 (10%)	^{129}I (1.6 10^7 years)
^{141}Ce	32.5 days	5.7	145 (49%)	^{141}Pr (stable)
$^{144}Ce+$ ^{144}Pr	285 days	6+0.3	134 (11%) 696 (1.4%)	^{144}Pr (17.3 min)
^{110m}Ag	250 days	—	657 (94%) 885 (76%)	^{110}Cd (stable)
^{125}Sb	2.7 years	0.021	938 (32%) 1384 (27%)	^{125}Te (stable)

* *University of Cluj-Napoca, Faculty of Mathematics and Physics, 3400 Cluj-Napoca, Romania*
** *Institute of Nuclear Physics and Engineering, Bucharest, Romania*
*** *Institute of Scientific Research and Technologic Engineering in Electronics, 3400 Cluj-Napoca, Romania*

The radioactive deposits were very nonuniforme since the rains, especially the storms spectacularly increased the radioactive fall-out [3—6]. The torrential rain that fall on May 1-st, 1986 in the western half of Cluj-Napoca caused an intense contamination of short-life isotopes. $^{132}Te + ^{132}I$, ^{131}I, $^{140}Ba + ^{140}La$, $^{99}Mo + ^{99}Tc$, etc. [6]. Compared to the initial gamma global activity of this rain (4μCi/l), a decrease of $\simeq 40$ times was found in the radioactivity of the sample of water measured at the end of the year 1986, when the activity is given specially by the medium and the long-life isotopes ^{103}Ru, $^{106}Ru + ^{106}Rh$, $^{95}Zr + ^{95}Nb$, ^{137}Cs and ^{134}Cs

Experimental Method. Gamma global activity of the samples was measured by a 4 channel analysor of NP—424 type coupled to a NaI(Tl) detector of ample size(75 × 45 mm) The samples were measured in $\pi - 2\pi$ geometry put from the frontal face of the detector or in Marinelli type geometry [7]

The gamma spectra were obtained by a 512 channel analysor of NTA—512 type coupled to a GeLi detector of Kovo 327-1 type Also, it was used a 4096 channel analysor of Canberra type coupled to a GeLi detector of 65 cm^3 from (I F.I N) IPNE—Bucharest Efficiency and energy calibration was made using calibration sources measured in a similar geometry of 25 cm^3 The analysed sediment sample was collected from the roof of a building in the Mănăştur district (the western part of the city) on May 17, 1986 This sample, therefore, contains deposits collected from the period of April 29 to May 17, 1986 The volatile elements ^{131}I, ^{132}I, ^{103}Ru and ^{106}Ru partially left the sediment and so the analysed sample is somewhat deprived of these nuclides

The sediment was collected from around a fluvial drain (C) over a circular surface with a diameter of $\simeq 1.4$ m (zone B), Figure 1 The drain collects the water over a surface of 50 m^2 (zone A) After the sample got dry, the amount of collected sediment weighted 1 kg and represented $\simeq 75\%$ of the total amount of sediment existing in zone B This sample was then homogenised and parts of various weights from it were measured.

Results and discussions. From the gamma global activity measured at the date of collection ($1.8\ 10^6$ imp/100 s 30 g), considering the detection geometry and efficiency of the detector, as well as of the radionuclides presented in the gamma spectrum, a radioactive deposit of $\simeq 1000-1200$ kBq/m^2 was estimated for this area, much larger than the average estimated for Romania [8]. This fact finds its explanation in the torrential rain and storm that affected this area on May 1-st, 1986, date which coincides with the crossing of the radioactive cloud.

The dynamics of the evolution of the radioactivity of the sample of sediment is shown in Fig 2—5, which presents the gamma spectra of the sample recorded on various dates. May 17,1986, Nov 20, 1986; March 4, 1987, and July 7, 1988.

The spectra presented in Figures 2—3 are merely energetically calibrated, so they may be used only for the identification of radionuclides, whereas those in Fig. 4—5 are also calibrated in efficiency which permits the determination of the specific activity of each radionuclide. As one can see in Fig 5 the long-life radioactive isotopes in the examined deposit are · ^{137}Cs, ^{134}Cs, ^{144}Ce, ^{125}Sb, $^{106}Ru +$ $+ ^{106}Rh$ and ^{110m}Ag. On the spectrum from

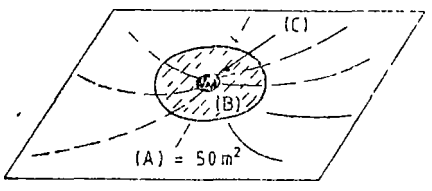

Fig 1. Zone of sample collection

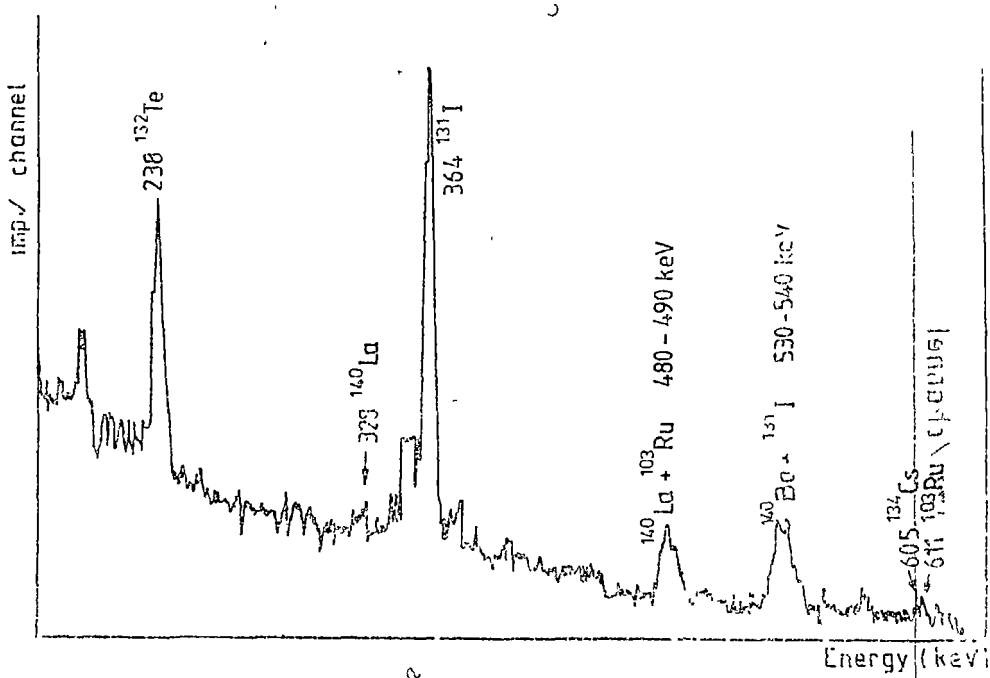

Fig. 2 Gamma spectrum of sample of May 17, 1986 (analyser NTA—512 M)

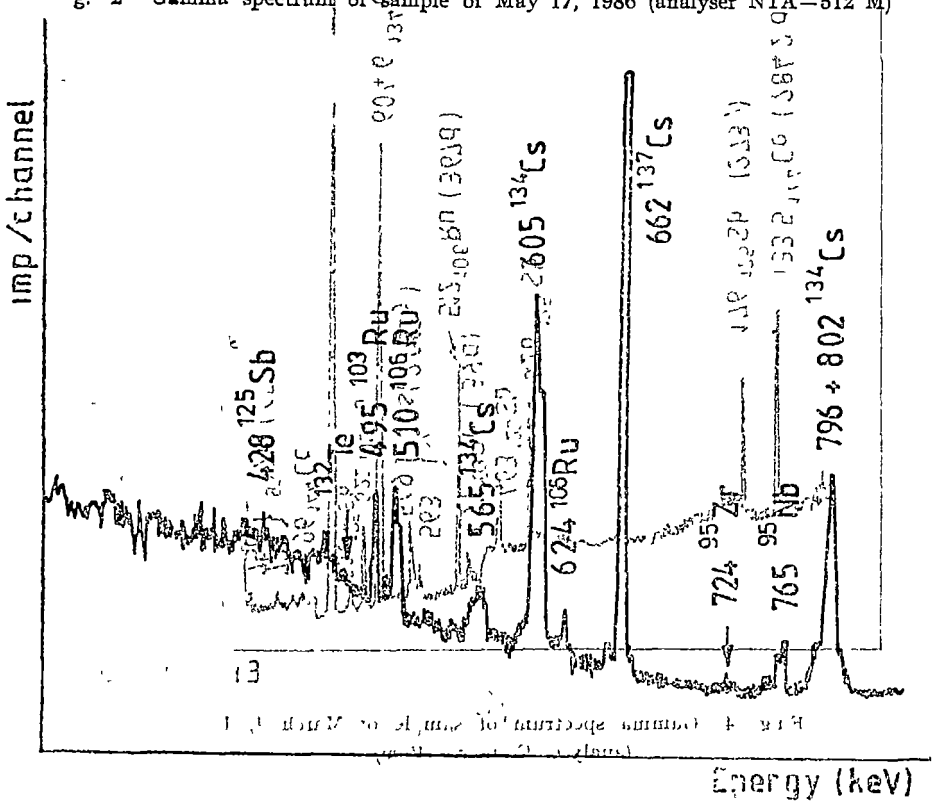

Fig 3. Gamma spectrum of sample of November 20, 1986 (analyser NTA—512 M)

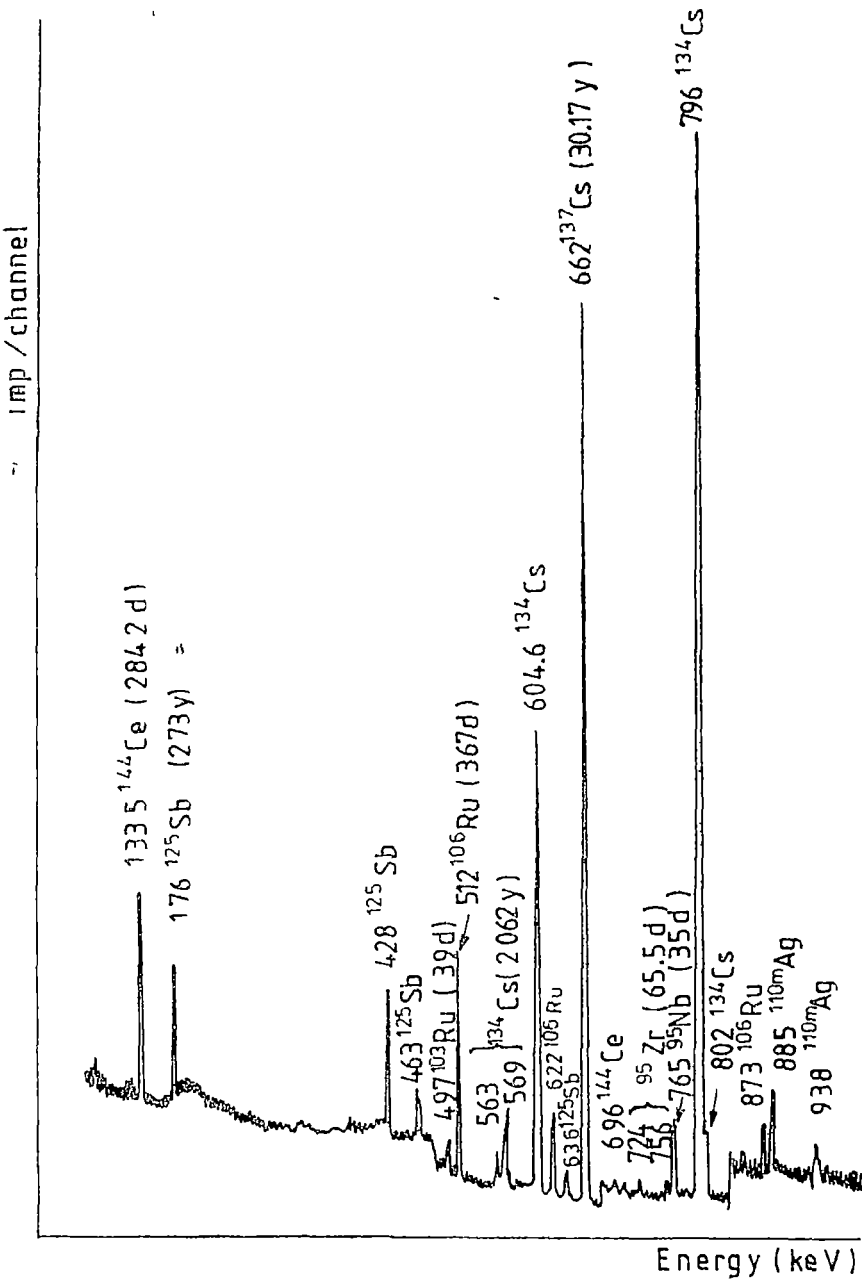

Fig 4 Gamma spectrum of sample of March 4, 1987
(analyser Canberra 4096)

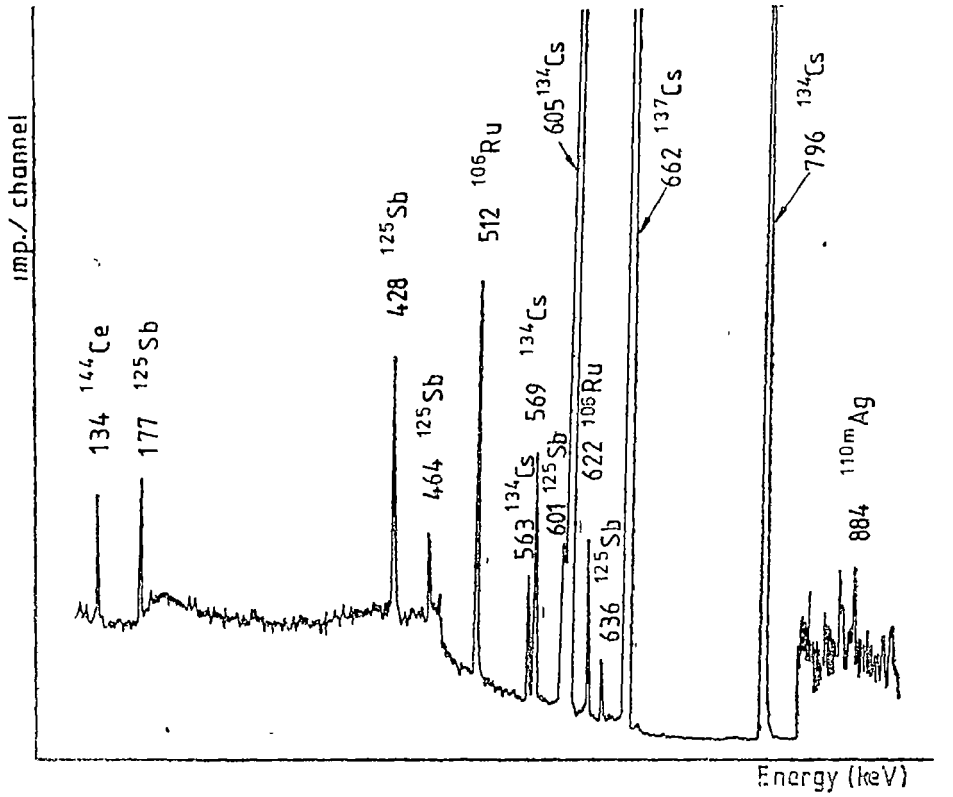

Fig 5 Gamma spectrum of sample of July 7, 1988
(analyser Canberra 4096)

Fig 3 and Fig 4 there also appear some mid-life isotopes $^{95}Nb + ^{95}Zr$ and ^{103}Ru

The composition of the mid-life and long-life radionuclides was calculated from these spectra at the moment of collection, Table 2, carried out with the relation

$$A_0 = A \cdot e^{\lambda \Delta t} \tag{1}$$

As for ^{95}Nb allowance was made for the fact that ^{95}Nb is not only a fission product but it also accumulates from ^{95}Zr, according to the scheme

$$^{95}Zr \xrightarrow[65,d\ 5ays]{\beta^-} {}^{95}Nb \xrightarrow[35\ days]{\beta^-} \ldots \tag{2}$$

while the ^{95}Nb activity is given by the relation

$$A_{Nb} = \frac{\lambda_{Nb}}{\lambda_{Nb} - \lambda_{Zr}} A_{Zr}(0) \left(e^{-\lambda_{Zr} t} - e^{-\lambda_{Nb} t}\right) \tag{3}$$

The radionuclides presented in Table 2, comprise a total beta deposit of 105 150 Bq/m^2 On analysing the spectra in Fig 2—4 one may calculate the

ratio $^{103}Ru/^{106}Ru \simeq 4$ This value coincides fairly well with the value that may becaluclated in Table 2, as well as with the values given by other authors [9—10] The ^{141}Ce contribution may be calculated from the ratio $^{141}Ce/^{144}Ce = 1.2$ [9] as well as from the value for ^{144}Ce in Table 1 The result being a contribution of 12 000 Bq/m^2 for ^{141}Ce.

Table 2

Activity of mid-life and long-life radionuclides at the moment of collection (May 17-th, 1986)

Nuclide	$T_{1/2}$	Specific activity (Bq/kg)	Deposit (Bq/m^2)
$^{144}Ce + ^{144}Pr$	284 days	190 500 ± 5%	10 000
^{125}Sb	2,73 years	76 400 ± 4%	2 000
^{103}Ru	39 days	1 628 600 ± 7%	43 200
$^{106}Ru + ^{106}Rh$	367 days	441 900 ± 4%	24 000
^{95}Zr	65,5 days	97 400 ± 12%	2 600
^{95}Nb	35 days	557 600 ± 5%	14 800
^{134}Cs	2.06 years	210 100 ± 1%	5 600
^{137}Cs	30 years	482 500 ± 1%	12 800
^{110m}Ag	250 days	5 300 ± 20%	150

For the ratio $^{131}I/^{103}Ru$ we consider a mean value of $\simeq 4$ This value results from the spectrum in Fig. 2 whereas a similar value was obtained by others as well [11]. In the rain water of May, 1-st, this ratio was about 6

For other ratios we take into consideration the following mean values, from Fig. 2—5: $^{132}Te/^{131}I \simeq 2$, $^{103}Ru/^{140}Ba \simeq 0{,}6$ and $^{103}Ru/^{129m}Te \simeq 1$ [11].

With these data we can calculate the contribution of the short-life radionuclides: 172 000 Bq/m^2 for ^{131}I, 688 000 Bq/m^2 for $^{132}Te + ^{132}I$, 120 000 Bq/m^2 for $^{140}Ba + ^{140}La$ and 43 000 Bq/m^3 for ^{129m}Te. For the total contribution we obtain the value of 1130 kBq/m^2, much larger than the average in Romania [8]. Recent determinations [12] have established for deposits in the city of Cluj-Napoca area a ratio of $^{90}Sr/^{137}Cs = 1/8$ The value for the deposit of ^{90}Sr in Bucharest area is 860 Bq/m^2 [13].

BIBLIOGRAPHY

1 A. A Abaghian *et al*, *Atomnaia Energhia*, **61** (5) 301 (1986)
2 * * * *Proceedings of AEIA Conference on the Nuclear Accident Tchernobyl*, Wien, 1986.
3 G. Kossl, W Varburgg, *PTB Mitteilungen*, **96**, 4, 249 (1986)
4 * * * *Radioactivity survey Data in Japan*, **80**, April, 1988.
5 * * * *Science et Vie*, **837**, May 1987.
6. C. Cosma *et al*, *Proc of Symposium „Meth, Models, Tech. in Phys"*, Cluj-Napca, 1987, p. 160.
7 C. Cosma *et al*, *Studia Univ. B—B ser. Physica*, **32** (2), 47 (1987)
8 D. Galeriu, M. Oncescu, *Preprint ICEFIZ*, RB—1987, Bucureşti—Măgurele 1987
9. S. Sonoc *et al*, *Proceedings of ICEFIZ Conference*, 23—24, oct 1987, Bucureşti—Măgurele, p. 73.
10. I. A Izrael *et al*, *Meteorologhia i ghidrologhia*, **2**, 5 (1987)
11 A Andrasi *et al*, *KFKI—1986—42/K Report*, Budapest, 1986
12. C. Cosma, A. Negoescu, *Proceedings of ICEFIZ Conference*, 7—8 oct 1988, Constanţa, p. 592.
13. N. Păunescu, I. Vâţă, *J. Radioanal. Chem*, *Letters*, **126** (2), 97 (1988).

STUDIA UNIV BABEŞ-BOLYAI, PHYSICA, XXXIII, 2, 1988

EPR INVESTIGATIONS IN THE SUPERCONDUCTOR $GdBa_2Cu_3O_x$

AL. NICULA*, A. V. POP*, AL. DAROBONT** and L. GIURGIU**

Received November 7, 1988

ABSTRACT. — EPR from Gd^{3+} ions in the high $T_c \simeq 90$ K superconductor $GdBa_2Cu_3O_x$ is reported The asymmetric line, g value independent with temperature, linewidth and the role of mixed valence Cu^{2+}_{III}, Cu^{2+}_{II} and Cu^{3+} is discussed The resonance of Gd^{3+} must be associated with a Cu^{2+} component of the signal, wich influences linewidth

Introduction. Since the discovery of high critical temperature T_c superconducting oxides [1 ; 2] a number of magnetic investigations have been achieved on the family of $YBa_2Cu_3O_{7-\delta}$ [3—10] The decrease of the mean Landé factor value g from 2 22 to 2 07, between $T = 4$ K and $T = T_c$, is ascriebed to a hole being transferred from cooper to oxygen [3] For T < 90 K, the thermal variations of lineshapes, g-values and intensities are differing This implies that the line at $g > 2{,}12$ cannot be related to a nonsuperconducting fraction of the orthorombic phase [4] Therefore the hole transfer from oxygen to cooper with decreasing T is characteristic of the orthorombic structure The EPR sigual and microwave absorption in thin films and bluk samples of $RBa_2Cu_3O_{7-\delta}$ (R = Y, Sm) is ascriebed to Cu^{2+} ions in non-superconducting regions and the low field one to flux penetration [5]

EPR investigations of Gd doped $YBa_2Cu_3O_{7-\delta}$ [4] evidence the shape modifications of the Gd^{3+} probe spectrum at lowest temperatures, being in relation with the fraction of Cu^{2+} ions in a non superconducting orthorhombic phase and the hole transfer from oxygen to cooper

Superconductor $GdBa_2Cu_3O_x$ studies were reported by [5; 10]

In this paper we report on the paramagnetic resonance of Gd^{3+} and discuss the role of mixed valence of Cu in superconductor $GdBa_2Cu_3O_x$

Experimental. The samples were prepared from stoichiometric amounts of dried high purity poweders of Gd_2O_3, $BaCO_3$ and CuO First the well mixed powder was heated to 850 °C in air for 24 h The product was reground, pressed into pellets and sintered to 950 °C in oxygen atmosphere for 18 h

The presence of a superconducting phase with $T_c > 80$ K was established by testing the Meissner effect on the samples cooled in liquid nitrogen

The electron paramagnetic resonance measurements were carried out at an ITIM spectrometer, in X band, on powder samples in silicon feet Merck, between room temperature and $T < T_c$.

Results and Discussion. The spectrum consists of a single, slightly-asymmetric line of width 1160 G at room temperature and 1040 G at 77 K (Fig 1). The asymmetry, wich is quite small as compared with even poor metals is

* *University of Cluj-Napoca, Faculty of Mathematics and Physics, 3400 Cluj-Napoca, Romania*
** *ITIM Cluj-Napoca, 3400 Cluj-Napoca, Romania*

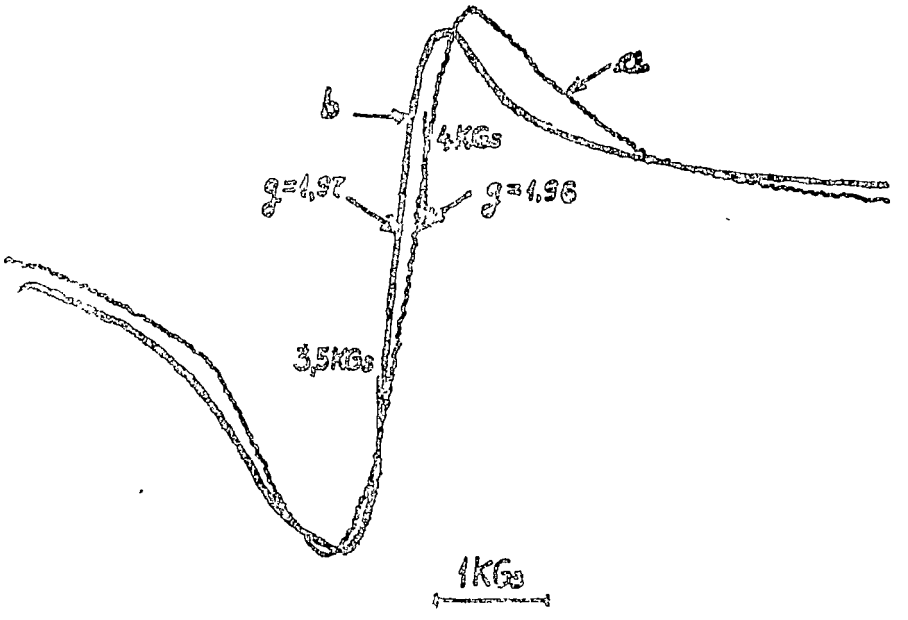

Fig. 1. EPR spectra recorded at room temperature (a) and at 77 K (b) from a superconductive sample $GdBa_2Cu_3O_x$

temperature independent. An asymmetric line shape can also be associated with internal field distributions in concentrated magnetic systems and the granular structure of sample.

The g-value of 1.96 ± 0.01 is temperature independent. This value corresponds Gd^{3+} in intermetallic compounds ($GdAl_2$, PdGd, AgGd with 3% Gd). The negative g shift from the unshifted $g = 2$, can not be explained the change and superchange interactions this to causeing the positive shift, an alternative being the occurrence of negative polarizations in superconductivity state.

The linewidth decreases with decreasing temperature, minimum value of this corresponds to $T_1 \simeq 90°K$. For $T < T_c$ the linewidth increases, therefore, T_1 correspounds to transition temperature T_c.

The different types of paramagnetic ions in superconducting samples influence specifically the linewidth. For the ion with great relaxation thime the resonance signal appears, the contribution of other paramagnetic ions being found in the shift and linewidth of the signal. The resonance of Gd^{3+} must be associated with a Cu^{2+} component of the signal, which influences linewidth [6]. In compounds such as "1—2—3 ($GdBa_2Cu_3O_7 = Gd^{3+}Ba_2^{2+}Cu^{3+}Cu_2^{2+}O_7^{2-}$) having both Cu—O, planes and chains Cu^{3+}-holes appear in the reaction $Cu^{3+} + O^{2-} \rightarrow Cu^{2+} + O^{1-}$, which transfer into the p-system A decrease in the number of holes (growth of Cu^{2+} content) and oxygen vacancies is formed primanly in chains, and eleads to increasein resistence. O. Oudet [8] has introduced a distinction between the notion of valence (or oxidation number o n) and that of ionicity,

this leads to the hypotesis of 3d cations of ionicity 2+ and o n higher than two (Cu^{2+}_{III} have o.n. III and ionicity 2+) Let us now describe the covalent bond between the cation Cu^{2+}_{III} and the oxigen O^{1-}_{II} The covalent bond is the result of an attraction between the third deep valence electron of the cation and the nucleus of the anions

In summary, we consider the Gd^{3+} ions with spin 7/2 not compensated, a part of the Gd— Gd interaction must be mediated by the polarization of conduction electrons on the Cu The temperature dependence of the linewidth for Gd^{3+} ions in the vicinity of T_c are related to the corresponding characteristics of the Cu^{2+} ions

REFERENCES

1 J G. Bednorz and K B Muller, *Z Physik*, **B 64** (1986), 189
2 M K Wu *et al*, *Phys Rev Lett*, **58** (1987), 908
3. S Benakki *et al*, *J Mater Res* **2** (6), Nov. Dec 1987, p 765—767
4 S Benakki *et al*, *Internat Conf of High. Temperat Supercond*, Interlaken Febr 29 — Mar 4, 1988, Swirzerland
5 J. Dumas *et al*, *Internat Conf of High Temperat Supercond*, Interlaken, Febr 29—Mar 4, 1988, Switzerland
6. F. Mehran *et al*, *Phys Rev*, vol. 36, nr 13, 1987
7. D Shaltiel *et al*, Solid State Commun (1987)
8 X Oudet, *Internat Conf of High Temperature Supercond*, Interlaken Feb 29—Mar 4 1988 Switzerland
9 I Ursu *et al*, *Rev Roum Phys*, Tome 33, Nr 2, p 175— 1988
10 H. Lutgemeir, *Internat Conf of High Temperature Supercond*, Interlaken Feb 29— Mar. 4, 1988, Switzerland.

STUDIA UNIV BABEŞ-BOLYAI, PHYSICA, XXXIII, 2, 1988

ELECTRON-POLARON INTERACTION IN HIGH TEMPERATURE SUPERCONDUCTORS

I. GROSU*

Received February 15, 1988

ABSTRACT. — Electron bipolaron interaction has been studied for a high temperature superconductor The bipolarons occur from the electrons which are in y narrow band and interact strongly with the phonons The electron-bipolaron interaction is described by a mixing term between the wide band electrons and the localized electrons with modified energy and Coulombian interaction The critical temperature of the superconductor is drastically enhanced and an increasing of T_c is possible

1 **Introduction.** The high temperature superconductivity recently discovered by Bednorz and Muller [1] has been explained by different authors through several non-phononic mechanisms, conventional phononic mechanism, the Bose concentration of the bipolarons or a mechanism related to the Jahn-Teller effect [2] At the present time, it is generally accepted (even if the isotopic effect was observed only for La-systems) that the electron-phonon interaction has an important contribution in the electron-electron interaction Chakraverty [3] showed that for a very strong electron-phonon interaction the electrons from a narrow band form pairs with opposite spins which are in fact called bipolarons If in a system there is an interaction between the itinerant electrons from a wide band and the localized electrons, the localized pairs can be transferred in the wide band and become delocalized via the interaction between two kinds of electrons

If the one-site repulsive Coulomb interaction between two electrons with opposite spins is weak, occurence of one-site bipolaron is possible The bipolaron sites can be regarded as a negative U-center, and influence of these centers on the superconducting critical temperature T_c of the wide band electrons has been studied previously [4] In Section 2 we present the model, and in Section 3 order parameters and critical temperatures are calculated, using the strongcoupling formalism from the theory of superconductivity We also analyse the dependence of U on concentration [5] in the case of the systems $(La_{1-x}M_x)_2CuO_{4-\delta}$ in connection with the variation of the lattice constant a with concentration x

* *University of Cluj-Napoca, Faculty of Mathematics and Physics, 3100 Cluj-Napoca, Romania*

2. The Effective Hamiltonian. ι) *Normal State.* We consider a system consisting of itinerat electrons "e" and a system of localized electrons interacting with the phonons If the electron-phonon is strong enough, the localized electrons behave like small polarons which are unstable against the bi-polaron formation This system (Fig 1) is described by the Hamiltonian

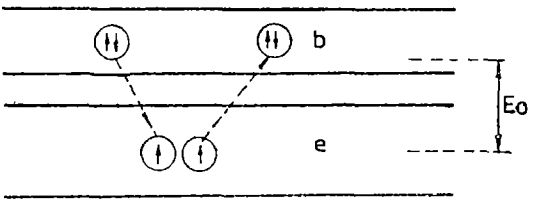

Fig 1

$$\mathcal{H} = \mathcal{H}_s + \mathcal{H}_t + \mathcal{H}_{\text{int}} \tag{1}$$

where

$$\mathcal{H}_t = \sum_{i} E_i c_i^+ c_i + U \sum_{i,\alpha} n_{i\alpha}\, n_{i-\alpha} \tag{2}$$

$$\mathcal{H}_s = \sum_{\vec{p},\alpha} [\varepsilon(\vec{p}) - E_0]\, c_{\vec{p}\alpha}^+ c_{\vec{p}\alpha} - g \sum_{\vec{p},\vec{p}'} c_{\vec{p}\uparrow}^+ c_{\vec{p}'\downarrow}^+ c_{\vec{p}'\downarrow} c_{\vec{p}\uparrow} \tag{3}$$

$$\mathcal{H}_{s-t} = \sum_{i,\vec{p}} [T_i(\vec{p})\, c_{\vec{p}}^+ c_i + h \quad c] \tag{4}$$

In the Hamiltonian (1) $\varepsilon(\vec{p})$ is the energy of the s-electrons, $c_{p\alpha}^+$, $c_{p\alpha}$ the operators of creation and annihilation of the itinerant electrons system, E_0 the difference between the centers of the two bands, E_i is given by

$$E_i = E_0 + \frac{\lambda^2}{v} \sum_{\vec{q}} \frac{1}{\omega(\vec{q})} \tag{5}$$

$$U = U_{a,b} - J - \frac{2\lambda^2}{v} \sum_{\vec{q}} \frac{1}{\omega(\vec{q})}\, e^{i\vec{q}(\vec{a}-\vec{b})} \tag{6}$$

where E_0 is the energy of the local level, $\omega(\vec{q})$ the phonon energy, $U_{a,b}$ the repulsive interaction between the nearest neighbours localized electrons, J is the superexchange, and $T_i(q)$ is the coupling constant between the localized electrons described by operators c_i^+ and c_i) and the itinerant electrons)

ι) *Superconducting state.* We introduce the superconducting order parameter

$$\Delta = g \sum_{\vec{p},\omega} \langle c_{\vec{p}\uparrow}\, c_{-p\downarrow} \rangle \tag{7}$$

and

$$\Delta_i = -\, U \sum_{i} \langle c_{i\uparrow}\, c_{i\downarrow} \rangle \tag{8}$$

which describes the electron-electron due to the interaction In the mean-field approximation we consider the Hamiltonian

$$\mathcal{H} = \mathcal{H}_s + \mathcal{H}_t + \mathcal{H}_{\text{int}} \tag{9}$$

where

$$\mathcal{H}_s = \sum_{\vec{p},\alpha} \varepsilon(\vec{p}) c^+_{\vec{p}\alpha} c_{\vec{p}\alpha} - \Delta \sum_{\vec{p}} (c^+_{\vec{p}\uparrow} c^+_{\vec{p}\downarrow} + h \cdot c) \tag{10a}$$

$$\mathcal{H}_t = \sum_{\alpha,\beta} E_{i\alpha}(n_{i\alpha\alpha} + n_{i\beta\beta}) - \Delta_t \sum_i (c^+_{i\alpha\alpha} c^+_{j\beta\beta} + h \quad c) \tag{10b}$$

$$\mathcal{H}_{\text{int}} = \sum_{i,\vec{p},\alpha} T_i(p)(c^+_{i\alpha} c_{p\alpha} + h \quad c) \tag{11}$$

In (10 b) the energy of the localized electrons was defined as $E_t = E_0 + U\langle n_{ja,\alpha}\rangle$, and we will consider the non-magnetic states of the localized electrons If we take a-site and b-site as a single site, the model corresponds to the negative U-center discussed by Anderson [6] and reconsidered recently by different authors [7—8] for the high-temperature superconductivity

3 **The Order Parameter.** In order to calculate the critical temperature of the superconducting state described by the order parameter (7) we will study for the beginning the spectrum of the superconducting elementary excitations at $T = 0$ The Green function for the itinerant electron is

$$\hat{G}^{-2}(\vec{p}, z) = zZ(z)\hat{\tau}_0 - \varepsilon(\vec{p})\hat{\tau}_3 - \Phi(z)\hat{\tau}_1 = z\hat{\tau}_s - \varepsilon(\vec{p})\hat{\tau}_3 - \hat{\Sigma}_s(z) \tag{12}$$

and for the localized electron is

$$\hat{G}_t(z) = zZ_t(z)\hat{\tau}_0 - E_t\hat{\tau}_3 - \Phi_t(z)\hat{\tau}_1 = z\hat{\tau}_s - E_t\hat{\tau}_3 - \hat{\Sigma}_t(z) \tag{13}$$

where the self energies $\hat{\Sigma}_s(z)$ and $\hat{\Sigma}_t$ can be calculated using $T_i(p)$ as a perturbation

In the framework of the strong-coupling theory [9] we get

$$Z(z) = 1 + \frac{|T_i(p)|^2 Z_i(z)}{D(z)} \tag{14a}$$

$$\Phi(z) = \Delta + \frac{|T_i(p)|^2 \Phi_i(z)}{D(z)} \tag{14b}$$

and

$$Z_t(z) = 1 + \frac{|T_i(p)|^2 \pi N(0)\Phi(z)}{[\Phi^2(z) - z^2Z^2(z)]^{1/2}} \tag{15a}$$

$$\Phi_t(z) = \Delta_t + \frac{|T_i(p)|^2 \pi N(0)\Phi(z)}{[\Phi^2(z) - z^2Z^2(z)]^{1/2}} \tag{15b}$$

where

$$D(z) = \Phi_i^2(z) + E_i^2 - z^2Z_i^2(z) \tag{16}$$

and N(0) is the density of states for the itinerant electrons at the Fermi level With these results we can analyse the spectrum of the elementary excitations and calculate critical temperatures

a) *The energy spectrum* Let us define

$$\Phi(z) = \Delta_g(z)Z(z) \tag{17}$$

where $\Delta_g(z)$ is the gap in the energy spectrum of the superconducting elementary excitations.

From Eqs. (14)—(15) we obtain

$$\Delta_g(z) = \Delta \frac{[1 - dF(z)]}{[1 + dF(z)]} \tag{18}$$

where

$$F(z) = \frac{|T_s(p)|^2}{D(z)} \tag{19}$$

and

$$d = -\Delta_s/\Delta \tag{20}$$

Eq (16) can be transformed using Eqs (14)—(15) as

$$D(z) = V^2 + E_s^2 - z^2 + 2z \frac{[\Delta_s \Phi(z) - z^2 Z^2(z)]}{[\Phi^2(z) - z^2 Z^2(z)]^{1/2}} \tag{21}$$

where $V = \pi N(0)|T_s(p_0)|^2$, p_0 being the Fermi wave vector In the limit $V \gg \omega_D \gg \Delta_g(z)$ and $\omega \ll \omega_D$ (the parameter ω_D is of the order 700 K for the high temperature superconductors)

Eq (21) becomes

$$D(z) \cong V^2 + E_s^2 \tag{22}$$

and the gap will be expressed as

$$\Delta_g = f\Delta \tag{23}$$

where

$$f = \frac{1 - ad}{1 + a} \tag{24}$$

$$a = \frac{V}{\pi N(0)(V^2 + E_s^2)} \qquad d = \frac{N_s(0)}{N(0)}, \; N_s(0) = \frac{V}{\pi(V^2 + E_s^2)} \tag{25}$$

is the effective density of states for the localized electrons at the Fermi level.

Eq. (23) shows that gap is not identical with the order parameter if the superconducting electrons interact with the localized ones.

b) *The Critical Temperatures.* In order to calculate the critical temperatures T_p (defined by $\Delta(T_p) = 0$) and T_c (defined by $\Delta(T_c) = 0$), we consider the self — consistent equations (7) and (8) written as

$$\Delta = N(0)g\pi T \sum_{p\,\omega} \frac{\Phi(\omega)}{[\Phi^2(\omega) + \omega^2 Z^2(\omega)]^{1/2}} \tag{27}$$

and

$$\Delta_s = -U\pi T \sum_{\omega} \frac{\Delta}{D(\omega)} + \sum_{\omega} \frac{V\Phi(\omega)}{[\Phi^2(\omega) + \omega^2 Z^2(\omega)]^{1/2}} \tag{28}$$

where we performed the analytical $z + i\delta \to i\omega$ and $\omega = (2n + 1)\pi T$.

From Eq (28) we get

$$T_p = \frac{E_i}{\ln \frac{\tilde{U} + 2E_i}{\tilde{U} + 2E_i}} \tag{29}$$

where

$$\tilde{U} = U\left(1 + \frac{V}{dE_i}\right) \tag{30}$$

Eq. (29) can be approximated as

$$T_p \cong \frac{U}{2}\left(1 + \frac{VE_i}{d}\right) \tag{31}$$

and using for a the expression given by Keiser [9]

$$T_p = \frac{U}{2}\left[1 + \frac{VN(0)|g|E_i}{N_i(0)U_{\text{eff}}}\right] \tag{32}$$

where

$$U_{\text{eff}} = \frac{U}{1 + U/\pi E_i \tan^{-1}\frac{E_i}{V}} \tag{33}$$

Eq. (32) can be considered as the expression for the occurrence of the polarons which appear to be pairs of localized electrons due to the potential U, which is in fact the Coulomb interaction strongly enhanced by the electron-phonon interaction (See Appendix)

From Eqs (27) and (17) we can calculate the critical temperature T_c from the equation

$$\Delta_g = fg\pi T \sum_{\omega} \frac{\Delta_g}{\sqrt{\Delta_g^2 + \omega^2}} \tag{34}$$

using the result

$$\Delta_g(0) \equiv \Delta_g(T = 0) = \frac{2\omega_D}{f} \exp\left[-\frac{1}{N(0)|g|f}\right] \tag{35}$$

The critical temperature T_c will be given by

$$\ln \frac{T_c}{T_{co}} = \frac{f - 1}{fN(0)g} \tag{36}$$

which gives

$$T_c = T_{co} \exp\left[\frac{a(d+1)}{ad - 1}\right] \tag{37}$$

and we see from Eq (37) that if

$$\left(\frac{N_i(0)}{N(0)}\right)^2 U_{\text{eff}} > 0 \tag{38}$$

he critical temperature T_c increases with U_{eff} for a fixed g. If V is small J_{eff} can be approximated by U and using now

Eq. (6), we get (See Appendix)

$$U = U_0 + \frac{\lambda^2}{a} C \tag{39}$$

where C is a constant.

Fukuyama and Hasegawa [5] considered that the electron-phonon coupling constant depends on x by as

$$\lambda = \frac{N(0) f(x)}{\omega_D} \tag{40}$$

where

$$f(x) = \begin{cases} b_0 + x b_1; & x < x_c \\ b_1; & x > x_c \end{cases}$$

x_c being a critical concentration obtained from the variation with x of the lattice constant $a(x)$ This variation has the form

$$a(x) = \begin{cases} a - \alpha x; & x < x_c \\ \beta; & x > x_c \end{cases} \tag{441}$$

where b_0, b_1, α and β are constants.

For Eqs. (39—41) we see that for $x < x_c$, $U(x)$ will increase with x which makes the condition (38) plausible.

4 **Discussions.** We showed that the strong electron-phonon coupling may give rise to an increasing in the critical temperature of superconducting electrons interacting with the polarons. Coulomb interaction U has been calculated for this system and is drastically affected by the concentration x in the systems $(La_{1-x}M_x)_2CuO_4$ If V is small and $U \cong 0.2$ eV the polarons appear above $T_p \cong$ $\cong$ 600 K and in this case the critical concentration is $x = 0\,2$. The $T_c(x)$ has a maximum at $x = 0\,05$ which is 60 K is $\omega_D = 700$ K.

Appendix

Let us consider the coulombian interaction U given by (6) as

$$U = U_{ab} - I - \frac{2\lambda^2}{V} \sum_{\vec{q}} \frac{1}{\omega(\vec{q})} e^{i\vec{q}\vec{R}} \tag{A 1}$$

where we will consider

$$\omega^2(q) = \omega_0^2 + \omega_1^2 \cos qa$$

a being the constant lattice

The summation over q can be transformed in an integral and we have

$$S = \frac{1}{V} \sum_{\vec{q}} \frac{1}{\sqrt{\omega_0^2 + \omega_1^2 \cos qa}} e^{i\vec{q}\vec{R}} = \frac{4\pi}{(2\pi)^3} \int \frac{q\, dq \sin qR}{\sqrt{\omega_0^2 + \omega_1^2 \cos qa}} \tag{A.2}$$

In (a 2) we take $R = a$ and the expression for S becomes

$$S = \frac{1}{2\pi^2 a^2 \omega_0^2} \int_0^{q_D} \frac{x \sin x}{\sqrt{1 + \Omega^2 \cos x}}\, dx \tag{A 3}$$

where $\Omega^2 = \omega_1^2/\omega_0^2$ and q_D is the wave vector associated with the Debye energy ω_0 The integral (A 3) can be performed and we get

$$S = -\frac{1}{\pi^2 \omega_0^2 \Omega^2} \left[q_D^2 a (1 + \cos q_D a \cdot \Omega^2) + \mathbf{E}\left(\frac{q_D a}{2}, \sqrt{\frac{2\Omega^2}{1 + \Omega^2}} \right) \right] \tag{A 4}$$

where $E(\varphi, k)$ is the elliptic integral

$$\mathbf{E}(\varphi, k) = \int_0^{\varphi} d\theta \sqrt{1 - k^2 \sin^2 \theta} \tag{A 5}$$

For small values of Ω ($\omega_0 \gg \omega_1$) we obtain

$$S = -\frac{q_D}{\pi \omega_1^2 a} \tag{A 6}$$

Then we can write (A 1) as

$$U = U_0 + \frac{2\lambda^2}{a} C \tag{A.7}$$

where

$$C = \frac{q_D}{\pi \omega_1^2}, \quad U_0 = U_{ab} - I$$

REFERENCES

1. J. G Bednorz and K A Muller, *Z Phys*, **B 64,** 189 (1986)
2 T.M Rice, *Z. Phys* **B 67,** 141 (1987)
3 B. K Chakraverty, *J Physique*, **42,** 1351 (1981)
4 C S Ting, D N Talwar and K L. Nagi, *Phys Rev Lett*, **45,** 1213 (1980)
5 H. Fukuyama and Y Hasegawa, *J Phys Soc Jpn*, **56,** 1312 (1987)
6. P W Anderson, *Phys Rev Lett*, **34,** 953 (1975)
7 J Ranninger and S Robaszkiewich, *Physica*, **135 B,** 468 (1985)
8 K Nasu, *Phys Rev*, **B 35,** 1748 (1987)
9 A B Kaiser, *J Phys*, **C 3,** 410 (1970)

STUDIA UNIV. BABEŞ—BOLYAI, PHYSICA, XXXIII, 2, 1988

DECONVOLUŢIA DE TIP SPLINE APLICATĂ ÎN SPECTROSCOPIA RES LOCALIZATĂ

AL. NICULA*, S. AŞTILEAN*, S. NICULA** and AL. DUNCA***

Received December 10, 1988

ABSTRACT. — **Spline-Type Deconvolution Applied in Localized RES Spectra.** A deconvolution method is used for ESR imaging, in which ESR spectrum is divided into picewise functions and each function is approximated to a cubic spline function and then deconvolution using the momentum of the resolution function The obtained results show that the method works best when the width of picewise function is equivalent to that of the resolution function and is very strong against noise

Introducere. Formarea imaginilor de spin în spectroscopia RES localizată (ESR Imaging), presupune prelucrarea proiecţiilor densităţii de spin [1, 2]. Deconvoluţia spectrală este una din problemele de maximă importanţă. În RES localizată apar, pe lîngă fenomenele intrinseci care lărgesc linia, lărgiri suplimentare datorate gradientului de cîmp magnetic. Ţinînd seama de valorile practic limitate ale gradientului utilizat, este dificil uneori de a distinge între componentele spectrale datorate despicărilor hiperfine, de exemplu, şi cele datorate gradientului. Astfel, în cîmp magnetic de gradient constant lărgimea liniei spectrale ΔB este:

$$\Delta B = \Delta B_i + \Delta B_g \tag{1}$$

unde ΔB_i este lărgimea intrinsecă, iar ΔB_g este lărgimea introdusă de gradient.

Scopul metodelor de deconvoluţie în RES localizată constă în decodificarea distribuţiilor spaţiale ale centrilor paramagnetici din spectrele-proiecţie.

Deconvoluţia spectrelor proiecţie. Să admitem prin funcţia $g(B)$ reprezentarea distribuţiei spectrale intrinseci a răspunsului sistemului de spini sau funcţia de formă a liniei de absorbţie RES în cîmp uniform. Fie distribuţia eterogenă $\rho\ (x, y, z)$ a spinilor electronici din probă. Putem defini funcţia de distribuţie în lungul unei axe.

$$n(z) = \int\int \rho(x, y, z)\, dxdy \tag{2}$$

Dacă proba este plasată într-un cîmp magnetic de gradient constant, atunci suprafeţele pe care se integrează relaţia (2) vor fi secţiuni plasate în acelaşi cîmp magnetic. Pentru oricare altă orientare a gradientului relaţia (2) poate fi scrisă în mod corespunzător.

* *Facultatea de Matematică şi Fizică, Univ din Cluj-Napoca, 3400 Cluj-Napoca, Romania*
** *Liceul „Dragoş Vodă", 4925 Sighetu Marmaţiei, Romania*
*** *Şc. Gen Nr 2, 3475 Dej, Somania*

Dependența liniară între cîmpul magnetic și coordonata pe axă ne permite să stabilim relația.

$$n(z) = f(B_z)\frac{dB_z}{dz} = f(B_z)G_z \tag{3}$$

unde $f(B_z)$ este distribuția de spini exprimată în coordonate experimentale Semnificația fizică a produsului de convoluție între două funcții ne permite exprimarea analitică a unui spectru în RES localizată

$$s(B) = \int_{-\infty}^{+\infty} f(B')\, g(B - B')\, dB' \tag{4}$$

Astfel spectrul convoluat $s(B)$ codifică distribuțiile spațiale prin funcția $f(B)$. Rezolvarea acestei ecuații, sau deconvoluția, va stabili $f(B)$ pe baza cunoașterii formei liniei $g(B)$ (în cîmp magnetic omogen) și a spectrului proiecție $s(B)$ (în cîmp magnetic de gradient constant și la diferite orientări)

În practica reconstrucției distribuției spațiale de spini, corectitudinea imaginilor produse va depinde esențial de acuratețea deconvoluției realizate. Proiecțiile deconvoluate formează datele de intrare în algoritmii de reconstrucție

În literatură cele mai utilizate metode de deconvoluție sînt de tip Fourier [3, 4]. În această lucrare prezentăm posibilitatea de realizare a deconvoluției în spectroscopia RES localizată printr-o metodă de tip *spline*

Deconvoluția de tip spline. Dezvoltată numeric, metoda prelucrează spectrele proiecții în spațiul datelor experimentale. Deși binecunoscute avantajele funcțiilor spline, metoda nu a fost valorificată încă efectiv în spectroscopia RES localizată (ESR Imaging), optimizarea fiind în curs de elaborare [5] Admitem că funcția — proiecție $f(x)$ din relația (4) poate fi dezvoltată în serie Taylor

$$f(x - l) = f(x) - f'(x)\, l + \frac{2}{2} f''(x) l^2 - \frac{1}{6} f'''(x)\, l^3 + \ldots \tag{5}$$

substituind în relația (4), se obține.

$$s(x) = f(x)\, M_0 - f'(x)\, M_1 + \frac{1}{2} f''(x)\, M_2 - \frac{1}{6} f'''(x)\, M_3 \tag{6}$$

unde:

$$M_m = \int_{-\infty}^{+\infty} l^m g(l)\, dl$$

reprezintă *momentele* funcției de formă a liniei de RES Admitem că $f(x)$ poate fi reprezentată pe subintervale prin funcții spline cubice

$$f(x) = \sum_{k=1}^{n-1} s_k(x) \tag{7}$$

unde

$$\check{s}_k(x) = \begin{cases} 0 & \text{dacă } x < \xi_k \\ a_k x^3 + b_k x^2 + c_k x + d_k, & \text{dacă } \xi_k \leqslant x \leqslant \xi_{k+1} \\ 0 & \text{dacă } x > \xi_{k+1} \end{cases} \tag{8}$$

$\xi_1, \xi_2, \ldots, \xi_n$, fiind nodurile funcțiilor spline definite mai sus Alegem astfel nodurile încît $f(x) = 0$ dacă $x > \xi_n$ și $x < \xi_1$, iar în seria Taylor (5) termenii de ordin > 4 să poată fi neglijați Admitem că spectrul convoluat poate fi dezvoltat prin funcții spline cubice, cu aceleași noduri dar cu coeficienți diferiți:

$$s(x) = \sum_{k=1}^{n-1} \check{S}_k(x) \tag{9}$$

unde

$$\check{S}_k(x) = \begin{cases} 0 & \text{dacă } x < \xi_k \\ A_k x^3 + B_k x^2 + C_k x + D_k, & \text{dacă } \xi_k \leqslant x \leqslant \xi_{k+1} \\ 0 & \text{dacă } x < \xi_{k+1} \end{cases}$$

Prin identificare se stabilesc relațiile

$$\begin{aligned} a_k &= A_k/M_0 \\ b_k &= B_k/M_0 + 3a_k M_1/M_0 \\ c_k &= C_k/M_0 + 2b_k M_1/M_0 - 3a_k M_2/M_0 \\ d_k &= D_k/M_0 + C_k M_1/M_0 - b_k M_2/M_0 + a_k M_3/M_0 \end{aligned} \tag{10}$$

Să notăm că o funcție de formă simetrică (liniile RES Gaussiene sau Lorentziene) are toate momentele de ordin impar nule Algoritmul procedurii va cuprinde următorii pași

a) se interpolează spectrul proiecție experimental $s(x)$ prin setul de funcții spline cubice din relația (9), stabilindu-se astfel nodurile ξ_k și setul de coeficienți $\{A_k\}$, $\{B_k\}$, $\{C_k\}$ și $\{D_k\}$, pentru $k = \overline{1, n-1}$.

b) se calculează primele patru momente ale liniei RES în cîmp omogen.

c) pe baza relațiilor (10) se exprimă setul de coeficienți $\{a_k\}$, $\{b_k\}$, $\{c_k\}$ și $\{d_k\}$, pentru $k = 1, n-1$

d) Acești coeficienți împreună cu nodurile ξ_k determină complet pe baza relației (7) valorile funcției proiecție pentru orice $x \in [\xi_1, \xi_n]$

Dacă admitem dezvoltarea proiecției prin setul de funcții spline din relația (7), atunci dezvoltarea în serie Taylor din relația (5) este riguroasă numai dacă argumentele l și $x - l$ aparțin la același subinterval de definiție a unei funcții spline, adică $l \in [\xi_k, \xi_{k+1}]$, și de asemenea $x - l \in [\xi_k, \xi_{k+1}]$. Această condiție este aproximativ îndeplinită numai dacă funcția de formă a liniei este destul de rapid descrescătoare spre zero cu creșterea lui $|x|$ În spectroscopia RES localizată această metodă dă cu siguranță rezultate corecte dacă lărgimea funcției spline între noduri este comparabilă cu lărgimea liniei RES Erorile care apar inevitabil în exprimarea proiecției cînd $x \to \xi_k$ pot fi reduse prin extrapolări și alegerea unui număr corespunzător de noduri

Concluzii: În concluzie se remarcă posibilitatea aplicării cu succes a metode spline în spectroscopia RES localizată. Sînt evidente următoarele avantaje a) fiind procedură monopas nu amplifică diferitele tipuri de erori, în contrast cu procedurile iterative; b) se evită netezirile exagerate şi oscilaţiile parazite c) erorile de trunchiere nu afectează restul valorilor proiecţiilor în contrast cu metodele Fourier [6].

Metoda de tip spline îmbogăţeşte astfel numărul procedurilor de deconvoluţie practicate în RES localizată (ESR Imaging), neexistînd în fond o metodă universal valabilă.

BIBLIOGRAFIE

1 K Ohno, *Magnetic Resonance Review*, vol 11, 275—310, (1987).
2 Al Nicula, S. Aştilean, M. Todică, *Stud. şi Cercet. de Fiz.*, nr. 2, (1989) (sub tipar).
3 H Fujii, L. I. Berliner, *J. Magn. Reson.*, Vol. 68, 377—382, (1986).
4. D C. Champeney, „Fourier Transforms and Their Physical Applications", Acad Press (1973)
5 K Ohno *Bull. of the Fac. of Eng.*, no. 114, 33—40, (1983).
6. Deutsch, M., Beniaminy I., *Rev. Sci. Intru.*, vol. 53, p. 90 (1982).

STUDIA UNIV BABEŞ—BOLYAI, PHYSICA, XXXIII, 2, 1988

UNSTABLE ORBITS AROUND PULSATING STARS

VASILE MIOC*, ÁRPÁD PÁL and IOACHIM GIURGIU*****

Received December 15, 1988

ABSTRACT. — The motion of a particle around a pulsating star is studied from three points of view stability, evolution of the unstable orbit, and time scale for perturbations Two applications are made, for an RR Lyrae pulsating star and for a long-periodic variable. The orbits are proved to be unstable at different time scales, according to the initial distance of the particle.

1. **Perturbing Acceleration and Equation of Motion.** Let us consider a pulsating star of constant mass M and radius R, whose luminosity L changes according to a law of the type (e.g. [2, 6, 9]):

$$L(t) = L_0(1 + a_p \sin (n_p t)), \tag{1}$$

or:

$$L(t) = L_0(1 + a_p \sin (2\pi t/T_p)), \tag{2}$$

where L_0 is a mean luminosity, while a_p, n_p, T_p are respectively the amplitude, frequency and period of pulsation. Also consider a spherical, homogeneous particle of constant albedo, orbiting the given star at a distance r. If the only two forces acting on the particle are the gravitation and the radiative force, the perturbing acceleration undergone by the particle will be

$$F_r = K/r^2, \tag{3}$$

where we denoted

$$K = AL(t)/(4\pi mc), \tag{4}$$

or (equivalent):

$$K = 3L(t)/(16\pi r' \rho c). \tag{5}$$

In these formulae, A is the effective cross-sectional area of the particle, m, r', ρ are respectively the mass, radius and density of the particle, while c denotes the speed of light.

Since the resulting force acting on the particle is central, the motion will be plane and featured by the differential equation

$$d^2r/dt^2 - C^2/r^3 = -G(M + m)/r^2 + K/r^2, \tag{6}$$

where C is the constant angular momentum and G is the gravitational constant.

* *Centre for Astronomy and Space Sciences, 3400 Cluj-Napoca, Romania*
** *University of Cluj-Napoca, Faculty of Mathematics-Physics, 3400 Cluj-Napoca, Romania*
*** *Industrial Secondary School, 3379, Baia de Arieş, Romania*

If we introduce the notations

$$H = G(M + m) - 3L_0/(16\pi r' \rho c), \tag{7}$$

$$f(t) = (G(M + m)/H - 1)\, a_p \sin(2\pi t/T_p), \tag{8}$$

$$\mu = H\,(1 - f(t)), \tag{9}$$

the equation of motion (6) will acquire the form

$$d^2r/dt^2 - C^2/r^3 = -\mu/r^2, \tag{10}$$

namely the same form as in the case of the two-body problem, but this time μ is time-dependent. In other words, we deal with a generalization of the Kepler problem [7].

In order to have always the particle under the gravitational influence of the star, we naturally suppose that $\mu > 0$. Taking into account (7)—(9), this condition can be written as follows

$$0 < G(M + m)/H - 1 < 1 \tag{11}$$

For subsequent purposes we shall denote

$$\alpha = a_p(G(M + m)/H - 1), \tag{12}$$

$$g(t) = \sin(2\pi t/T_p) \tag{13}$$

One easily observes that $0 < \alpha < 1$. We shall consider that the pulsation amplitude is sufficiently small to have $0 < \alpha \ll 1$. In this case, with (8), (12) and (13), we can write

$$f(t) = \alpha g(t), \tag{14}$$

where α is a small parameter.

2. **Stroboscopic Equations of Motion.** Consider that at the initial instant $f(0) = 0$. Also consider that the initial orbit is circular of radius r_0. In this case at the moment $t = 0$ we are in the frame of the two-body problem and we have $r_0 = C^2/H$.

Let us introduce the dimensionless variables $x(|x| < 1)$ and τ [2, 7—9,13] by means of the relations

$$r = r_0(1 + x), \tag{15}$$

$$t = r_0^{3/2} H^{-1/2} \tau. \tag{16}$$

In other words, x is the dimensionless perturbation of the radius vector, while τ is a dimensionless time. One easily sees that (16) can also be written

$$\tau = 2\pi t/T_0, \tag{17}$$

where T_0 is the period of the Keplerian motion on a circular orbit of radius r_0.

Replacing (15) and (16) into (10), taking into account (9), and expanding in x, the equation of motion becomes to first order in x

$$d^2x/d\tau^2 + (1 + 2f(\tau))x = f(\tau) \tag{18}$$

In order to study the motion featured by (18), we apply the stroboscopic method [4], whose principle was described in [7—9, 13] and will not be repeated here. For this purpose, we consider the trajectory in the phase plane $(x, dx/d\tau)$, in polar coordinates $(y^{1/2}, \psi)$ introduced as follows:

$$\begin{aligned} y &= x^2 + (dx/d\tau)^2, \\ \psi &= \tan^{-1}((dx/d\tau)/x), \end{aligned} \tag{19}$$

or:

$$\begin{aligned} x &= y^{1/2}\cos\psi, \\ dx/d\tau &= y^{1/2}\sin\psi. \end{aligned} \tag{20}$$

We also must take into account the following relations

$$f(\tau) = \alpha g(\tau), \tag{21}$$

$$\hat{\tau} = \alpha\tau, \tag{22}$$

$$\Delta\theta = \Delta\psi + 2\pi. \tag{23}$$

The equation (21) is (14) written for the dimensionless time. By (22) we introduced a new dimensionless time, $\hat{\tau}$, called stroboscopic time. As to (23), the variation of the polar angle ψ was replaced by its variation modulo 2π, since this is all we are interested in; the symbol Δ signifies the variation of the respective quantity corresponding to a variation of τ between 0 and 2π.

With all these considerations, we can pass from (18) to an equivalent first order system. The process is long enough and was exposed in detail in [2, 7, 9] We shall not repeat here the successive transformations of the equation (18); at the end one obtains the system.

$$\begin{aligned} dy/d\hat{\tau} &= ((C_1\sin\theta - S_1\cos\theta)y^{1/2} - (C_2\sin(2\theta) - S_2\cos(2\theta))y)/\pi, \\ d\theta/d\hat{\tau} &= ((C_1\cos\theta + S_1\sin\theta)y^{-1/2} - C_2\cos(2\theta) - S_2\sin(2\theta) - C_0)/(2\pi), \end{aligned} \tag{24}$$

where we denoted:

$$S_j = \int_0^{2\pi} g(\tau)\sin(j\tau)d\tau, \; C_j = \int_0^{2\pi} g(\tau)\cos(j\tau)\,d\tau, \tag{25}$$

with $j = 0, 1, 2$. By (13) and (17), we have in (25)

$$g(\tau) = \sin(k\tau), \tag{26}$$

in which we introduced the notation:

$$k = T_0/T_p. \tag{27}$$

Equations (24) are the stroboscopic equations of motion. They are very useful for studying the motion over very long time intervals.

3. **Unstable Orbit.** We have shown [7] that the stroboscopic equations in the form (24) admit an equilibrium point, whose polar coordinates in the phase plane are given by

$$\tan \theta_e = (C_1S_2 - S_1(C_2 + C_0))/(S_1S_2 + C_1(C_2 - C_2)), \tag{28}$$

$$y_e^{1|2} = C_1/((C_2 + C_0) \cos \theta_e + S_2 \sin \theta_e) \tag{29}$$

The explicit expressions of $y_e^{1|2}$ and $\tan \theta_e$ were given in [2, 13], they are functions only of k

The stability of this equilibrium point is given by the nature of the roots of the characteristic equation of the system (24) One showed [2, 9, 13] that for $k < 0\,845$ the equilibrium point is a centre or a weak focus, the motion has a neutral stability or is weakly stable For $k < 0\,845$, the equilibrium point is a sabble point, the motion is unstable

The direction in which the unstable orbit moves can be determined from the first equation (24), for very small values of y_i (initial value of y) For such values we must have $dy/d\tau < 0$, in order to avoid imaginary values for x or $dx/d\tau$ (see the first equation (19)) From the first equation (24), and taking into account (25) and (26), we deduce the existence of a critical polar angle in the phase plane, given by [2, 13]

$$\tan \theta_c = \sin (2\pi k)/(k(1 - \cos (2\pi k))), \tag{30}$$

for which $dy/d\tau = 0$ Consequently, the initial polar angle θ_i may lie only in certain domains on the trigonometric circle The study of the possible different situations [2, 5, 9] leads to the following results (θ_c being considered as lying in the first quadrant)

If $\sin (2\pi k) < 0$, $k < 1$, we obtain

$$\begin{aligned} &\theta_i \in (\theta_c, \pi) \rightleftharpoons x \text{ increases}, \\ &\theta_i \in (\pi, \theta_c + \pi) \Rightarrow x \text{ decreases} \end{aligned} \tag{31}$$

If $\sin (2\pi k) < 0$, $k < 1$, we obtain

$$\begin{aligned} &\theta_i \in (\theta_c - \pi/2, 0) \Rightarrow x \text{ decreases}, \\ &\theta_i \in (0, \theta_c + \pi/2) \Rightarrow x \text{ increases} \end{aligned} \tag{32}$$

If $\sin (2\pi k) < 0$, $k < 1$, we obtain

$$\begin{aligned} &\theta_i \in (\theta_c - \pi, 0) \Rightarrow x \text{ decreases}, \\ &\theta_i \in (0, \theta_c) \rightleftharpoons x \text{ increases}. \end{aligned} \tag{33}$$

Finally, if $\sin (2\pi k) < 0$, $k < 1$, we obtain

$$\begin{aligned} &\theta_i \in (\theta_c + \pi/2, \pi) \Rightarrow x \text{ increases}, \\ &\theta_i \in (\pi, \theta_c + 3\pi/2) \Rightarrow x \text{ decreases} \end{aligned} \tag{34}$$

The increase or decrease of x were established on the basis of the second relation (20) If x increases, the unstable orbit moves outward with respect to the initial circular orbit, if x decreases, the motion is performed inward

The time scale for perturbations to become significant (characteristic time) can also be determined from the first stroboscopic equation (24) Denote by y_p the value of y after a stroboscopic time interval of length $\hat{\tau}_p$, when the perturbation became appreciable Integrating the first equation (24) for fixed θ_*, we obtain [10]

$$\tau_p = (2\pi/Y_2 \ln ((Y_1 - Y_2 y_p^{1/2})/(Y_1 - Y_2 y_p^{1/2})), \tag{35}$$

where we denoted $Y_j = S_j \cos(j\theta_*) - C_j \sin(j\theta_*)$, $j = 1, 2$

For our applications we considered [2, 13]

$$y_* = 0, \qquad y_p = 1/4 \tag{36}$$

With (22), (25), (26), (35) and (36), the dimensionless characteristic time becomes:

$$\tau_p = \pi(k^2 - 1) \cos\theta_c/(\alpha k(1 - \cos(2\pi k)) \sin(\theta_* - \theta_c)) \tag{37}$$

From here, with (16), one can determine the physical characteristic time, t_p.

A last remark all considerations made in this section are valid only for nonintegral values of the ration k [2, 9, 13]. Integer values of k lead to resonances.

4 **Physical Initial Conditions.** We can now study the motion of a particle around a pulsating star by means of the mathematical model briefly exposed in Sections 2 and 3 In order to have not a repulsive radiative force exceeding (in module) the gravitational attraction, we took care to fulfil the condition (11).

Taking into account the natural values of the density of the particle (1—4 g/cm^3), the condition (11) imposed inferior limits for the acceptable dimensions of the particle So, in the two cases we studied, there was necessary to consider limitative values for the radius r' of the particle ($r' = 0\,01$ cm in the case of an RR Lyrae pulsating star, and $r' = 1$ cm in the case of a long-periodic variable). If we consider smaller values (as to the order of magnitude), the condition (11) is no longer fulfilled.

As to the central body of the dynamical system (a pulsating star), we had firstly in view the RR Lyrae pulsating stars They are well known observationally and well studied, representing characteristic types for the oscillating cosmic phenomena [3] But, as we shall remark in the next section, the orbits of the particles around such stars are a priori unstable Consequently, it was necessary to consider as central body a long-periodic pulsating star, too

In the next sections we shall study the evolution of the orbit of a particle around a pulsating star from three points of view stability of the motion, evolution of the unstable orbit with respect to the initial circular orbit, characteristic time for perturbations to become significant

5 **Orbits around an RR Lyrae Star.** Let the pulsating star taken into account as central body of our dynamical system be an RR Lyrae variable. We considered this star as having the features of XZ Cygni (RR Lyrae pulsating variable), namely [12]

$$\begin{aligned} M &= 1\,036 \quad 10^{33}\text{g}, \\ L_{max} &= 1\,886 \quad 10^{34}\ \text{cm}^2\text{g/s}^3, \\ L_{min} &= 0\,842 \quad 10^{34}\ \text{cm}^2\text{g/s}^3, \\ R &= 3 \quad 2138 \quad 10^{11}\ \text{cm}, \\ T_* &= 0.46647\ \text{days}. \end{aligned} \tag{38}$$

For the particle we considered $r' = 0\,01$ cm, $\rho = 3$ g/cm^3

We determined firstly the period of a "zero satellite" (a fictitious satellite orbiting the star at the distance R), denoted T_s. From Kepler's third law written for this case:

$$T_s = 2\pi R^{3/2} H^{-1/2}, \tag{39}$$

we found $T_s = 2\,31$ days.

One observes immediately that, even without considering the small variations of the stellar radius [1, 3, 12], the minimum value which can be reached by the ratio k (for $T_0 = T_s$) is $k = 4\,95$. Therefore, as we showed in Section 3, every eventual equilibrium point will be a saddle point, which is unstable. The tests performed for other concrete RR Lyrae stars gave not qualitatively different results Consequently, taking into account the fact that all RR Lyrae variables have sensibly the same characteristics [3, 12], we may extrapolate the conclusion: the motion of a particle (body with reduced absolute dimensions) around an RR Lyrae pulsating star is a priori unstable Of course, as we shall see, the characteristic time for perturbations can be very long, but the motion of the particle, at this time scale, is however unstable.

Coming back to the central pulsating star with the features of XZ Cygni, we adopted for the initial circular orbit the radius $r_0 = 3 \quad 10^{14}$ cm, which leads to a revolution period $T_0 = 5.692 \cdot 10^6$s, namely $k = 141238\ 7$.

The singular point of the stroboscopic equations of motion has the polar coordinates in the phase plane:

$$y_e^{1/2} = 0.5, \qquad \theta_e = -0^\circ\,0003. \tag{40}$$

This is, as we showed, an unstable equilibrium point.

In order to determine the evolution of the unstable orbit, we applied the considerations made in Section 3 (see also [5]). We found.

$$\theta_* \in (359^\circ\,9997, 360^\circ \Rightarrow)\ x \text{ decreases},$$

$$\theta_* \in (0^\circ, 179^\circ.9997) \Rightarrow x \text{ increases},$$

namely, in the great majority of cases, starting with initial conditions near those of the unperturbed motion (in the permitted domains for θ_*); the general tendency of the unstable orbit for very long time intervals will be a motion outward with respect to the initial orbit.

As to the time scale for perturbations, adopting the restrictions (36), we obtained $t_p \cong 28 \quad 10^6$ years. This value corresponds to the most favourable case: $\theta_* = 89^\circ.9997$, for which t_p is minimum The more θ_* is far from this value, in the domains (41), the longer t_p will be.

Greater (or even much greater) values for r' do not lead to significantly different values for the domains in which θ_* may lie and for the minimum characteristic time.

Letting r_0 vary, notable results appear only at the estimate of the characteristic time. So, assigning to r_0 a double value as against that previously considered, one obtains practically for the orbit only the tendency of motion outward with respect to the initial orbit. The perturbations being smaller, one finds for the characteristic time a value of about 13 10 years (minimum value).

6 **Orbits around a Long-Periodic Variable.** We saw that in the case of the short-periodic pulsating stars (as the RR Lyrae variables are) the orbital motion of a particle is implicitly unstable due to the great value of the ratio k. In order to find stars whose features (obviously, conjugated with the characteristics of the satellite particle) lead to the fulfilling of the condition $k < 0.845$, we dwelt upon the long-periodic variables of the type Mira Ceti (see e.g. [3, 11, 14]). These ones are generally red supergiants of spectral classes M, R, N or S, and their pulsation periods can reach 700 days [11].

In order to model the orbital motion of a particle around such a variable star, we considered a fictitious long-periodic variable with the following features

$$\begin{aligned} M &= 20\ M_\odot, \\ L_0 &= 2.7 \quad 10^4 L_\odot, \\ R &= 500\ R_\odot, \\ T_p &= 700 \text{ days}, \\ a_p &= 0.1, \end{aligned} \tag{42}$$

with $M_\odot = 1.989 \cdot 10^{33}$ g, $L_\odot = 3.826 \cdot 10^{33}$ cm^{2}g/s^3, $R_\odot = 6.96 \quad 10^{10}$ cm (solar mass, luminosity and radius, respectively). With the following characteristics of the particle $r' = 1$ cm, $\rho = 3$ g/cm^3, the condition (11) is fulfilled.

As in the previous section, we determined firstly the "zero satellite" period, obtaining $T_s = 306.07$ days. Therefore we can consider in this case real satellites of the star for which $k < 0.845$. We started with the initial radius $r_0 = 5 \quad 10^{13}$cm (or $T_0 = 4.554 \quad 10^7$s), which leads to $k = 0.753$.

Determining the polar coordinates in the phase plane of the singular point of the stroboscopic equations, we obtained

$$y_e^{1/2} = 4.0, \quad \theta_e = 138^\circ\ 3. \tag{43}$$

This equilibrium point is stable, the motion of the particle can be stable and periodic for initial conditions in the neighbourhood of this point, but the value of its polar radius is too great to be considered. For realistic initial conditions, the motion will hence be unstable.

We determined as previously the direction of the evolution of the unstable orbit in the permitted domains for θ_i.

$$\begin{aligned} &\theta_i \in (126^\circ\ 46,\ 180^\circ) \Rightarrow x \text{ increases}, \\ &\theta_i \in (180^\circ,\ 306^\circ\ 46) \Rightarrow x \text{ decreases} \end{aligned} \tag{44}$$

In the first case, the unstable orbit will move outward with respect to the initial orbit (the particle moves away from the star), in the second case, the motion will be performed inward. At limit the particle will escape from the attraction sphere of the star, or, respectively, will fall on the star.

If θ_i takes, in the domains (44), values near 126° 46 or 306° 46, the characteristic time for perturbations will be very long. The minimum value of this one is obtained for $\theta_i = 216^\circ\ 46$, condition which leads to $t_p \cong 25$ years. The orbit is hence very soon destabilized, in a direction or another. This is according to expectation, having in view the relatively small radius of the initial orbit of the particle (about 1.5 R), therefore the great perturbations.

We also performed some tests with the initial condition $r_0 = 5\,39 \cdot 10^{13}$ cm, which leads to $k = 0.843$ (near the critical value). The results are not significantly different from the previous ones, except the position of the equilibrium point of the stroboscopic equations of motion, one obtains $y_e^{1/2} = 223$, an excessively great value to be considered

Keeping the conditions $r_0 = 5.39 \quad 10^{13}$ cm, $\rho = 3$ g/cm^3 (the density of a silicate), but letting r' vary (increase), we have not obtained sensibly different results. Even for an increase of r' with 4—5 orders of magnitude, the permitted domains for θ_1 remain roughly the same, and the perturbations become appreciable after a minimum interval of the order of 25 years.

Coming back to the conditions $r' = 1$ cm, $\rho = 3$ g/cm^3, we determined the characteristics of the motion for greater initial distances from the central star, for which the ratio k is greater than the critical value 0.845. So, for an initial orbital radius $r_0 = 5 \cdot 10^{14}$ cm, we obtained the equilibrium point·

$$y_e^{1/2} = 0\,5, \qquad \theta_e = -1°.7, \tag{45}$$

which is unstable. The domains for θ_1 which decide the direction of the evolution of the unstable orbit are:

$$\begin{aligned} &\theta_1 \in (356°\cdot 4,\ 360°) \Rightarrow x \text{ decreases}, \\ &\theta_1 \in (0°,\ 176°\cdot 4) \Rightarrow x \text{ increases}. \end{aligned} \tag{46}$$

The minimum characteristic time is of the order of 10^5 years.

Growing the initial radius at $r_0 = 5 \cdot 10^{15}$ cm, the singular point preserves its polar radius, but $\theta_e = 0°\cdot 016$. The direction of the evolution of the unstable orbit is given by:

$$\begin{aligned} &\theta_1 \in (0°\cdot 7,\ 180°) \Rightarrow x \text{ increases}, \\ &\theta_1 \in (180°,\ 180°\cdot 7) \Rightarrow x \text{ decreases}, \end{aligned} \tag{47}$$

while the minimum characteristic time for perturbations increases appreciably, reaching about 2.5 10^5 years.

Other determinations were performed for the same last two values of the initial orbitral radius, and for the same dimensions of the particle, but with a density of 1 g/cm^3 (corresponding to water ice grains). The results are in the main similar to the previous ones, with an exception. the characteristic time, which becomes sensibly shorter. This is natural, having in view the greater perturbations in this case (due to the smaller mass of the particle of the same dimensions).

7. **Concluding Remarks.** On the basis of the information provided by the applications performed in Sections 5 and 6, we can formulate some conclusions.

The motion around the RR Lyrae pulsating stars (and, generally, around the short-periodic intrinsic variables) is a priori unstable, due to the great value of the ratio k. According to the initial conditions, the direction of the instability is particularly outward with respect to the initial orbit; the particle tends to move away from the central star. The minimum physical time

after which the perturbations become significant is of the order of 10^7-10^8 years.

In the case of the long-periodic pulsating stars, there can appear situations in which the ratio k is smaller than the critical value, but these situations need equilibrium points unlikely far from the origin in the phase plane Consequently, a realistic orbital motion will be unstable

Choosing, for long-periodic pulsating stars, initial conditions leading to $k < 0\,845$ (critical value), the minimum time scale for perturbations to become appreciable is very short, such an orbit is destabilized after some 25 years

An important part in the determination of the minimum characteristic time is played by the pulsation amplitude and the initial distance of the particle. Small amplitudes and great initial distances lead to small perturbations, for which the time scale to become notable is of the order of hundred million years.

REFERENCES

1 Giurgiu, I, *Note on the Stellar Adiabatic Pulsations*, Babeş-Bolyai Univ, Fac Math Phys Res. Sem, Preprint 10 (1987), 177—182.
2 Giurgiu, I, *Contribuţii la studiul mişcării orbitale în cazul parametrului gravitaţional variabil, cu aplicaţii la stele pulsante*, Thesis, University of Cluj-Napoca, 1988
3. Lungu, N, *Pulsaţii stelare Teorie matematică*, Ed ştiinţifică şi enciclopedică, Bucureşti, 1982,
4. Minorsky, N, *Nonlinear Oscillations*, Van Nostrand, Princeton, 1962
5 Mioc, V, *Unstable Orbit Evolution in the Motion with Variable Gravitational Parameter*, Babeş-Bolyai Univ Fac Math Phys Res Sem, Preprint 10 (1988), 63—72
6 Mioc, V, Giurgiu, I, *Deformations of the Initially Circular Orbit of a Body Moving around a Pulsating Star*, Babeş-Bolyai Univ, Fac Math Phys Res Sem, Preprint 4 (1988), 57—68
7 Mioc, V, Pál, Á, Giurgiu, I., *A Method for Studying the Orbital Motion with Changing Gravitational Parameter*, Babeş-Bolyai Univ, Fac Math Phys Res Sem, Preprint 1 (1988) 79—90.
8 Mioc, V, Pál, Á, Giurgiu, I, *On the Motion around a Star of Linearly Increasing Magnitude*, Babeş-Bolyai Univ, Fac Math Phys Res Sem, Preprint 4 (1988), 41—56
9 Mioc, V, Pál, Á, Giurgiu, I, *Orbital Motion with Periodically Changing Gravitational Parameter*, Studia Univ Babeş-Bolyai, Mathematica, 33, (1988), No 4 (to appear)
10 Mioc, V, Pál, Á, Giurgiu, I, *Time Scale for Perturbations in the Orbital Motion with Changing Gravitational Parameter*, Proc Conf Appl Math, and Mech, Cluj-Napoca, 20—23 October 1988 (to appear)
11. Pecker, J C, Schatzman, E, *Astrophysique générale*, Masson et C-ie, Paris, 1959
12. Pop, V, *The Physical Parameters of RR Lyrae Stars*, Babeş-Bolyai Univ, Fac Math Res Sem., Preprint 2 (1985), 64—78
13. Saslaw, W. C, *Motion around a Source whose Luminosity Changes*, Astrophys, J, 226 (1978), 240—252
14. Ureche, V, *Universul*, Vol. 2, *Astrofizică*, Ed Dacia, Cluj-Napoca, 1987

STUDIA UNIV BABEŞ—BOLYAI, PHYSICA, XXXIII, 2, 1988

ORBITAL MOTION WITH MONOTONICALLY CHANGING GRAVITATIONAL PARAMETER

IOACHIM GIURGIU* and VASILE MIOC**

Received December 15, 1988

ABSTRACT. — An extension of Kepler's problem in the case of a secular variation of the gravitational parameter is done. The elements of the oscilating orbit corresponding to an arbitrary instant are determined analogously to the case of the two-body problem.

1 **Changing Gravitational Parameter.** Consider a point mass m orbiting another point mass $\mathcal{M}$, under the only influence of two forces: the gravitational attraction and a perturbing force which is central (its support containing the attractive centre $\mathcal{M}$) and obeys an inverse square law. Since the resulting force is also central, the motion will take place in a fixed plane (determined by the radius vector and the velocity vector at the initial instant $t = 0$), and will be featured by the equation (e.g. [11]):

$$d^2r/dt^2 - C^2/r^3 = -G(\mathcal{M} + m)/r^2 + K/r^2, \tag{1}$$

in which r = radius vector of m with respect to $\mathcal{M}$, G = gravitational constant, C = constant angular momentum, K/r^2 = perturbing acceleration undergone by m as an effect of the above mentioned perturbing force.

We shall consider that $\mathcal{M}$, m, K and even G are time-dependent; hence we can write.

$$q = q_0(1 + f_q(t)), \quad q \in \{\mathcal{M}, m, G, K\}, \tag{2}$$

where the quantities q_0 are constant and represent the initial values of the quantities q. This means that we imposed the restriction $f_q(0) = 0$.

Such variations of these quantities were considered by several authors (e.g. [1, 4, 6, 15, 17]; for a detailed list, see [2]), each peculiar case corresponding to a concrete astronomical problem or situation.

We have shown [5, 7, 8, 10] that in these conditions the problem is equivalent to Kepler's problem in the case of a time-variable gravitational parameter. Indeed introducing the notations

$$H = G_0(\mathcal{M}_0 + m_0) - K_0, \tag{3}$$

where the constant H is called effective gravity and consists of the constant part of $G(\mathcal{M} + m)$, this one being the purely gravitational parameter, and the constant part of K (which features the perturbing force), and

$$\begin{aligned} f(t) = (K_0 f_K(t) - G_0((\mathcal{M}_0 + m_0) f_G(t) + (1 + f_G(t)) \\ (\mathcal{M} f_{\mathcal{M}}(t) + m_0 f_m(t)))/(G_0(\mathcal{M}_0 + m_0) - K_0), \end{aligned} \tag{4}$$

* *Industrial Secondary School, 3379 Baia de Arieș, Romania*
** *Centre for Astronomy and Space Sciences, 3400 Cluj-Napoca, Romania*

he equation of motion (1) acquires the form

$$d^2r/dt^2 - C^2/r^3 = -\mu/r^2, \tag{5}$$

where we denoted

$$\mu = H(1 - f(t)) \tag{6}$$

Observe that the equation (5) has the same form as the equation of motion in the classical two-body problem, but here μ is function of time. That is why we called μ of the form (6), which appears in (5), *changing gravitational parameter*. This is somehow an abuse of language, since the nature of the perturbing force is not specified.

We mention that some natural restrictions must be imposed to the functions $f_q(t)$ from (2), in order to illustrate realistic concrete astronomical situations Such restrictions were discussed in [5]

2 **Basic Formulae.** In some previous papers [6—10] we considered that the initial motion is circular and studied different problems concerning the perturbed orbit by means of the method described in [5] In this paper we shall consider that the initial orbit is elliptic (of arbitrary subunitary eccentricity) and use another method, in order to determine the osculating orbit and dis uss some features of this one We impose to the function $f(t)$ a single condition to be a monotonic function, that is the gravitational parameter undergoes a secular variation

We start with the basic equation of the trajectory, which, by (5) and (6), can be written in the form

$$d^2r/dt^2 - C^2/r^3 = -H(1 - f(t))/r^2 \tag{7}$$

Since the point mass m moves under the action of a central force, its motion must observe the theorem of angular momentum, which we use in the form [14]

$$r^2du/dt = C, \tag{8}$$

where u is the argument of latitude

We also use the integral of energy in polar coordinates [14]

$$(dr/dt)^2 + r^2(du/dt)^2 = 2\mu/r + h \tag{9}$$

In the classical two-body problem, μ is the purely gravitational parameter (constant) and h denotes the constant of energy In the case of our extension of Kepler's problem, μ is time-dependent, according to the law (6), and h will be time-dependent, too

Replacing (6) and (8) in (9), the integral of energy can be written as prime integral of the basic equation (7) under the form

$$(dr/dt)^2 + C^2/r^2 - 2H(1 - f(t))/r = h(t) \tag{10}$$

The time-dependence of the orbital energy is given by

$$dh(t)/dt = (2H/r)\, df(t)/dt, \tag{11}$$

formula which can immediately be verified by differentiating (10) with respect to time and taking into account the equation (7) of the trajectory.

As we said, the problem we study is the determination of the osculating orbit at an arbitrary instant. So, we tackle this generalized Kepler problem as $h(t)$ were constant (see [9, 15]).

Consider in the Euclidean three-space E_3 an inertial, rectangular, right-handed frame $\mathcal{M}xyz$, with the axes directed towards fixed points in space. In this frame, the constant angular momentum vector $\vec{C}$ will have the components

$$\vec{C} = \vec{C}(C_x, C_y, C_z), \tag{12}$$

such that

$$C^2 = C_x^2 + C_y^2 + C_z^2, \tag{13}$$

where $C = |\vec{C}|$. Analogously, Laplace's vector $\vec{f}_L$ will have the components

$$\vec{f}_L = \vec{f}_L(f_{L,x}, f_{L,y}, f_{L,z}), \tag{14}$$

such that

$$f_L^2 = f_{L,x}^2 + f_{L,y}^2 + f_{L,z}^2, \tag{15}$$

where $f_L = |\vec{f}_L|$.

Consider now the orbital elements $\{a, e, \Omega, \iota, \omega, t_p\}$, where a = semimajor axis, e = eccentricity, Ω = longitude of the ascending node, ι = inclination, ω = argument of pericentre, t_p = instant of pericentre (dynamical element). The relationships between the orbital elements and the Cartesian coordinates and velocity components are well known (e.g. [1, 12, 14, 16]). Here we are interested in the relationships between the components of the vectors $\vec{C}$ and $\vec{f}_L$ and the orbital parameters.

The components of $\vec{C}$ are [1]:

$$\begin{aligned} C_x &= C \sin\Omega \sin\iota, \\ C_y &= -C \cos\Omega \sin\iota, \\ C_z &= C \cos\iota, \end{aligned} \tag{16}$$

while the components of $\vec{f}_L$ are [1]

$$\begin{aligned} f_{L,x} &= f_L\ (\cos\Omega \cos\omega - \sin\Omega \sin\omega \cos\iota), \\ f_{L,y} &= f_L\ (\sin\Omega \cos\omega + \cos\Omega \sin\omega \cos\iota), \\ f_{L,z} &= f_L \sin\omega \sin\iota \end{aligned} \tag{17}$$

We know that in the two-body problem there exists the following relationship between the integration constants $\vec{C}$, $\vec{f}_L$ and h (see e.g. [1, 12, 16])

$$f_L^2 = \mu^2 + C^2 h. \tag{18}$$

In our generalized case, taking into account (6), the equation (18) becomes

$$f_L(t) = (H^2(1 - f(t))^2 + C^2 h(t))^{1/2}. \tag{19}$$

With all these considerations and formulae, we can now determine the osculating orbit at an arbitrary instant.

3. **Shape and Dimensions of the Orbit.** The shape of the orbit is precised by the eccentricity From the formula

$$e = f_L/\mu, \tag{20}$$

we find the instantaneous eccentricity as function of time.

$$e = (1 + C^2h(t)/(H^2(1 - f(t))^2))^{1/2}. \tag{21}$$

We deduce from (21) two features concerning $h(t)$ on one hand, $h(t)$ must have the dimension of the square of the velocity, on the other hand, $h(t)$ must be such that

$$f(t) \to 1 \Rightarrow e \to 1, \tag{22}$$

namely $h(t)$ tends to zero faster than $1 - f(t)$

The dimensions of the orbit are precised by its semimajor axis Taking into account the relationship (e g [1])

$$a(1 - e^2) = C^2/\mu, \tag{23}$$

we obtain the semimajor axis written in our case as function of time

$$a = -H(1 - f(t))/h(t). \tag{24}$$

Observe that, since $h(t)$ is negative (elliptic-type motion) and due to the fact that $h(t)$ tends to zero faster than $1 - f(t)$, the semimajor axis will be positive insofar $f(t) < 1$, $a \to \infty$ for $f(t) \to 1$, and will become negative (hyperbolic-type orbit) when $f(t)$ exceeds the unity.

4. **Position of the Orbit Plane.** As it is known, the position of the orbit plane with respect to the $\mathcal{M}xyz$ frame is specified by the angles Ω (angle between the $\mathcal{M}x$ — axis and the intersection of the orbit plane with the $\mathcal{M}xy$—plane) and i (angle between the orbit plane and the $\mathcal{M}xy$—plane) Since the point mass m undergoes the action of a central resulting force, its motion takes place in a fixed plane (determined, as we already said, by the initial positions of the radius vector and velocity vector) So, we have

$$\Omega = \Omega_0, \; i = i_0, \tag{25}$$

where the index signifies the values at the initial instant $t = 0$

5. **Position of the Orbit in its Plane.** Laplace's vector determines the position of the orbit in its plane, the direction of this vector coincides with the line of apsides (semimajor axis). In order to find this direction we need the argument of pericentre (angle in the orbit plane between the line of nodes (intersection of the orbit plane with the $\mathcal{M}xy$—plane) and the direction towards the pericentre). This angle can be determined on the basis of Laplace's vector and angular momentum, according to the formula

$$\tan \omega = f_{L,z}C/(f_{L,y}C_x - f_{L,x}C_y) \tag{26}$$

The argument of pericentre can also be deduced, in a perturbative manner from the corresponding equation of the Newton-Euler system (in the case of a central perturbing force)

$$d\omega/dt = -(S/e)\cos v, \tag{27}$$

where S is the (only nonzero) radial component of the perturbing acceleration ($S = K/r^2$), the eccentricity is given by (21), while the true anomaly (v) can be obtained from the orbit equation in polar coordinates

$$r = a(1 - e^2)/(1 + e\cos v). \tag{28}$$

6 **Instant of Pericentre.** The true anomaly being determined, one can find the eccentric anomaly (E) on the basis of the formula

$$\tan(E/2) = ((1 - e)/(1 + e))^{1/2}\tan(v/2), \tag{29}$$

with e given by (21) Having the eccentricity and the eccentric anomaly, one solves Kepler's equation (e.g. [12, 13])

$$M = E - e\sin E, \tag{30}$$

obtaining in this way the mean anomaly (M)

Let us now consider the formula for the mean motion

$$n = a^{-3/2}\mu^{1/2}, \tag{31}$$

or, in our case, by (6) and (24)

$$n = (-h(t))^{3/2}/(H(1 - f(t))). \tag{32}$$

With M given by (30) and n given by (32), we finally find the instant of pericentre

$$t_p = t - M/n = t - MH(1 - f(t))/(-h(t))^{3/2} \tag{33}$$

Now the problem is completely solved for the case of the elliptic-type motion

7 **Comments.** Interesting information about the limits between which the radius vector can lie are obtained from (21) and (24), by taking into account the well-known relationships.

$$r_{\min} = a(1 - e), \qquad r_{\max} = a(1 + e) \tag{34}$$

One finds [9, 15]

$$C^2/(2H(1 - f(t))) < r_{\min} \leqslant C^2/(H(1 - f(t))) \leqslant r_{\max} < \infty. \tag{35}$$

Analogous results can be obtained from (11) and (35) for the orbital energy [9]:

$$\begin{aligned} 0 < (dh/dt)_{\min} &\leqslant (2H^2(1 - f(t))/C^2)df(t)/dt \leqslant \\ &\leqslant (dh/dt)_{\max} < (4H^2(1 - f(t))/C^2)df(t)/dt. \end{aligned} \tag{36}$$

Observe from (36) that, for $f(t) < 1$, if the function f is increasing (the gravitational parameter decreases) the orbital energy will increase, too. Conversely,

if the gravitational parameter increases (hence the function f decreases), the orbital energy will decrease

We must emphasize that these results are valid only if $f(t)$ is a monotonic function

Of course, the evolution of the orbit in the case of a secular variation of the gravitational parameter can be studied by other methods, too. As examples, we mention the method used by us in [5], or that used in [15] If the secular change of the gravitational parameter is very slow as against the dynamic time scale, the problem can be also studied by using the theory of adiabatic invariants (e.g [3])

REFERENCES

1 Duboshin, G N, *Celestial Mechanics Basic Problems and Methods*, Gos Izd Fiz -Mat Lit, Moscow, 1963 (Russ)

2 Giurgiu, I, *Contribuţii la studiul mişcării orbitale în cazul parametrului gravitaţional variabil cu aplicaţii la stele pulsante*, thesis, University of Cluj-Napoca, 1988

3 Landau, L D, Lifshitz, E M, *Mechanics*, Pergamon Press, Oxford, 1960

4 Lyttleton, R. A, Finch, J P, *Effect of a Changing G on the Moment of Inertia of the Earth*, Astrophys J, **221** (1978), 412—413

5 Mioc, V, Pál, Á, Giurgiu, I, *A Method for Studying the Orbital Motion with Changing Gravitational Parameter*, Babeş-Bolyai, Univ, Fac Math Phys Res Sem, Preprint 1 (1988), 79—90

6. Mioc, V, Pál Á, Giurgiu, I, *On the Motion around a Star of Linearly Increasing Magnitude*, Babeş-Bolyai Univ, Fac Math. Phys Res Sem, Preprint 4 (1988), 41—56

7 Mioc, V, Pál, Á, Giurgiu, I., *Orbital Motion with Linearly Changing Gravitational Parameter*, Babeş-Bolyai Univ, Fac Math Phys Res Sem, Preprint 10 (1988), 3—20

8 Mioc, V, Pál, Á, Giurgiu, I, *Perturbations in the Initially Circular Motion with Parabolically Changing Gravitational Parameter*, Babeş-Bolyai Univ, Fac Math Phys Res Sem, Preprint 10 (1988), 21—34.

9 Mioc, V, Pál, Á, Giurgiu, I, *Limit Values for the Radius Vector and Orbital Energy in the Motion with Monotonically Changing Gravitational Parameter*, Babeş-Bolyai Univ, Fac Math. Phys Res Sem, Preprint 10 (1988), 91—102

10. Mioc, V, Pál, Á, Giurgiu, I, *Orbital Motion with Periodically Changing Gravitational Parameter*, Studia Univ Babeş-Bolyai, Mathematica, **33** (1988), No 4

11 Moulton, F R, *An Introduction to Celestial Mechanics*, 13-th ed., Macmillan, New York, 1959

12 Oproiu, T, Pál, Á, Pop, V, Ureche, V, *Astronomie Culegere de exerciţii, probleme şi programe de calcul*, University of Cluj-Napoca, 1985

13 Pál, Á, Pârv, B, *On the Efficency of Numerical Methods for Kepler's Equation Solution*, Babeş-Bolyai Univ, Fac Math Phys Res Sem, Preprint 10 (1988), 115—134

14. Pál, Á, Ureche, V, *Astronomie*, Ed didactică şi pedagogică, Bucureşti, 1983

15. Saslaw, W C, *Motion around a Source whose Luminosity Changes*, Astrophys. J, **226** (1978), 240—252

16. Subbotin, M F, *Lectures on Celestial Mechanics*, 2-nd ed, Vol. 1, Gos Izd Tehn-Teor Lit, Leningrad, Moscow, 1941 (Russ.).

17 Will, C M, *Relativistic Gravity in the Solar System II Anisotropy in the Newtonian Gravitational Constant*, Astrophys J, **169** (1971), 141—155

STUDIA UNIV BABEŞ-BOLYAI, PHYSICA, XXXIII, 2, 1988

RECENZII

INSTITUTUL CENTRAL DE FIZICĂ
INSTITUTUL DE ÎNVĂŢĂMÎNT SUPERIOR CONSTANŢA
COMITETUL NAŢIONAL ROMÂN DE FIZICĂ
INSTITUTUL ROMÂN DE CERCETĂRI MARINE
ÎNTREPRINDEREA CONSTRUCŢII NAVALE CONSTANŢA

PROGRESE ÎN FIZICĂ

A 10-A SESIUNE ANUALĂ DE COMUNICĂRI A INSTITUTULUI CENTRAL DE FIZICĂ

CONSTANŢA, 6–8 octombrie 1988

ROMANIAN PHYSICS IN 1988

The 1988 Romanian Physics moment, hallmarked by the X-th Scientific Session of Romania's Central Institute of Physics, on October 6—8, is particularly significant for the complex field of activity and of knowledge, at both national and international level, in that concurrently came out the written text of the 1988 edition of "Progress in Physics" (pp 828) Even when merely reading this generic heading — consistently repeated year by year for a decade of scientific information, not only by the caption of previous such events but also by the publishing of some precursory books of the like —, the truth that any science evolves from the past (more remote or nearer), develops in the present and wends its way toward the future — a future expected to yield as many a concept as has done its progress from the past to the present — once again turns out to be right This brief primordial idea will help readers understand, we trust, why "Progress in Physics" has been glossed as such and preserved through the short past of a decade and viewed for the coming future of this imposing domain of scientific knowledge

The book "Progress in Physics" (1988) is for the physicists in our country — and not only for them, but also for those abroad, for researschers both old or young — a valuable means of information and optimum documentation about the achievements of the experienced researcher in investigation and exploration of the physical phenomena, of the laws of relative stability or instability of varied physico-chemical substances The long beaten paths by the pioneer physicists, by the forerunners, and devisers of research methodologies in the so diversified field of physics justify our calling the recent researcher — of which the text of the book is largely evincive — as "physicist-perfecter"

The syntagm *progress in physics* was coined in 1979 by the then whole group of Romanian physicists and assigned to be the generic headline of the domain scientific sessions on both the research plane and of the education and economic-industrial production in our country.

"Progress in Physics", as set out — maintaining the format of the previous editions (1984, 1985, 1986 and 1987) —, carries no foreward or afterword for readers, which makes the anonymous reader — whether physicst or not — elaborate it himself, but hardly achievable yet not impossible, and with brain pains relied on certain hermeneutic principles.

The text of the book complies with and ensures the information flow abreast of the scientific standards and actuality towards depth and details in the description of physical phenomena, especially through extension and correlation of the operational procedures both in the intradisciplinary domain of physics and in other fields of knowledge as exacting to the methodology of physics That is why we consider it more appropriate to make an euristical description on the type of the book, and lay by the

preface and postface for some other future review

A first, general view of the text is evincive to the physicist researchers' having imposed themselves to mirror succintly and concisedly, rigorously and in a sample manner the accomplishments of the daily practice of the object (matter substance, body, phenomenon, physical and physico-chemical law structural-functionally applied etc) subject to investigations And, as it is well known fact that in any field of activity to be modern is to be applicative — both theoretically and practically —, physics itself being no exemption from that, it follows that, while exhaustively consulting the text of the book, one is called for a close look upon the three differentiated ways of application the self-application of physics — which secures its progress as distinctive science, external application i e in other domains, and, finally, the application of other domains in physics These three disciplinary and interdisciplinary application requirements and conditions, with large dependence and interdependence on scope methods of investigation in physics, compels, us, as first readers of the text, to view the relation author-reader of an informational text from three essential standpoints

First, in the book the authors make known to one another their accomplishments, benefitting each from the other's experience and from the information amount their texts convey Second, the researchers as authors (of written text) inform their readers about sound knowledge of specialty (physics), which circulates at the international level and is characterized by scientific standards and actuality, by profoundness and minuteness, by extention and correlation among the varied chapters This event of the human cognition, always in extention, and the ever more extensive expansion of the scientist's intellect are known today as "informational outburst". But to have this informational outburst take place on an interdisciplinary level, this event has been and is preceded beforehand by another scientific event which occurs inside each scientific branch, — as a specific event of it — denoted "informational explosion" Therefore the text of the book evidences a recent informational break-out in physics, which extends over other domains (interdisciplinarity), outlining the informational outburst of physics

Third, the text of the book is indicative to readers that due to previons development the nowadays physics has won an autonomous scientific status and poses a smooth progress, making itself dominated by such a specialized "information" that it not only contributes to education of the natural intteligence of the human person (for those educating themselves through it), but also by theory and practice to the soft driven operation of what is known of late to be the "artificial intelligence and robotistic" When physics by its experimental methods and theoretical ratiocination has turned out to be a source of promoting information from other disciplines — no matter which they are —, we can say it has reached the "performance' stage Thereby, the text of the here reviewed book must be looked upon as a competent and performant text

All the three requirements of the dyad author-reader of informational text in physics being met — as illustrated by the book in question — fully prove that the Romanian physicists have touched the competence stage to write in their own field and endeavour to maintain this scientific spirit state In the light of the above considerations, it comes out that the book title "Progress in Physics" is no mere pun, a syntagm to be ignored, but a so-called "generic informational-informative" title also denoted "Compendium of Presentday Physics", having its own paradigms and hermeneutic The book is edited accurately by a prestigeous editorial team of the Central Institute of Physics It contains 828 pages, with a complex profile and well outlined evolvement direction in all the recent branches of physics, as follows Nuclear and hard ions physics (68 subjects), Atomic and molecular physics (34 subjects), Field theory and elementary particles, statistical and mathematical physics (34 subjects), Condeused state physics (88 subjects), Plasma physics optics, spectroscopy and lasers (73 subjects), Biophysics, radiobiology, radioimmunology (22 subjects), Radiometry and dosimetry of the environment (54 subjects), Earth physics, astronomy and astrophysics (45 subjects) and, Nonconventional physics and technologies (45 subjects),

The title of each subject was principally established by authors according to the substance subject to expriments, the choice of the phenomenon specific to this substance, the choice and logical ordering of the essential parameters of the phenomenon as function of the way in which they render out its law character and, finally, the outline of the conditions of useful application of the investigated substance in laboratory or technics (industry) Scientific evaluation of the obtained results is clearly emergent from the calculations progress, from the drawing of the graphs and the law interpretation of the phenomenon investigated

The graphs and tabulations accompanying the written text, with newest references ensure a deep insight into the specific characteristics of the substances envolved, and the accurate language of the text makes it easily compre-

hensible even by nonphysicists studying physics interdisciplinarily

A general view of the whole body of concepts employed in the book and of the chapter vocabulary is indicative of a rather wide reccurrence in the text discourse of the structural components of the matter such as substance, molecule, atom, atomic nucleus, neutron, proton, mezon, neutrino, elementary particle, of the terms denoting physical constants as, for example h, c, l etc, of many physical parameters as well as of laboratory instrumentation, of terms designating physical or chemical phenomena namely fission, fussion, (re)crystallization, x-radiation emission, γ-radiation, uv-radiation, levels of electromagnetic energy a s o

The informational load of more than 10 000 terms with semantic marks specific to physics, chemistry, biology, mathematics and to other disciplines such as technical disciplines — prerequisites of the laboratory experiments and researches, of the large scale industrial application, respectively — enabler esearches to documentate thoroughly in his specialty field

The over 550 authors signing the contributions, either individually or collectively, carry out research activity specific of the theme — theoretical or experimental —, in laboratories — either didactic or non-didactic — belonging to universities, pilot stations of industrial aggregates or of enterprises and technological installations, all these having research planning under the Central Institute of Physics in our country

Informationally and documentarily, the poster-like text desplay turns out an informational treasury and column of sound knowledge in the modern field of theoretical and applied physics The information bursting from the texts goes in part to the informational flow levelling international congresses, while some other in the country and for other varieties of scientific literature such as specialty treatise, lexicons and dictionaries, school text-books, and quite good a share comes to mass media sicentific and technical literature

As for the researchers — authors of the papers in the here reviewed collection, many of them having also authored the texts of previous volumes — they are heading upstream toward next year and the followings, with an ever more enriching experience

PETRU POGÂNCEANU

K Baumgartel and K Sauer, **topics on nonlinear wave-plasma interaction**, Birkhauser Verlag, Basel—Boston—Stuttgart, 1987, 222 pp

This monograph is devoted to theoretical asnects of nonlinear processes at the interaction of intense electromagnetic radiation with unmagnetized fully ionized plasmas The book covers several selected topics on nonlinear wave-plasma interaction in a treatment based on a hydrodynamic plasma description The interest in these processes has increased in connection with the effort to bring about laser-driven fusion and with active wave experiments in cosmic plasmas too

The text is divided into main parts dealing respectively with nonlinear processes which involve only electrons (high-frequency processes) and phenomena which include ion motion (low-frequency processes) The book has 11 chapters

Part I presents the derivation of the basic equations for both high-frequency and low-frequency processes from two-fluid equations of a plasma A review on basic features of linear wave propagation in nonuniform plasmas (resonance absorbtion structure, resonances) is given in the Part II Chapters 6—7 (Part III) are devoted to high-frequency nonlinear phenomena as the generation of harmonics, stimulated Raman scattering and two-plasmon decay

Part IV (chapters 9—11) deals with low-frequency phenomena as the stimulated Mandelstam-Brillouin scattering, density profile deformation, non-linear skin effect, envelope solutions superreflexion

A list of General References is added and at the book end an Appendix containing some peculiar calculations is given

The content of this book is partly introductory and presents current results obtained as research contributions by the authors

The book is very useful for students and scientists too, not only in field of plasma physics

SPERANȚA COLDEA

L Munchow, R Reif, **Recent Developments in the Nuclear Many-Body Problem**, *Strong interactions and nuclear structure*, vol 1, Teubner-Texte, zur Physik, Leipzig, 1985, 152 pg , *Nuclear reactions and dynamics*, vol 2, 1987, 180 pg

This book treats modern approaches to the nuclear many-body problem sterssing the conceptional points of view as well as the links

to other fields in physics. The text is divided into six chapters, vol 1, and ten chapters, vol. 2.

Vol 1 The first chapter gives some informations on substantial content of nuclei in terms of nucleons and quarks The classification of baryons and mesons and quark-theoretical interpretation are sketched together with the attempts to explain the mass spectra within a phenomenological bag model including gluon exchange between quarks In chapter two, the basic features of the free nucleon-nucleon interaction are discussed There are also included some comments on quark theoretical aspects of the strong interactions between nucleons Chapter 3 contains the present status of mean field theories, starting from the phenomenological shell model with configuration mixing More principal considerations are based on the Hartree-Fock method The concept of nuclear matter and the treatment of hard-core correlations and Brueckner theory are given in chapter 4 In chapter 5 collective vibrations of nuclei are investigated The modern aspects as rotational alignment and backbending phenomena are discussed in chapter 6

A list of 140 references is added. The book is very useful for students and scientists which are interested in modern nuclear research.

Vol 2 The basic concepts and formal elements of the quantum mechanical collisions theory, the description of nuclear reactions in terms of the R-matrix and projection operator techniques are presented (chapters 1—4). For a comparison of theoretical results and experimental data only few illustrative examples have been selected.

The phenomenological optical model, direct reactions, distorted wave Born approximation, zero-range approximation, coupled-channel approximation for inelastic scattering, direct reactions as a tool of reaction spectroscopy and statistical aspects of nuclear reactions are discussed in chapters 5—7.

The treatment of the few-body problem in nuclear reactions is based on the Fadeev equations (chapter 8)

In the last two chapters (9—10), the authors present the classical and semiclassical theory of heavy-ion collisions, the phenomenon of nuclear friction and the time-dependent mean-field approach to heavy-ion induced reactions

Some approaches which could not be discussed in detail are listed in a final section and a list of 220 references is added, too

ONUC COZAR

Stephen Parrott, **Relativistic Electrodynamics and Differential Geometry,** Springer-Verlag, New York, Inc 1987

This book is a complete exposition of the logical structure of classical relativistic electrodynamics written in the language of coordinate-free differential geometry

In Chapter 1 (Special Relativity) and Chapter 2 (Mathematical Tools) the necessary concepts from special relativity and differential geometry are presented Chapter 3 formulates the part of electrodynamics which deals with continuous distributions of charge Chapter 4 treats the radiation and presents the motivation leading to the Lorentz-Dirac equation The last chapter, which is of a more specialized nature, explores further difficulties with the usual formulation of electrodynamics and discusses alternate approaches Much of this chapter is drawn from the reasearch literature

Each chapter contains also exercises with solutions

This very interesting book is addressed to the mathematicians and physicists which are familiar with the language of modern mathematics (differential geometry) and with electromagnetic theory

STELIANA CODREANU

Dimensions and Entropies in Chaotic Systems, *Quantification of Complex Behavior,* Springer-Verlag Berlin Heidelberg, 1986 (G Mayer-Kress, Editor)

This volume contains the papers contributed to the International Workshop on „Dimensions and Entropies in Chaotic Systems" at the Pecos River Conference Center on the Pecos River Ranch in September 1985 The workshop was held by the Center for Nonlinear Studies of the Los Alamos National Laboratory It is known that at the Center for Nonlinear Studies the investigation of chaotic dynamics and especially the quantification of complex behavior has a long tradition

In September 1985 was brought together an indisciplinary group of scientists who worked for one week The results was published in this book which contains seven parts Introduction., General Theory, Mathematical Aspects of Dimensions, Basic Problems, Numerical and Experimental Problems in the Calculation of Dimensions and Entropies, Computation of Lyapunov Exponents, Reliability, Accuracy and Data-Requirements of Different Algorithms, Analy-

sing Spatio-Temporal Chaos, Experimental Results and Applications

The volume is very useful for the researches and serious students foi their own research in the field of nonlinear chaotic dynamics

STELIANA CODREANU

Quantum Chaos and Statistical Nuclear Physics, *Lecture Notes in Physics* 263, Springer-Verlag Berlin Heidelberg 1986, (T H Seligman and H Nishioka, Editors)

This volume contains the proceedings of the 2nd International Conference on Quantum Chaos and of the 4th International Colloquium on Statistical Nuclear Physics, held at Cuernavaca Mexico, in January 6—10, 1986 The convergence in quantum chaos and statistical nuclear physics of methods and physical background justify the meeting on both subjects

The sections of these proceedings are Introduction, Spectra and States, Time dependent systems, Nuclear reactions, Other topics

This volume, which concentrates the latest research results, is very useful for the researches on both domains

STELIANA CODREANU

Roger Penrose, Wolfgang Rindler, **Spinors and Space-time**, *Two-Spinors Calculus and Relativistic Fields*, vol I, Cambridge University Press, 1984, England, reprinted with corections, 1986, 458 pg

The present book represent the first monography in which is given a concise treating of the space-time geometry in frame of spinorial formalism The twistor theory is presented (a development of Dirac's bispinor) which had been created in 1968 and strengthened as unitar theory in '70 years

The interest for twistor theory is related with its applications at the autodual solutions from field theory (the instanton, the monopol), the construction of supersymmetrical spaces, in gravity theory

The authors don't need a special introduction, they are well-known by gravity-physiciens through the terms which had already become customary "Penrose diagramms", "Radon-Penrose transformation", "Newman-Penrose formalism", "Rindler metric", "Rindler vacuum".

The first volume is composed from a preface, five chapters an appedix containing writting diagrammatical system, the bibliography with 203 titles and an index of terms

Chapter 1 — *Geometry of world-vectors and spin-vectors* The simplest spinorial object is defined-a spin-vector complex with 2-components, together with its geometrical image in space-time-"the isotrop flag" determined by the isotropical direction (the support of the flag) and bidimensional isotropical semiplane (the sheet of the flag) It is also given a geometrical interpretation for all spinorial operations

Chaper 2 — *Abstract indices and spinor algebra* The necessity of the abstract indices is explained in the tensorial algebra and from the analogy of the tensorial structure with that of the spin-vectors, spinorial algebra is build

Chapter 3 — *Spinors and world-tensors* It is indicated how the spinorial structure of space-time naturally leads to the isotrop tensorial structure, which is defined by 4 complex liniar independent vectors — the NewmanPenrose isotrop tetrada The basic ideea of isotrop tetrada led to the Newman-Penrose formalism used in the search for solutions of Einstein's ecuations.

Chapter 4 — *Diferentiation and curvature* The curvature spinors conform Weyl and Ricci are analysed and a spinorial formulation for Einstein theory and that of the Bianchi relations is given Using the exterior forms the spinorial coeficients method is described, a method which managed the substantiation of black-hole-fields ot arbitrar spin interactions As an application the topology of bidimensional surfaces is discussed, choosing as an important case,a he 2-sphere in Minkowski's space and the theory of sferical harmonics with spinorial weight is build.

Chapter 5 — *Fields in space-time* In gauge field theory the matter fields (fermions), sections are considered in vectorial bundles and the gauge fields (bosons) would be the conexions of these bundles, over basevariety (Minkowski's space). In this way electromagnetic and Yang-Mills fields is approached. Also the general notion of conformal invariance, valid for curved space-time, is introduced.

EMIL VINȚELER

ÎNTREPRINDEREA POLIGRAFICĂ CLUJ,
Municipiul Cluj-Napoca, Cd. nr. 575

În cel de al XXXIII-lea an (1988) *Studia Universitatis Babeş-Bolyai* apare în specialităţile:

matematică

fizică

chimie

geologie-geografie

biologie

filosofie

ştiinţe economice

ştiinţe juridice

istorie

filologie

In the XXXIII-rd year of its publication (1988), *Studia Universitatis Babeş-Bolyai* is issued as follows:

mathematics

physics

chemistry

geology-geography

biology

philosophy

economic sciences

juridical sciences

history

philology

Dans sa XXXIII-e année (1988), *Studia Universitatis Babeş-Bolyai* paraît dans les spécialités:

mathématiques

physique

chimie

géologie-géographie

biologie

philosophie

sciences économiques

sciences juridiques

histoire

philologie

Abonamentele se fac la oficiile poștale, prin factorii poștali și prin difuzorii de presă, iar pentru străinătate prin „ROMPRESFILATELIA", sectorul export-import presă, P. O. Box 12—201, telex. 10376 prsfir, București, Calea Griviței nr. 64—66

Lei 35